

KADIR HAS UNIVERSITY

SCHOOL OF GRADUATE STUDIES

PROGRAM OF COMPUTATIONAL BIOLOGY AND BIOINFORMATICS

**DEVELOPMENT OF NOVEL AND POTENT INHIBITORS FOR
GABA-AT ENZYME VIA IN SILICO SCREENING METHODS**

ANAS ABDULQADER ABBAS AL-OBAIDI

MASTER THESIS

ISTANBUL, NOVEMBER 2020



**DEVELOPMENT OF NOVEL AND POTENT INHIBITORS FOR
GABA-AT ENZYME VIA IN SILICO SCREENING METHODS**

ANAS ABDULQADER ABBAS AL-OBAIDI

MASTER THESIS

Submitted to the School of Graduate Studies
of Kadir Has University in Partial Fulfillment of the Requirements for the Degree
of Master in the Program of Computational Biology and Bioinformatics

ISTANBUL, NOVEMBER 2020

ANAS ABDULQADER ABBAS AL-OBAYDI

MASTER THESIS

2020



DECLARATION OF RESEARCH ETHICS /

METHODS OF DISSEMINATION

I, ANAS ABDULQADER ABBAS AL-OBAIDI, hereby declare that;

this Master's Thesis is my own original work and that due references have been appropriately provided on all supporting literature and resources;

this Master's Thesis contains no material that has been submitted or accepted for a degree or diploma in any other educational institution;

I have followed "Kadir Has University Academic Ethics Principles" prepared in accordance with the "The Council of Higher Education's Ethical Conduct Principles"

In addition, I understand that any false claim in respect of this work will result in disciplinary action in accordance with University regulations.

Furthermore, both printed and electronic copies of my work will be kept in Kadir Has Information Center under the following condition as indicated below:

The full content of my thesis/project will be accessible from everywhere by all means.

ANAS ABDULQADER ABBAS AL-OBAIDI

11/11/2020

KADIR HAS UNIVERSITY
SCHOOL OF GRADUATE STUDIES

ACCEPTANCE AND APPROVAL

This work entitled DEVELOPMENT OF NOVEL AND POTENT INHIBITORS FOR GABA-AT ENZYME VIA IN SILICO SCREENING METHODS prepared by ANAS ABDULQADER ABBAS ALO-OBAIDI has been judged to be successful at the defense exam held on 11/11/2020 and accepted by our jury as MASTER THESIS.

APPROVED BY:

Prof. Dr. Kemal YELEKÇİ (Advisor) (Kadir Has University) _____

Prof. Dr. Safiye S. ERDEM (Marmara University) _____

Asst. Prof. Dr. Deniz EROĞLU (Kadir Has University) _____

I certify that the above signatures belong to the faculty members named above.

Prof. Dr. Emine Füsun Aliođlu
Dean of School of Graduate Studies
DATE OF APPROVAL: (11/11/2020)

TABLE OF CONTENTS

TABLE OF CONTENTS	vi
ABSTRACT	i
LIST OF TABLES	v
LIST OF FIGURES	vi
LIST OF ABBREVIATIONS	viii
1. INTRODUCTION	1
1.1 Neurological disorders and GABA-AT	1
1.1.1 Epilepsy	1
1.1.2 Parkinson	2
1.2 GABA-AT	2
1.2.1 GABA-AT Inactivating Mechanism	3
1.2.2 GABA-AT inhibition	6
1.2.3 PLP	6
1.3 GABA-AT approved drugs	7
1.3.1 Vigabatrin	7
1.4 Computer-Aided Drug Design	8
1.4.1 Virtual Screening	9
1.4.1.1 Structure-Based	10
1.4.1.2 ADMET	10
1.4.1.3 Molecular Docking	11
1.4.1.4 Active Site	11
1.5 Molecular dynamics simulation	12
1.6 Homology Modeling	13
1.7 Enzymes	14
1.7.1 Coenzymes	14
1.8 Blood-Brain Barrier	14
2. Materials	16
2.1 Tools and Softwares	16
2.2 Homology Modeling	16

2.3 Homology Modeling Validation.....	17
2.3.1 Align Structures	17
2.3.2 Model Score	17
2.3.3 Ramachandran Plot.....	18
2.3.4 ProSA-web.....	18
2.3.5 Verify3D.....	18
2.3.6 MD Simulation	18
2.3.7 Known Inhibitor	18
2.4 Virtual Screening	24
2.4.1 Database.....	24
2.4.2 ADMET and Lipinski's Rule of Five	24
2.4.3 GOLD	25
2.4.4 VINA	25
2.4.5 AUTODOCK.....	25
2.4.6 MD Simulation Analysis.....	25
3. Results and Discussion	28
3.1 Homology Modeling.....	28
3.1.1 Align Structures	32
3.1.2 Ramachandran Plot.....	33
3.1.3 ProSA-web.....	34
3.1.4 Verify 3D.....	35
3.1.5 MD Simulation	36
3.1.6 Known Inhibitors.....	38
3.1.3.1 Vigabatrin MD Simulation.....	45
2.5 Virtual screening.....	48
3.2.1 Database.....	48
2.5.2 ADMET and Lipinski's Rule of Five	48
3.2.3 Gold	49
3.2.4 Vina	51
3.2.5 AutoDock.....	51
3.2.6 MD Simulation Analysis	52
References:.....	69

DEVELOPMENT OF NOVEL AND POTENT INHIBITORS FOR GABA-AT ENZYME VIA IN SILICO SCREENING METHODS

ABSTRACT

γ -aminobutyric acid aminotransferase (GABA-AT) is a pyridoxal 5'-phosphate (PLP)-dependent enzyme which degrades γ -aminobutyric acid (GABA) in the brain. GABA is an important inhibitory neurotransmitter that plays important neurological roles in the brain. Therefore, GABA-AT is an important drug target which regulates the GABA level. Novel and potent drug development to inhibit GABA-AT is still very challenging task. In this study, we aimed to devise some novel and potent inhibitors against GABA-AT using computer-aided drug design (CADD) tools. However, the human GABA-AT crystal structure is not available yet, and we built the 3D structure of human GABA-AT based on the crystal structure of pig's liver (*Sus Scrofa*) enzyme as a template. The generated model was validated with numerous tools such as ProSA and PROCHECK. A set of selected well-known inhibitors have been tested against the modeled GABA-AT. Molecular docking studies have been accomplished via application of Genetic Optimization for Ligand Docking (GOLD), Vina and Autodock 4.2 software to search for potent inhibitors. The best two candidate inhibitors have been computationally examined for absorption, distribution, metabolism, elimination and toxicity descriptors (ADMET) and Lipinski's rule of 5. Lastly, molecular dynamics (MD) simulations were carried out to inspect the ligands' binding mode and stability of the active site of human GABA-AT over time. The top ranked ligands exhibited reliable stability throughout the MD simulation. The selected compounds are promising candidates and might be tested experimentally for the inhibition of human GABA-AT enzyme.

Keywords: Gaba aminotransferase, homology modeling, virtual screening, ADMET descriptors, Lipinski's rule of five, molecular dynamics simulation, GABA-AT selective inhibitors.

ÖZET

γ -aminobütirik asit aminotransferaz (GABA-AT) piridoksal 5'-fosfat (PLP)-kofaktörlü bir enzimdir ve beyinde γ -aminobütirik asit (GABA) miktarını azaltır. GABA, beyinde önemli nörolojik görevleri olan engelleyici (inhibitory) bir nörotransmitterdir. GABA seviyesini düzenleyen GABA-AT enzimi de önemli bir ilaç hedefidir. GABA-AT'yi inhibe etmek için yeni ve güçlü ilaç geliştirme, hala çok zorlu bir görevdir. Bu tez çalışmasında, bilgisayar destekli ilaç tasarımı (CADD) araçlarını kullanarak GABA-AT'ye karşı bazı yeni ve güçlü inhibitörler tasarlamayı amaçladık. Ancak, insan GABA-AT enziminin kristal yapısı henüz mevcut değil ve bu çalışmada domuz karaciğeri (Sus Scrofa) GABA-AT enziminin mevcut olan kristal yapısı şablon olarak kullanılarak insan GABA-AT'nin üç boyutlu yapısı holoji modelleme yöntemi ile oluşturulmuştur. Oluşturulan model, ProSA ve PROCHECK gibi araçları kullanılarak doğrulanmıştır. Deneysel inhibisyon değeri iyi bilinen bir dizi seçilmiş inhibitörler, GABA-AT'ye karşı test edilerek hesapsal değerler elde edilmiştir. Hesapsal ve deneysel değerler karşılaştırılarak modellenen enzimin doğruluğu sağlanmıştır. Potansiyel inhibitörleri taramak için moleküler yerleştirme (doklama) metotlarından , Genetik Optimizasyon (GOLD), Vina ve Autodock 4.2 yazılımları kullanılmıştır. En iyi iki aday inhibitör, absorpsiyon, dağıtım, metabolizma, eliminasyon ve toksisite tanımlayıcıları (ADMET) ve Lipinski'nin 5 kuralı için hesaplamalı olarak incelenmiştir. Son olarak, ligandların bağlanma modunu ve insan GABA-AT'nin aktif bölgesinin zaman içindeki kararlılığını incelemek için moleküler dinamik (MD) simülasyonları gerçekleştirilmiştir. En iyi ligandlar, MD simülasyonu boyunca güvenilir bir kararlılık göstermişlerdir. Seçilen bileşikler umut verici ilaç adaylardır ve insan GABA-AT enziminin inhibisyonu için deneysel olarak test edilebilecek niteliktedir.

Anahtar Kelimeler: Gaba aminotransferaz, homoloji modelleme, sanal tarama, ADMET tanımlayıcıları, Lipinski'nin beş kuralı, moleküler dinamik simülasyonu, GABA-AT seçici inhibitörleri.

ACKNOWLEDGEMENTS

First and major, praise be to Almighty ALLAH on whom ultimately, we rely for sustenance and guidance. I thank ALLAH for the gift of life and all that he has made feasible for me to perform with it.

My deepest gratitude to my parents, **Abdulkadir Al-OBAIDI** and **Amal Al-QADHI**, for the unconditional support, and incredible love they have offered me throughout my life. I pray to ALLAH to reward the paradise.

I am massively indebted to my wife, **Hind Abdul Kareem** who has always been supportive of my dreams, and who demonstrate a senior deal of supporting, patience and understanding, and of course, to my children, **Sama and Ahmad**.

My sincere appreciation to my supervisor, **Professor Dr. Kemal Yelekçi** for introducing me to this field, giving me all the freedom to pursue my research, and providing enabling environment for me to thrive.

DEDICATION



To my beloved mother and wife,

Amal Al-QADHI

Hind ALSAEED

LIST OF TABLES

Table 2. 1. Known Inhibitors for Human and Rat with 2D structures.	19
Table 3. 1. The Homology Modeling results and scores, GABT_HUMAN.M0012 the highlighted one was the best result.	30
Table 3. 2. Known Inhibitors and the Active site residues interactions.	39
Table 3. 3. Known inhibitors and their experimental Ki and IC50 with docked Ki results with binding affinity and with 2D structures of their interactions.	40
Table 3. 4. Gold CHEMPLP Scoring Function scores for Known Inhibitors.	50
Table 3. 5. Best 30 ligand's binding energy and Ki.	51
Table 3. 6. The best 5-ligand interaction with Active Site before and after MD Simulation.	65
Table 3. 7. System energy for free GABA-AT and VIGABATRIN and the best 5 compounds after MD simulation and Ligand ΔG	66
Table 3. 8. physiochemical features for the top-ranked ligands.	66
Table 3. 9 MM/PBSA energy calculation for the six systems via CaFE tool.	67

LIST OF FIGURES

Figure 1. 1 (a). Conversion from PLP to PMP by the GABA-AT catalyzes (b). Conversion from PMP to PLP also by GABA-AT catalyzes (Silverman, 2018).....	4
Figure 1. 2. GABA enters GABA shunt (Silverman, 2018).	4
Figure1. 3. Relationship and the importance of GABA-AT and how can be an effect on GABA concentration (Silverman, 2018).	5
Figure1. 4. Chemical Interactions between PLP and Active Site of GABA-AT (Silverman, 2018).	7
Figure1. 5. Vigabatrin 2D and 3D structures.	8
Figure1. 6. Various types of CADD (Arodola & Soliman, 2017).	9
Figure 2. 1. The BLAST search result and the best was 1OHV.	17
Figure 2. 2 A workflow explaining all the steps has been followed in this chapter.	27
Figure 3. 1. 95.9% Similarity and 98.3% Identity and 100% Active Site similarity between Human FASTA and 1OHV FASTA ■ α helix ➔ β sheet ■ loops.....	29
Figure 3. 2. The modeled Protein with PLP.....	31
Figure 3. 3. PLP interaction residue before Homology Modeling.....	31
Figure 3. 4. PLP after Homology Modeling.	32
Figure 3. 5. Aligned 1OHV with PLP (yellow highlighted) and modeled protein with PLP.....	33
Figure 3. 6. Ramachandran plot showing the energetically allowed regions of the modeled protein.	34
Figure 3. 7. Modeled GABA-AT result from ProSA-web, ● indicates the GABA-AT location between the X-ray regions.	35
Figure 3. 8. Verify 3D shows 89.59% of the residues have averaged 3D score ≥ 0.2 . 35	35
Figure 3. 9. Modeled GABA-AT free RMSD for 50 Nanoseconds.	36
Figure 3. 10 A. Modeled GABA-AT RMSF, B. Modeled GABA-AT Rg.....	37
Figure 3. 11. Modeled GABA-AT after MD simulation showing charge surface with PLP interaction.....	37
Figure 3. 12. PLP interaction after MD Simulation.	38
Figure 3. 13. The modeled complex (GABA-AT with Vigabatrin) RMSD.	46
Figure 3. 14 A. GABA-AT with VIGABATRIN RMSF, B. GABA-AT with VIGABATRIN Rg.	46

Figure 3. 15. Docked Vigabatrin interaction with the Active Site and PLP.	47
Figure 3. 16. Simulated Vigabatrin interaction with the Active Site and PLP.	47
Figure 3. 17. Docked and Simulated Vigabatrin 2D interactions with the Active Site and PLP.	48
Figure 3. 18. ADMET Descriptors for Zinc, Otava and ChEMBL databases.	49
Figure 3. 19. GABA-AT and ZINC000635903250 complex's RMSD.	54
Figure 3. 20 A. GABA-AT and ZINC000635903250 complex's RMSF, B. GABA-AT and ZINC000635903250 complex's Rg.	54
Figure 3. 21. Docked 3D and simulated 3D for ZINC000635903250.	55
Figure 3. 22. Docked 2D and simulated 2D for ZINC000635903250.	55
Figure 3. 23. GABA-AT and ZINC000364721779 complex's RMSD.	56
Figure 3. 24 A. GABA-AT and ZINC000364721779 complex's RMSF, B. GABA-AT and ZINC000364721779 complex's Rg.	56
Figure 3. 25. Docked 3D and simulated 3D for ZINC000364721779.	57
Figure 3. 26. Docked 2D and simulated 2D for ZINC000364721779.	57
Figure 3. 27. GABA-AT and P6240926 complex's RMSD.	58
Figure 3. 28 A. GABA-AT and P6240926 RMSF, B. GABA-AT and P6240926 Rg. ...	58
Figure 3. 29. Docked 3D and simulated 3D for P6240926.	59
Figure 3. 30. Docked 2D and simulated 2D for P6240926.	59
Figure 3. 31. GABA-AT and ChEMBL1235738 complex's RMSD.	60
Figure 3. 32 A. GABA-AT and ChEMBL1235738 RMSF, B. GABA-AT and ChEMBL1235738 Rg.	60
Figure 3. 33. Docked 3D and simulated 3D for ChEMBL1235738.	61
Figure 3. 34. Docked 2D and simulated 2D for ChEMBL1235738.	61
Figure 3. 35. GABA-AT and ChEMBL1740350 complex's RMSD.	62
Figure 3. 36 A. GABA-AT and ChEMBL1740350 RMSF, B. GABA-AT and ChEMBL1740350 Rg.	62
Figure 3. 37. Docked 3D and simulated 3D for ChEMBL1740350.	63
Figure 3. 38. Docked 2D and simulated 2D for ChEMBL1740350.	63
Figure 3. 39. Comparison of all systems' RMSD.	64
Figure 3. 40 A. Comparison of all systems' RMSF B. Comparison of all systems' Rg.	64

LIST OF ABBREVIATIONS

ADMET: Absorption, Distribution, Metabolism, Elimination and Toxicity

BLAST: Basic Local Alignment Search Tool

BBB: Blood-Brain Barrier

CHARMM: Chemistry at Harvard Macromolecular Mechanics

CNS: Central Nervous System

CADD: Computer-Aided Drug Design

DS: Discovery Studio

FDA: Food and Drug Administration

GA: Genetic Algorithm

GABA: Gamma-Aminobutyric Acid

GABA-AT: Gaba Aminotransferase

IC₅₀: the half-maximal inhibitory concentration

K_i: Inhibitor constant

MM/PBSA: Molecular Mechanics Poisson-Boltzmann Surface Area

MD: Molecular Dynamics

NAMD: Nanoscale Molecular Dynamics

PDB: Protein Data Bank

R_g: Radius of gyration

RMSD: Root-Mean-Squared Deviation

RMSF: Root-Mean-Squared Fluctuations

1. INTRODUCTION

1.1 Neurological Disorders and GABA-AT

In order to understand the involvement of gamma-aminobutyric acid (GABA) in neurological disorders, we should understand the mechanism between normal brain and GABA. In the normal brain, the glia and neurons are regulating GABA. Poor regularity of GABA will lead to a huge effect on the brain functions and it will be the major factor for the neurological disorders (Kim & Yoon, 2017). The disturbing of GABA occurs in the brain either of mutation or systemic issues and ecological impacts (Al-Obaidi, Elmezayen, & Yelekçi, 2020). There are different types of electrochemical signaling and all of them carried out with neurotransmitters, when these neurotransmitters disturbed, the function of the brain will also be affected (Yizhar et al., 2011). As growing old the possibility of occurring the neurological disorders will increase resulting in Alzheimer disease and Parkinson disease and Epilepsy (Masten, Faden, Zucker, & Spear, 2009). Also, the newborn could have these disorders but with lower probability. Even for other stages of life, these diseases could be occurring but the major cause will be growing old (Visser, Danielson, Bitsko, Perou, & Blumberg, 2013). These disorders classified lately in 2016 by the National Institute of Mental Health (NIMH) as early, mature and late stages (Christensen et al., 2018).

1.1.1 Epilepsy

The distribution of epilepsy is around 10 for every 1000 human and the coverage is different between diverse races and different countries. Based on multiple studies and statistics epilepsy is more common in men more than women (Solomon & McHale, 2012). There are two types of the most prevalent epilepsy: generalized seizures and focal seizures. Generalized seizures appear in hemispheres, on the other hand, focal seizures

appear in a precise and specific place of the brain, these types depended on the duration and the age of the patient (Pearl, 2018). Epilepsy is more related to GABA^A receptor, GABA Aminotransferase (GABA-AT) and GABA concentration in the brain (Kaila, Ruusuvuori, Seja, Voipio, & Puskarjov, 2014).

1.1.2 Parkinson

The prevalence of Parkinson disease is around 4.5–19 per 100,000 humans (de Lau & Breteler, 2006). Parkinson is distinguished and recognized by shaking and trembling. The injury and occurrence for this disease are not related to a specific sex or race or even for a region on the globe. Until now it is still hard to determinate Parkinson's disease before the injury. There are several techniques for confirming the injury of Parkinson's disease such as Positron discharge tomography Single-photon emanation automated tomography and a specific post-mortem change in the expression of GABA^A Receptor subunit genes in the substantia nigra and caudate nucleus for the patients (Luchetti, Huitinga, & Swaab, 2011)

1.2 GABA-AT

GABA-AT is known as a pyridoxal 5-phosphate (PLP) dependent enzyme responsible for the depletion of the inhibitory neurotransmitter GABA and catalyzes the degradation of the inhibitory neurotransmitter GABA to succinic semialdehyde (Silverman, 2018). GABA-AT is an important target for central nervous system (CNS) disorders drugs, because the highly selective inhibition of GABA increases concentrations of it in the brain (Storici et al., 2004). GABA-AT is a catabolic enzyme regulates the concentration of GABA (Cellini, Montioli, Oppici, & Voltattorni, 2012). Reduction in GABA concentration in the CNS has been related to some common neurological diseases such as Epilepsy, Alzheimer disease, Parkinson disease and Huntington disease as well as Tardive Dyskinesia Diseases (McConkey, Sobolev, & Edelman, 2002; Pearl, 2018; Seyfried & Yu, 1980). Increasing the concentration of GABA in the CNS has an anticonvulsant effect in the brain (Clift & Silverman, 2008). GABA especially plays a critical role in the CNS, brain activity and as expected is the most broadly conveyed inhibitory transmitter in the CNS (Tunnicliff, 1989). Normal function in the CNS is to

stabilize the inhibitory neuronal system. GABA is the main inhibitory neurotransmitter in the CNS of mammalian and L-glutamate is the considerable excitatory neurotransmitter (Krnjevic, 1974). GABA-AT was observed in different organs such as; brain, liver, kidney, and pancreas and it shows a higher specific activity in glial cells and presynaptic neurons (Jeremiah and Povey, 1981).

1.2.1 GABA-AT inactivating mechanism

Through intermediates 2-4 the bounded LYS 329 to PLP cofactor will be transformed to pyridoxamine 5'-phosphate (PMP), as a result PLP is transformed to PMP (Figure 1.1, 1.2), the GABA-AT will not be catalyst because the GABA-AT has been changed. For retransformation the PMP to PLP another catalyst should be happening. When the GABA-AT use α -ketoglutarate as a substrate, the retransform will be achieved and this procedure will lead to consequence the α -ketoglutarate is transformed into the excitant neurotransmitter L-glutamate. As a result, one molecule of GABA is transformed into an excitatory neurotransmitter (L-Glu) in this procedure. For that, the GABA-AT enzyme is crucial for the brain system levels with the neurotransmitters (Madsen, Larsson, & Schousboe, 2008).

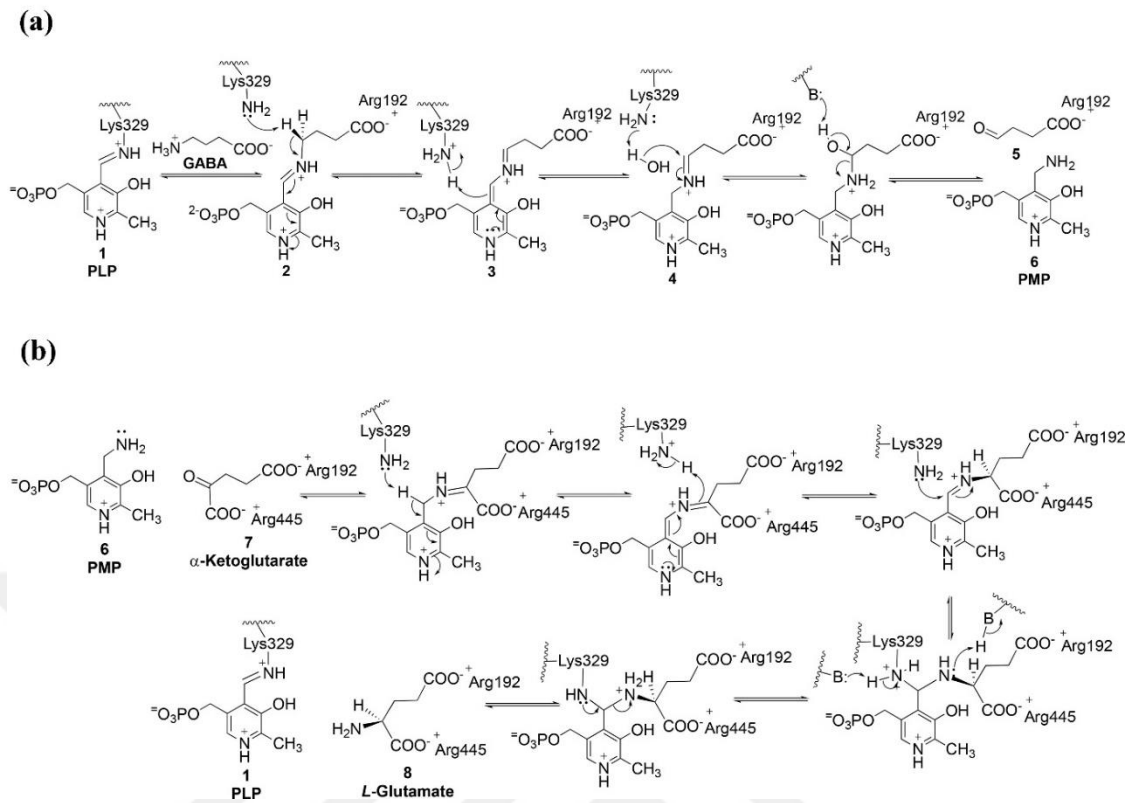


Figure 1. 1 (a). Conversion from PLP to PMP by the GABA-AT catalyzes (b). Conversion from PMP to PLP also by GABA-AT catalyzes (Silverman, 2018).

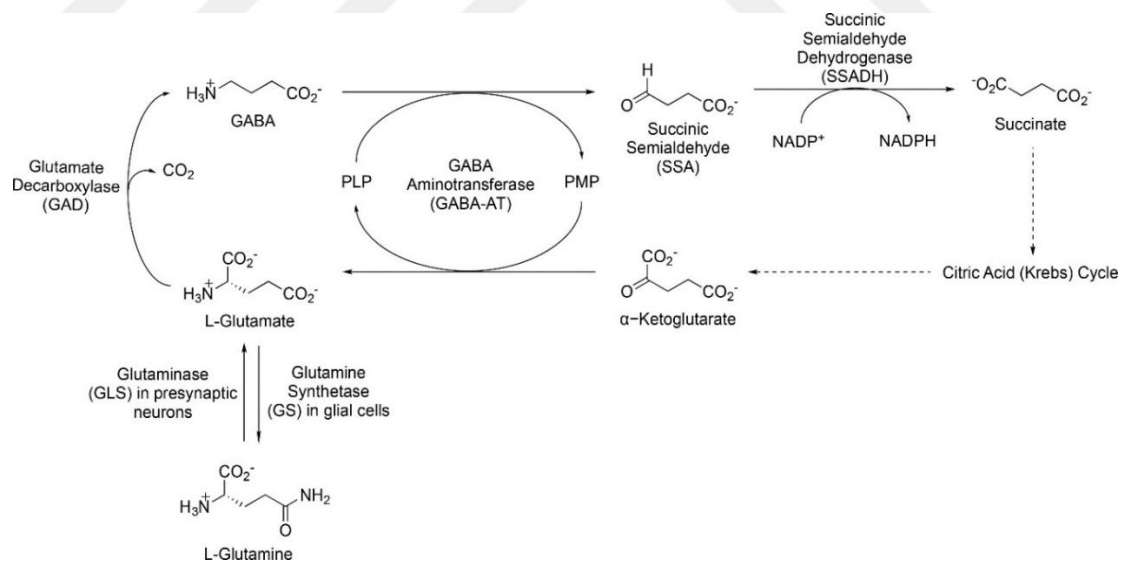


Figure 1. 2. GABA enters GABA shunt (Silverman, 2018).

From L-glutamate in presynaptic (GABAergic) nerve cells, GABA is created; depolarization of presynaptic nerve cells catalyzes GABA release and transport into the synaptic cleft by GABA transporters (GAT-1, GAT-2, GAT-3, and betaine-GABA

transporter) for neurotransmission (Krnjevic, 1974). GABA will bind to either GABA^A or GABA^B receptors when emitted into the synapse. If GABA bound to GABA^A receptor, this will lead to open the central chloride ion channel and this will lead to decrease the cell excitability and neuronal inhibition. If GABA bound to GABA^B receptor, this will lead to open linked potassium channels, hyperpolarization and like GABA^A receptor with neuronal inhibition (Silverman, 2018). GABA can be terminated by two ways; re-enter into presynaptic nerve cells or in glial cells by GABA transporters, GABA-AT in the glial cells will start to catabolize GABA either to PLP or PMP (Figure 1.3) (Bowery et al., 2002).

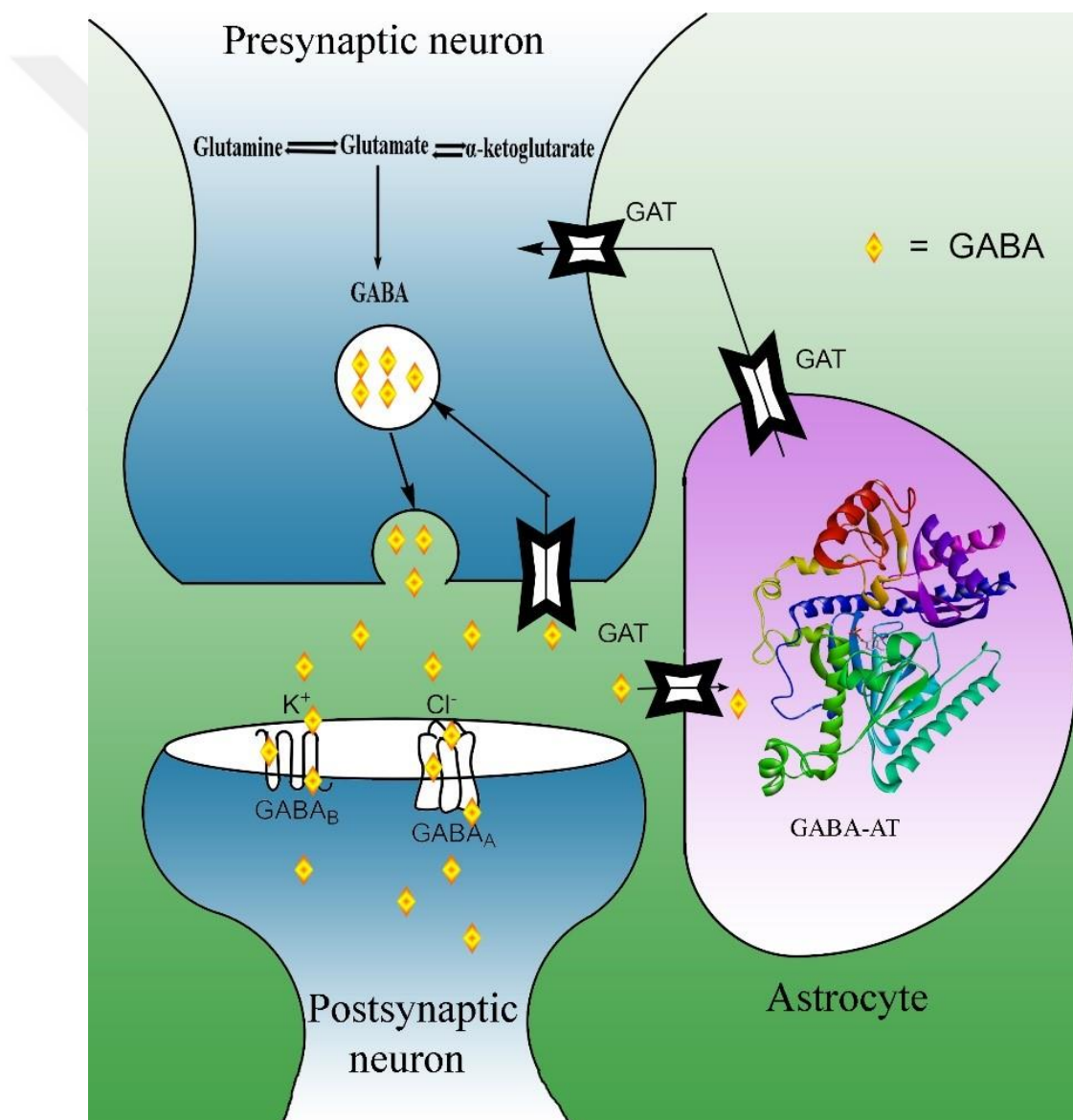


Figure1. 3. Relationship and the importance of GABA-AT and how can be an effect on GABA concentration (Silverman, 2018).

During these chemical reactions GABA in glial cells will be converted to L-glutamate and this will take more control in levels of central nervous neurotransmitters. GABA in glial and presynaptic neurons showing a very high specific activity, and can be a shift by Bi-Bi Ping Pong mechanism (Silverman, 2018).

1.2.2 GABA-AT inhibition

For the neurological disorders, the inhibition of GABA-AT is so important for the treatment or reduce symptoms of the neurological disorders because it will stop L-glutamate transformation from neurotransmitter GABA. The inhibition generally can be divided for two types: reversible inhibition which is a substrate bind reversibly to GABA-AT for decrease the function of GABA-AT and irreversible inhibition which a substrate will block GABA-AT with covalent bonds and will decrease the activity of GABA-AT (Rokita, 2000). In spite of the development in drug discovery, the GABA-AT inhibitory need to be investigated more intensely to find more and better inhibitors with less side effects in *silico*, *vitro* and *vivo* because of 20 to 40 % of patient with neurological disorders disease suffering from less activity of drugs in the market and not adequately treated (Pan, Qiu, & Silverman, 2003).

1.2.3 PLP

PLP refers to pyridoxal phosphate which is a vitamin's B6 derivative. PLP feasibly act for the most multifunction organic cofactor and used by multiple enzymes in all organisms (Percudani & Peracchi, 2003). Approximately all PLP-dependent enzymes (except glycogen phosphorylases) are related to biochemical pathways that include amino compounds, for the most part (Figure 1.4). The reactions completed by the PLP-dependent enzymes that take action on amino acids include the transfer of the amino group, decarboxylation (John, 1995).

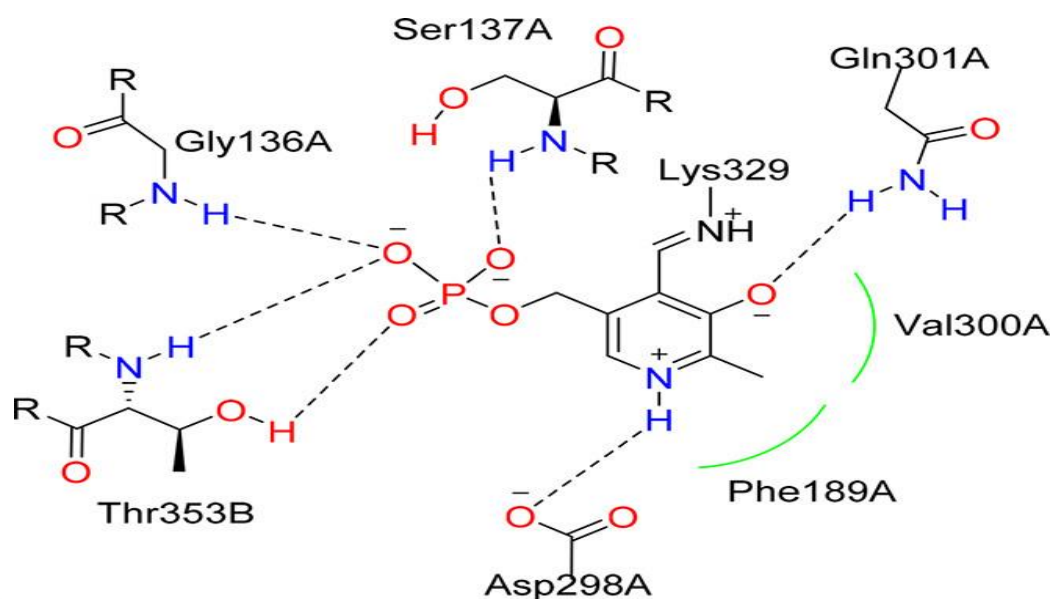


Figure 1. 4. Chemical Interactions between PLP and Active Site of GABA-AT (Silverman, 2018).

1.3 GABA-AT approved drugs

There is a huge number of experimental and *in silico* inhibitors were tested for inhibiting GABA-AT and a fewer number were moved on to become drugs and be available in the market. The most important in this field one drug was approved by the Food and Drug Administration (FDA) Vigabatrin (Boonstra et al., 2015).

1.3.1 Vigabatrin

Vigabatrin can be considered as an irreversible and analog substrate for GABA-AT. Vigabatrin an oral drug available in the market under the trade name “Sabril” since 1994-12-31. Vigabatrin is available with powder for solutions and tablets and the dosage 500 mg and 1 g. The half-life of Vigabatrin for newborns for each 50 mg/kg = 7.5 ± 2.1 hours, children each 50 mg/kg = 5.7 hours, adults each 50 mg/kg = 7.5 hours and for elderly each 50 mg/kg = 12 - 13 hours (Browne, 1998; Clayton et al., 2013; Gram, Larsson, Johnsen, & Schousboe, 1989; Hawker & Silverman, 2012; Lindberger, Luhr, Johannessen, Larsson, & Tomson, 2003; Tulloch, Carr, & Ensom, 2012; Zwanzger et al., 2001). Figure 1.5 shows 2D and 3D structure of Vigabatrin.

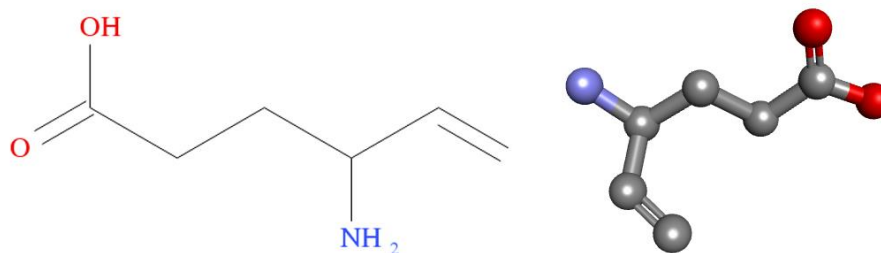


Figure 1. 5. Vigabatrin 2D and 3D structures.

1.4 Computer-Aided Drug Design

Computer-Aided Drug Design (CADD) is a computational approach used for designing drugs. Day after day CADD become so important because of the high cost of experimental techniques for discovering a new drug and it is time consuming. Developing a new drug and start to sell it in the market is very complicated and cost a massive amount of money and time can be reached between 10 and 14 years. So, for those reasons CADD is widely used now and rapidly growing. CADD contains two major pathways to discover a new drug: ligand-based drug design and structure-based drug design (Figure 1.7). CADD can reduce the time in discovering new drug up to 50 %, and can reject the unpromising drugs by studying their efficacy and absorption, distribution, metabolism, elimination and toxicity (ADMET), and can synthesis the protein-substrate interactions, and can test millions of substrates for one target before performed the best of them to the clinical trials. All of the previous features can minimize the failure rate at the experimental phases (Surabhi & Singh, 2018).

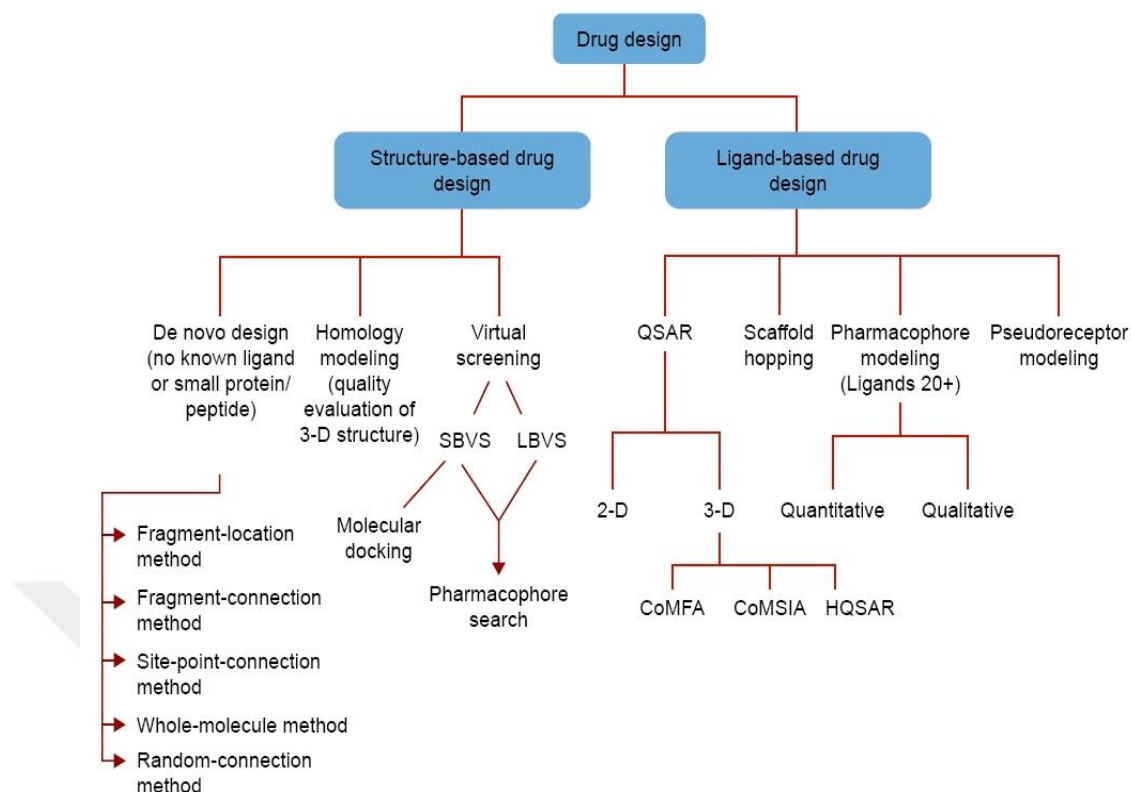


Figure1. 6. Various types of CADD (Arodola & Soliman, 2017).

1.4.1 Virtual Screening

Virtual screening is computational tactics to permeate all features of drug discovery (Jorgensen, 2004). Virtual screening is quick and logical drug discovery approach and has the feature of low cost and effective screening than the classic experimental high-throughput screening (Moitessier, Englebienne, Lee, Lawandi, & Corbeil, 2008). Virtual screening is split into two types: ligand-based and structure-based. The concept of ligand-based is to have an active known group of ligand molecules and no structural data is known for the target. The ligand-based techniques will be the best way to go through like pharmacophore modeling and quantitative structure-activity relationship (QSAR) (Kuntz, Blaney, Oatley, Langridge, & Ferrin, 1982). On the other hand, the concept of the structure-based drug design concept is having a 3D structure of target so, the molecular docking is the best way to have very good results for the targets and this technique is widely used and common since the early 1980s (Coupez & Lewis, 2006).

1.4.1.1 Structure-Based

The huge development in technology for the past years especially computational methods for drug design, drug discovery and genomics treatments and the increasing number for protein structures led to rapidly growing of structure-based technique and become widely used for virtual screening and giving more chances for lead discovery with shortening of time and decreasing the cost. (Jhoti, Rees, & Solari, 2013). In the 80s the first try was performed for structure-based design and the time wasted for obtaining a good result at that time. Until 90s was the first success realized for this approach with some publications. With the progress of computer technology and the advancement of algorithms, from that time till now, structure-based drug design techniques are growing very fast and used for virtual screening (Agrawal, 2013). For discovering a new drug with experimental trials, it will cost a huge amount of money such as approximately \$2.6 billion dollars from beginning until marketing and the cost are increasing even more because of the competition and will spend a lot of time for designing the drug even before test the drug with experimental here it comes the needing for the computational field for discover and design drugs, and structure base is one important technique for this approach (Wang, Song, Li, & Chen, 2018). Structure-based depends on four steps: protein prepare, recognizing the binding pocket, ligands preparation and docking with analyze the poses. These steps will change between the different programs but the concept is one (Gulerez & Gehring, 2014).

1.4.1.2 ADMET

ADMET feature can be considered as one of the virtual screening methods to predict pharmacokinetic quality of the substrates. ADMET tool can be considered a sub tool with a variety programs such as Biovia discovery studio (DS), OECD QSAR Toolbox 4.1, Toxtree, and the pkCSM approach or can be used by online servers such as SWISSADME (<http://www.swissadme.ch/>) (Biasini et al., 2014). ADMET considered as a leading feature in the virtual screening field because with this feature can determine whether the substrate will pass the clinical experiment or not and because of the high cost for discovering the drugs with clinical trials, this tool is so important in this field. This feature

can be used also for minimizing the virtual screening number of substrates at any stage of predicting the best substrate for the targets (Han et al., 2019).

1.4.1.3 Molecular Docking

Molecular docking is one type of bioinformatics modeling and it shows the interaction of the molecules and the target (Guedes, de Magalhães, & Dardenne, 2014). By counting on the binding features of molecules and target, it foretells the three-dimensional structure of the complexes (Seeliger & De Groot, 2010). Molecular docking leads to numerous conceivable adduct structures that are positioned and merged together utilizing scoring function almost in all software's (Shoichet, McGovern, Wei, & Irwin, 2002). Molecular docking calculates the conformation of docked molecules based on the total energy of the complex (Dar & Mir, 2017). The molecular docking technique used to show and demonstrate the interaction between ligand molecules and macromolecule (target protein) at an atomic level. Atomic level represents the behavior of ligand molecules in the active site of the proteins as well as to make clear the basics of biochemical processes (McConkey et al., 2002). The docking method contains two steps: prediction of the ligand confirmation, and it's coordinate with orientation within these sites with the evaluation of the binding affinity (Meng, Zhang, Mezei, & Cui, 2011). There are several programs using different algorithms such as Autodock, Dock, Gold, Vina, Zdock, and Glide which they are widely used for molecular docking and some of them used for rigid docking for both of ligand and protein and some for flexible ligand and rigid protein and some for protein-peptide docking. Despite different programs used for molecular docking approach but still sharing the same headline features such as lead optimization, hit identification and protein-ligand interaction. Also, there are several challenges in the molecular docking field such as ligand chemistry, protein flexibility and scoring function (Dar & Mir, 2017).

1.4.1.4 Active Site

Enzymes in fact are proteins catalyst which increase the speed of chemical reactions by decreasing their activation energy or increasing the ground state energy. This can be done

by enzymes making proper interactions with substrates. Enzymes usually can catalyze these substrates (which some of them naturally produced or chemically produced) to increase their reaction speed or to drive the whole chemical reaction to another way which could be happened without these substrates. Enzymes build-up by amino acids just like the proteins and that means they can make a variety active sites and their properties will be different depending on the amino acids kind which they are responsible for this active site (Ringe & Petsko, 2008). Active sites can be divided to several types: size and shape type which can be specifically for surrounding the substrate and polarity un-polarity type which the active site determined by its polarity and can reject the other type to make a better fit and charge type which depend on the active site charge if it's negative that mean it will be favorable for positive charge substrate and conversely to make a suitable fit, hydrophobicity or hydrophilicity type which is all of active site amino acids if were hydrophobic they will attract the hydrophobic molecule and conversely to make the best fit and special feature of cofactors. Vitamins and minerals are substantial because they help enzymes bind to substrates to make a better fit (Wiley, 2001). There are two theories about active sites: lock and key theory which mean that the enzyme and substrate can be shaped perfectly to be formed as one complex having different features with different levels of energy and the induced fit model theory which states that the pocket site and the ligand are not important to fit one another in their resting states and the ligand draws close to the enzyme and both of them change the shape as a result of interacting with each other and after the reaction has finished and new results are formed, the product and enzyme are no longer compatible and they separate (Kool, 2002).

1.5 Molecular Dynamics Simulation

X-ray crystallography has been developed and improving the techniques over decades to explain and describe the molecular structures of macromolecules. Molecular Dynamics (MD) simulation has turned into another significant procedure in the development of novel bioactive molecules by looking at the steadiness of molecular targets and ligand binding pose in time scale (Aqvist, Luzhkov, & Brandsdal, 2002). MD is a computational technique that uses structural data taken from experimentally to calculate the possible configuration of molecular systems. In traditional MD simulations, the potential energy

function frequently contributes as the “force field” characterize the interactions between atoms formed of bonded terms between covalently bound atoms (bonds, angles, torsions) and non-bond terms (Van der Waals interactions and electrostatic interactions). Classic molecular force fields like AMBER (Bayly et al., 1995), OPLS (Jorgensen & Tirado-Rives, 1988), Chemistry at Harvard Macromolecular Mechanics (CHARMM) (MacKerell et al., 1998) and GROMOS (Oostenbrink, Villa, Mark, & van Gunsteren, 2004) these force fields they show the interactions and the predicted motion for the systems (Aqvist et al., 2002). With the rapid evolution of technology in the field of MD, the computational power has been increased and MD simulations affected with this development and can be extended to microsecond with considering the decreasing in the timescale to enable significant competition to be observed (Maragakis et al., 2008).

1.6 Homology Modeling

When the crystal structure for a target protein is not available, homology modeling is the alternative way to build a model at atomic level depending on the sequence of the target protein and the similarity between the sequence and the most identity and similarity with any crystal structure taken from experimental by considering the highest identity and similarity between them. After aligning the sequences between homologous and the protein and the alignment result was below 20% of sequence identity, it will be definitely a very different structure and its unreliable to do the computational work on this predicted model (Chothia & Lesk, 1986). The sequence and the template which has been alignment between them will proceed to reproduce a new model based on the similarity between their sequences alignment and the crystal structure because the protein structure is devilishly conserved than sequence (Centeno, Planas-Iglesias, & Oliva, 2005). Generally, the homology modeling quality is located on the accuracy between the alignment of template structures and the sequences, in other words, the higher similarity and identity will produce a higher quality of the target with conceding the gaps between the template sequence and the target sequence and also the loops regions show more errors than the gaps because the template sequences and target sequences completely different than each other and sometimes even from different species ether (Park, Teichmann, Hubbard, & Chothia, 1997). With the exception of having a mutation because the mutation it can

cause another fold than the predicted and that will lead to another story of predictions, however, in the reality the protein, it should be folded in a proper way because it's under the constraint and the protein must carry out its function in the cell (Dalal, Balasubramanian, & Regan, 1997). Almost all the tools and software that are used for homology modeling are using four steps for the procedure: selecting the template, alignment between the template and target sequence, model building and evaluation of the predicted model (Martí-Renom et al., 2000).

1.7 Enzymes

Enzymes are macromolecules can speed up the chemical reactions in the organs. In all metabolic procedure's enzymes are needed to catalyze and speed up the reactions, thousands of chemical reactions can be catalyzed by enzymes by decreasing the activating energy of the enzymes. Enzymes are specific to their catalyzing. Enzymes activity can be affected by small molecules such as inhibitors which can lower the activity of enzyme and activators which can lift up the activity of enzymes (Silverman & Holladay, 2015).

1.7.1 Coenzymes

Coenzymes also called cofactor and for some enzymes cannot be catalyzed without coenzymes inside the active site for the enzyme. Some cofactors can be not organic such as: Zn and Fe and some can be produced organically in the body and this type specifically called coenzymes. Those coenzymes can be derived from vitamins such as PLP. Coenzymes can be considered transition carriers. Coenzymes are mainly related with the enzyme functions and also involved with the substrate metabolism by interacting with the required residues to provide to the enzyme with energy to activate the substrate during the enzyme-catalyze reaction (Silverman & Holladay, 2015).

1.8 Blood-Brain Barrier

The Blood-Brain Barrier (BBB) is an extremely selective membrane controlling the bypassing from blood to the CNS (Graff & Pollack, 2004). In 1908 Paul Ehrlich has been

awarded a Nobel prize for illuminated the existence of the BBB (Joó, 1993) with a 20 m² of the surface of BBB cells as a moderator between the blood and CNS. For drugs which related to the nervous system, the permeability should be high to navigate through the BBB to gain a better effect of the treatment. The substrate lipophilicity, hydrogen-bond desolvation potential, molecular weight, pKa/charge, and molecular size, all these factors can impact the permeability features with the BBB. The better factors for crossing the substrate the BBB, in general, is uncharged, lipophilic and low molecular weights (de Boer, van der Sandt, & Gaillard, 2003).



2. MATERIALS AND METHODS

2.1 Tools and Software Programs

In this study we used study several programs and tools for drug design and molecular docking such as biovia DS (BIOVIA, 2017), AutoDock tools and Autodock 4.2 (Morris et al., 2009), Autodock Vina (Trott & Olson, 2010) and GOLD (Jones, Willett, Glen, Leach, & Taylor, 1997).

2.2 Homology Modeling

There is no crystal structure resolved yet for human GABA-AT, we used homology modeling approach for predicting a model for human GABA-AT depending on the similarity between the GABA-AT sequence for human and the best template from another organism. The fasta sequence was retrieved from uniprot (Bateman, 2019). By using Basic Local Alignment Search Tool (BLAST) (Altschul, Gish, Miller, Myers, & Lipman, 1990) from biovia DS. The results showed that the higher similarity was from pig liver (*Sus Scrofa*) and Protein Data Bank (PDB) name 1OHV (Storici et al., 2004) chain A. 95% identity, 461 sequence, 938.717 Bit score, 0 E-value and 2.3 Å resolution (Figure 2.1).

	Title/Description	Accession	Identity %	Sequence Length	Alignment Length	Bit Score	E-value	Positive	Resolution	SCOP	Organism
1	4-AMINO BUTYRATE AMINOTRANSFERASE...	1OHV_A	95	461	461	938.717	0	98	2.3	c.67.1.4	Sus scrofa
✓	Uncharacterized protein [NCBI_tax_id=340	3HIU_D	46	152	30	28.8758	2.71853	63	1.85		Xanthomonas campestris pv. c.
<	putative phosphatase [NCBI_tax_id=83333	2B0C_A	40	199	25	29.6462	2.41383	72	2	c.108.1.2	Escherichia coli K-12
✓	Dishevelled-2 [NCBI_tax_id=9606	3CBZ_A	38	104	39	26.9498	8.42737	48	1.38	b.36.1.1	Homo sapiens
✓	Engineered Protein [NCBI_tax_id=671065	4HB5_B	37	162	43	28.8758	3.15886	58	2.294	d.211.1.0	Metallosphaera yellowstonensi.
✓	SERINE PALMITOYLTRANSFERASE [NCBI...	2IWT_A	34	398	98	31.5722	0.794387	50	1.25		Sphingomonas paucimobilis
✓	BETA-TRANSAMINASE [NCBI_tax_id=39...	2YKY_C	31	431	97	33.113	0.244404	43	1.69		Mesorhizobium sp. LUK
✓	D-phenylglycine aminotransferase [NCBI...	2CY8_A	31	402	61	41.5874	0.000519844	55	2.3		Pseudomonas stutzeri
✓	Sensory/regulatory protein rpfC [NCBI...	3M6M_D	29	118	65	30.0314	0.806932	50	2.5		Xanthomonas campestris pv. c.
✓	L-LYSINE-EPSILON AMINOTRANSFERASE...	2CJG_A	29	435	448	166.392	1.47288e-45	45	1.95		Mycobacterium tuberculosis
✓	Glutamate-1-semialdehyde 2,1-aminomut...	3BS8_A	28	430	122	45.4394	3.61767e-05	43	2.3	c.67.1.4	Bacillus subtilis
✓	419aa long hypothetical aminotransferase...	2E05_A	28	412	435	129.028	7.19574e-33	46	1.9		Sulfolobus tokodaii str. 7
✓	ornithine aminotransferase [NCBI_tax_id...	1Z7D_E	28	374	231	85.5001	3.90328e-18	45	2.1	c.67.1.4	Plasmodium yoelii yoelii
✓	Ornithine aminotransferase [NCBI_tax_id...	3LGD_B	28	385	201	84.3445	9.4678e-18	45	2.3	c.67.1.4	Plasmodium falciparum CDC/...
✓	CovR [NCBI_tax_id=1314	3RJP_A	28	96	59	30.0314	0.576667	50	1.5	a.4.6.0	Streptococcus pyogenes
✓	Aminotransferase, class III [NCBI_tax_id...	3I4J_D	27	379	218	67.781	2.47973e-12	41	1.7		Deinococcus radiodurans
✓	4-aminobutyrate transaminase [NCBI_tax...	3OKS_C	26	447	468	113.235	3.09458e-27	41	1.8	c.67.1.0	Mycobacterium smegmatis str...
✓	2,2-dialkylglycine decarboxylase [NCBI...	1ZOD_A	26	431	388	105.145	1.4821e-24	41	1.8	c.67.1.4	Burkholderia cepacia
✓	4-aminobutyrate aminotransferase GabT...	3R4T_A	26	444	472	110.923	1.60573e-26	42	2.5	c.67.1.0	Mycobacterium marinum M
✓	Glutamate-1-semialdehyde 2,1-aminomut...	3K28_A	26	423	122	36.5798	0.0204656	40	1.95	c.67.1.4	Bacillus anthracis str. Ames A...
✓	4-aminobutyrate aminotransferase (GabT...	4FFC_D	26	443	465	105.145	1.84261e-24	41	1.8	c.67.1.0	Mycobacterium abscessus AT...
✓	4-AMINO BUTYRATE TRANSAMINASE [N...	4ATQ_E	25	442	451	98.9821	2.2335e-22	42	2.75	c.67.1.0	Aerobacter aureescens TC1
✓	Pyruvate transaminase [NCBI_tax_id=676	4E3R_C	25	451	290	70.8626	3.09393e-13	41	1.9	c.67.1.0	Vibrio fluvialis
✓	4-aminobutyrate transaminase [NCBI_tax...	3O8N_A	25	438	471	109.768	4.63675e-26	41	2.05	c.67.1.0	Mycobacterium smegmatis str...
✓	Acetylornithine aminotransferase [NCBI...	2EH6_B	25	375	423	111.694	4.63759e-27	42	1.9	c.67.1.0	Aquifex aeolicus VF5
✓	4-aminobutyrate aminotransferase [NCBI...	1SFF_C	25	425	432	113.62	1.93353e-27	41	1.9	c.67.1.4	Escherichia coli

Figure 2. 1. The BLAST search result and the best was 1OHV.

The template protein (1OHV) was retrieved from protein data bank (Berman et al., 2000) and aligned with the Fasta sequence for human GABA-AT from uniProt by using “align sequences” plugin tool in Biovia DS, the model was built by using modeler (Webb & Sali, 2016) from biovia DS.

2.3 Homology Modeling Validation

2.3.1 Align Structures

The homology modeled protein was performed for aligning with 1OHV protein by using “align structures” from biovia DS and the C-alpha distance cutoff was set to 2.5 and length cutoff set to 50 and bin size set to 20.

2.3.2 Model Score

The homology modeling results produced 20 models and the best was chosen depending on the dope score and normalized dope score from Biovia DS.

2.3.3 Ramachandran Plot

The modeled protein was validated by using the Ramachandran plot from a web-based PROCHECK online server (<https://servicesn.mbi.ucla.edu/PROCHECK/>) (Laskowski, MacArthur, Moss, & Thornton, 1993).

2.3.4 ProSA-web

The modeled protein was also validated by using ProSA-web (web-based online server) (<https://prosa.services.came.sbg.ac.at/prosa.php>) (Wiederstein & Sippl, 2007).

2.3.5 Verify 3D

The modeled protein was further verified with Verify 3D from (Molecular Biology Institute and the DOE-MBI Institute at the University of California, Los Angeles) online server (<https://servicesn.mbi.ucla.edu/>) (Bowie, Lüthy, & Eisenberg, 1991).

2.3.6 MD Simulation

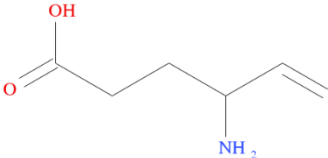
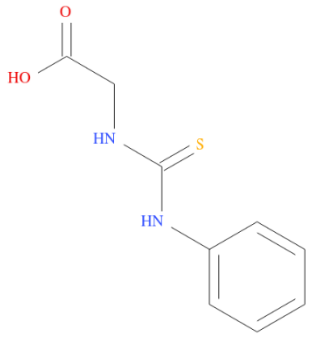
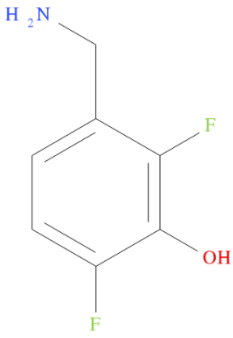
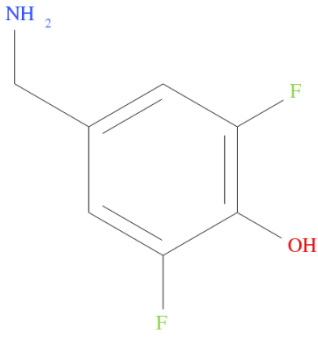
The modeled protein was performed for MD simulation to examine the stability of the free protein and we used charm GUI server a web-based graphical user interface for CHARMM (Jo, Kim, Iyer, & Im, 2008) for preparing the modeled protein for MD simulation. By using Nanoscale Molecular Dynamics (NAMD) software (Phillips et al., 2005) the modeled protein's energy was minimized to 10000 and equilibrated for 5 nanoseconds and simulated for 50 nanoseconds and the last frame were selected for continuing the study.

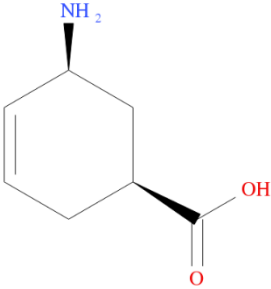
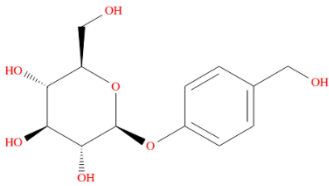
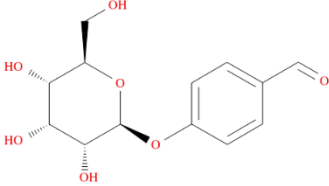
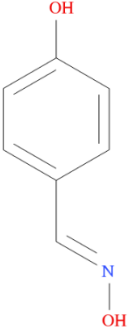
2.3.7 Known Inhibitor

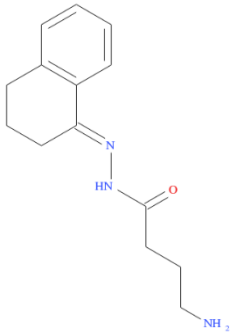
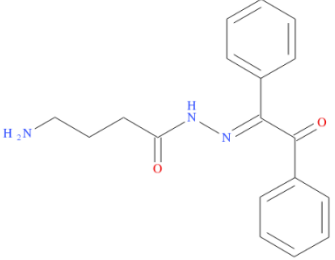
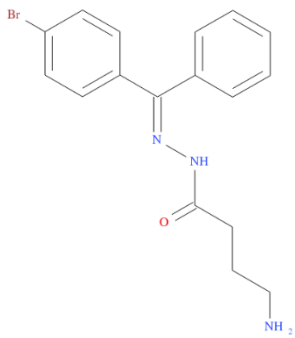
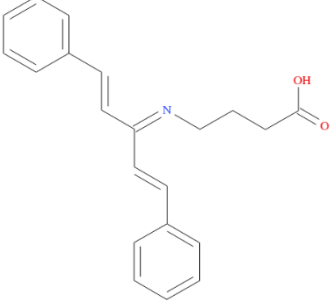
The known inhibitors were taken from ChEMBL database (Gaulton et al., 2012). All known inhibitors were experimentally tested for either human or rat (*Rattus norvegicus*). We retest these inhibitors computationally and compare the experimentally inhibitor constant

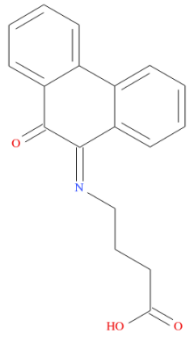
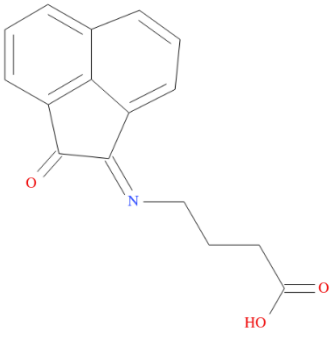
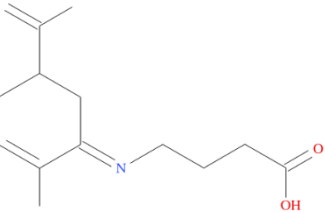
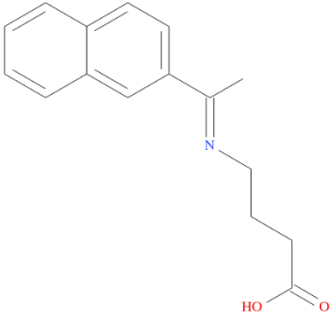
(Ki) and the half-maximal inhibitory concentration (IC50) with the docked results (Table 2.1).

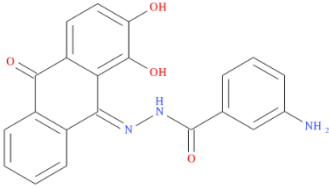
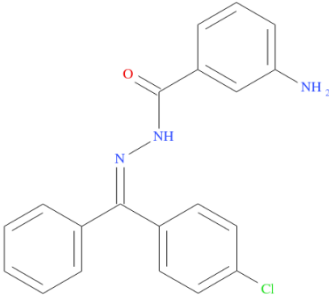
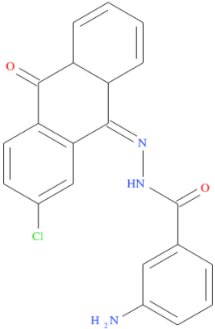
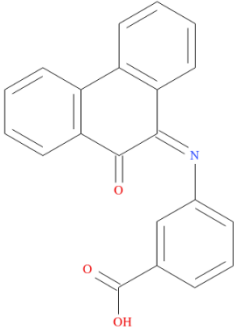
Table 2.1 Known Inhibitors for Human and Rat with 2D structures.

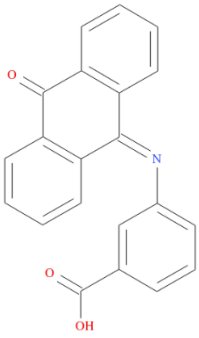
Inhibitor name	Organism	2D Structure	Literature
VIGABATRIN	human		(Choi & Silverman, 2002a)
Aryl aminopyridine derivative of GABA	human		(Wermuth et al., 1987)
“208” derivative difluorophenol	human		(Meanwell, 2011)
“209” derivative of difluorophenol	human		(Meanwell, 2011)

Cyclohexene analogue	human	<p style="text-align: right;">Chiral</p> 	(Choi & Silverman, 2002b)
GASTRODIN	human	<p style="text-align: right;">Chiral</p> 	(Tao, Yuan, Tang, Xu, & Yang, 2006)
HELICIDE	human		(Tao et al., 2006)
4-Hydroxybenzaldehyde	human		(Tao et al., 2006)

Tetrahydronaphthalen-1-one	Rat	 <p>The structure shows a tetrahydronaphthalene ring system with a hydrazide group (-NH-CO-) attached to the 1-position, and a 4-aminobutyl chain (-CH₂CH₂CH₂CH₂NH₂) attached to the nitrogen of the hydrazide group.</p>	(Bansal, Sinha, & Khosa, 2013)
CHEMBL2283209	Rat	 <p>The structure features a central carbon atom double-bonded to a phenyl ring and single-bonded to a benzoyl group (-CO-Ph). This carbon is also double-bonded to a nitrogen atom, which is part of a hydrazide linkage (-NH-CO-) connected to a 4-aminobutyl chain (-CH₂CH₂CH₂CH₂NH₂).</p>	(Bansal et al., 2013)
CHEMBL2283210	Rat	 <p>The structure shows a central carbon atom double-bonded to a phenyl ring and single-bonded to a 4-bromophenyl ring. This carbon is also double-bonded to a nitrogen atom, which is part of a hydrazide linkage (-NH-CO-) connected to a 4-aminobutyl chain (-CH₂CH₂CH₂CH₂NH₂).</p>	(Bansal et al., 2013)
CHEMBL2283211	Rat	 <p>The structure features a central carbon atom double-bonded to a phenyl ring and single-bonded to a propenoic acid chain (-CH=CH-COOH). This carbon is also double-bonded to a nitrogen atom, which is part of a hydrazide linkage (-NH-CO-) connected to a 4-aminobutyl chain (-CH₂CH₂CH₂CH₂NH₂).</p>	(Bansal et al., 2013)

CHEMBL2283213	Rat		(Bansal et al., 2013)
CHEMBL2283214	Rat		(Bansal et al., 2013)
CHEMBL2283217	Rat		(Bansal et al., 2013)
CHEMBL2283220	Rat		(Bansal et al., 2013)

CHEMBL2283221	Rat		(Bansal et al., 2013)
CHEMBL2283223	Rat		(Bansal et al., 2013)
CHEMBL2283224	Rat		(Bansal et al., 2013)
CHEMBL2283226	Rat		(Bansal et al., 2013)

CHEMBL2283227	Rat		(Bansal et al., 2013)
---------------	-----	------------------------------------------------------------------------------------	-----------------------

All the 21 known inhibitors were prepared by using Biovia DS and docked by AutoDock. The docked result for Vigabatrin was chosen for MD simulation. The modeled protein and vigabatrin (complex) were prepared for MD simulation by using charm GUI server and the energy minimization set for 10000 and equilibrated for 5 nanoseconds and simulated for 50 nanoseconds.

2.4 Virtual Screening

2.4.1 Databases

The database was retrieved from Zinc15 database (Sterling & Irwin, 2015), Otava CNS compound library (<http://www.otavachemicals.com/>) and ChEMBL database. We downloaded 5,000,000 ligands from zinc database depending on their LogP and molecular weight and we downloaded 2,372 ligands from Otava database, and we downloaded 1,870,461 ligands from ChEMBL.

2.4.2 ADMET and Lipinski's Rule of Five

All databases were performed for ADMET descriptor and Lipinski's rule of five to filter the molecules depending on the BBB values and Lipinski's rule of five. BBB penetration a quantitative linear regression model for the prediction of BBB penetration, as well as 95% and 99% confidence ellipses in the ADMET_PSA_2D versus ADMET_AlogP98. The range of BBB has been taken from more than eight hundred molecules that are well-

known CNS-permeable charismatics (Egan & Lauri, 2002). The pioneering research by Lipinski led to the well-known "Rule of five" for selecting drug-like molecules (Lipinski, Lombardo, Dominy, & Feeney, 1997). Human Intestinal Absorption (HIA) is widely predicted after oral administration. Ninety percent absorption indicates highly intestinal absorption drugs. The intestinal absorption model includes 95% and 99% confidence ellipses in the ADMET_PSA_2D versus ADMET_AlogP98. The Aqueous Solubility was generated relying on 775 different compounds from various classes and different generated plots extracted from experimental values (Cheng & Merz, 2003). The ADMET and Lipinski's features and pKa were performed by using biovia DS.

2.4.3 GOLD

495,539 ligands from zinc database and 2000 ligands from Otava database and 10333 ligands from ChEMBL database were docked with GOLD (Chemp1p scoring function) with 10 Genetic Algorithm (GA) run and select all atoms within 10 Å and with default protocols.

2.4.4 VINA

29,840 ligands from zinc and 803 ligands from Otava and 160 ligands from ChEMBL were docked with AutoDock Vina and the exhaustiveness was set for 8.

2.4.5 AUTODOCK

Twenty-nine ligands from zinc and 33 ligands from Otava and 27 ligands from ChEMBL were docked with AutoDock and the number of GA runs set for 20 and the maximum number of evals set for long (25,000,000) and the maximum number of generations set for 27,000.

2.4.6 MD Simulation Analysis

The best 2 ligands from zinc database and best 1 ligand from Otava and best 2 ligands from ChEMBL were prepared for MD simulation to evaluate their stability in the active

site of GABA-AT over time. We used charm GUI server for preparing the complexes for MD simulation. By using NAMD the complexes' energy was minimized to 10000 and equilibrated for 5 nanoseconds and simulated for 50 nanoseconds and the last frames were selected for study the stability of the complexes. All systems' last frame was picked for calculate the Potential, Van der Waals, Electrostatic and Solvation energies via Poisson Boltzmann with non-polar Surface Area (PBSA) plugin tool from Biovia DS. Ligand ΔG for all systems were calculated after MD simulation via the web-based K_{DEEP} (<https://www.playmolecule.org/Kdeep/>) (Jiménez, Škalič, Martínez-Rosell, & De Fabritiis, 2018). Binding free energy calculated via CaFE tool (Liu & Hou, 2016). CaFE tool calculate the gas-phase free energy, solvation free energy and the change in the system entropy. CaFE tool use molecular mechanics Poisson-Boltzmann surface area (MM/PBSA) method for calculate the free energy (Elmezayen, Al-Obaidi, Şahin, & Yelekçi, 2020). The last 10 ns for the six complex systems submitted to CaFE tool. Figure 2.2 can summarize all above mentioned methods in this chapter.

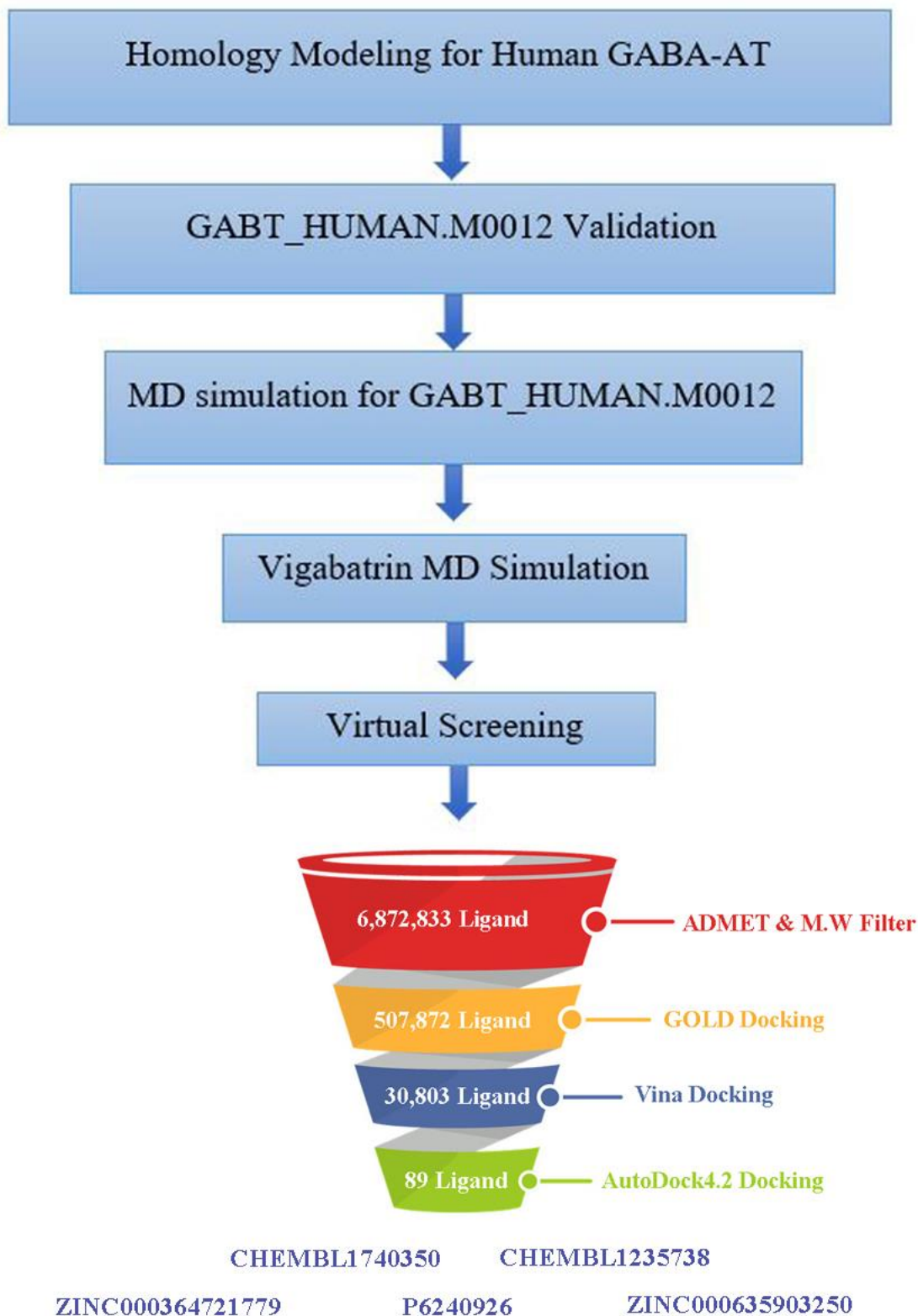


Figure 2. 2 A workflow explaining all the steps has been followed in this chapter.

3. Results and Discussion

3.1 Homology Modeling

We build a homology model for the human GABA-AT by using modeler from biovia DS. At first, we retrieved a Fasta sequence for the human GABA-AT from UniProt database with the entry P80404 (GABT_HUMAN). The sequence was used with BLAST search tool from biovia DS for searching the highest similarity protein from other organisms, the result shows that the GABA-AT from pig's liver (*Sus Scrofa*) was the highest identity with chain A and 95% identity and 461 sequences with 938.717-bit score with 0 E-value and 2.3 Å resolution (Figure 2.1). We retrieved the PDB for the pig liver GABA-AT from PDB website under the name of the protein 1OHV which has been deposited at 2003-06-02 and released at 2003-10-16. 1OHV was resolved with X-ray diffraction and the resolution was 2.3 Å and the R-value free 0.221 and the R-value work 0.188 (Storici et al., 2004). The protein has 4 chains A, B, C and D, chains B, C and D were excluded from the protein (1OHV) because the protein contains two homodimers and the four chains are 100% similar to each other. The protein was prepared by using “prepare protein” from biovia DS then the sequence for human GABA-AT aligned with the 1OHV sequence by using “align sequences” with biovia DS and the aligning shows that the main-chain RMSD was 0.21400 Å. The sequence identity was 95.9% and the sequence similarity was 98.3%. The aligned sequences show high similarity and 100% with the active site (Figure 3.1). If 30% at least sequence identity between a target and a template, proteins are expected to have similar structures if the aligned region is long enough. If two proteins have more than 50% sequence identity the quality of the model is generally considered excellent (Pevsner, 2009).

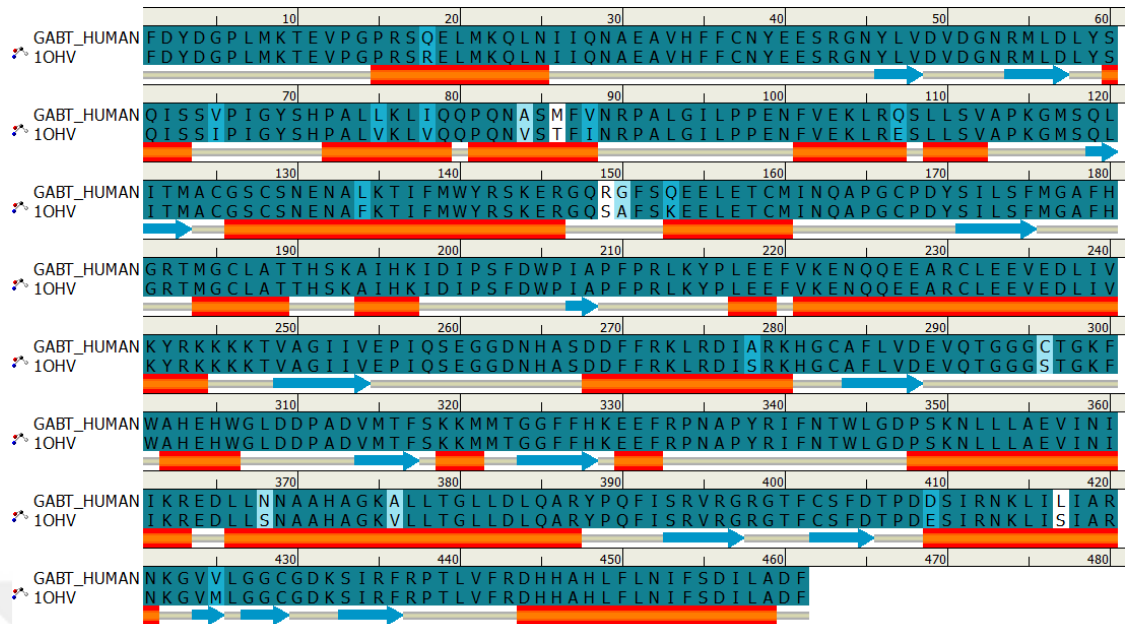


Figure 3. 1. 95.9% Similarity and 98.3% Identity and 100% Active Site similarity between Human FASTA and 10HV FASTA █ α helix ➔ β sheet loops.

We created a homology model for the human GABA-AT by using “build homology models” with biovia DS. The homology modeling created 20 models. To validate and choose the best model results were performed for “verify protein (Modeler)” from biovia DS. The best model was GABT_HUMAN.M0012 with dope score -54978.171875 and normalized dope score -1.206257 (Table 3.1).

Table 3. 1. The Homology Modeling results and scores, GABT_HUMAN.M0012 the highlighted one was the best result.

Protein Scores		
Name	DOPE Score	Normalized DOPE Score
GABT_HUMAN.M0007	-54759.050781	-1.172594
GABT_HUMAN.M0008	-54890.910156	-1.192851
GABT_HUMAN.M0012	-54978.171875	-1.206257
GABT_HUMAN.M0015	-54773.820313	-1.174863
GABT_HUMAN.M0001	-54787.460938	-1.176958
GABT_HUMAN.M0003	-54844.500000	-1.185721
GABT_HUMAN.M0018	-54816.351563	-1.181397
GABT_HUMAN.M0019	-54592.898438	-1.147069
GABT_HUMAN.M0006	-54718.898438	-1.166425
GABT_HUMAN.M0010	-54665.898438	-1.158283
GABT_HUMAN.M0005	-54757.914063	-1.172419
GABT_HUMAN.M0013	-54753.316406	-1.171713
GABT_HUMAN.M0016	-54858.902344	-1.187934
GABT_HUMAN.M0017	-54354.074219	-1.110379
GABT_HUMAN.M0002	-54919.933594	-1.197310
GABT_HUMAN.M0020	-54933.121094	-1.199336
GABT_HUMAN.M0004	-54828.503906	-1.183264
GABT_HUMAN.M0014	-54489.828125	-1.131234
GABT_HUMAN.M0011	-54466.957031	-1.127721
GABT_HUMAN.M0009	-53949.980469	-1.048300

The best model extracted and re-prepared by using “prepare protein” from biovia DS and the plp were put back into the same coordinate without losing the interacted residues (Figures 3.2, 3.3, 3.4).

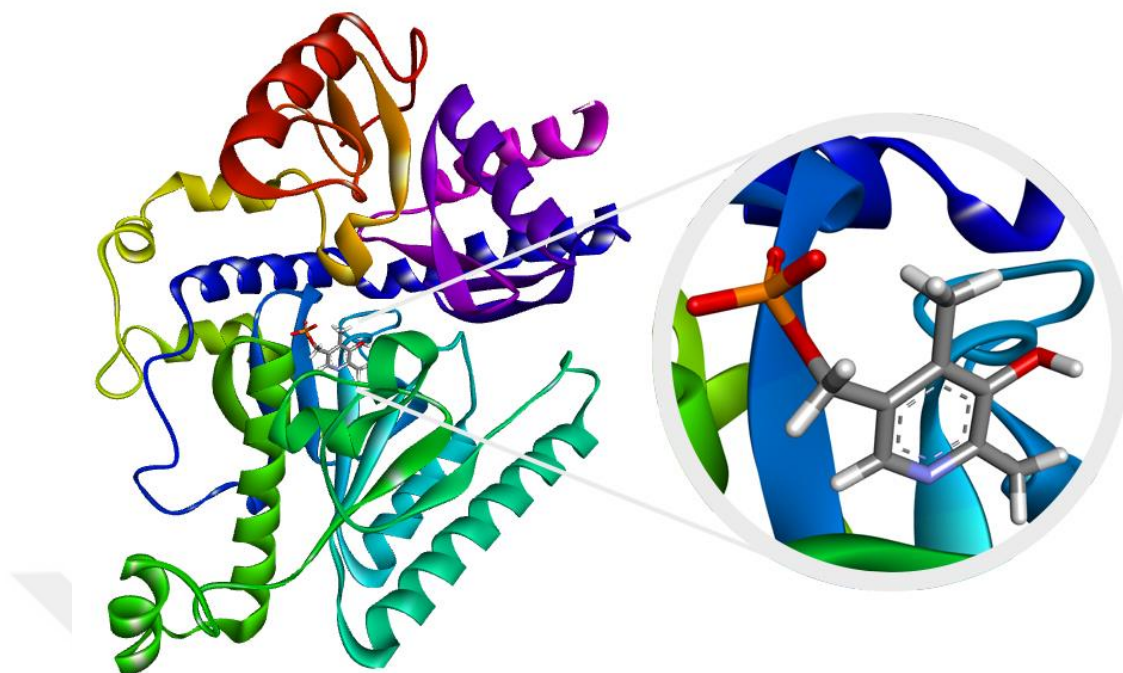
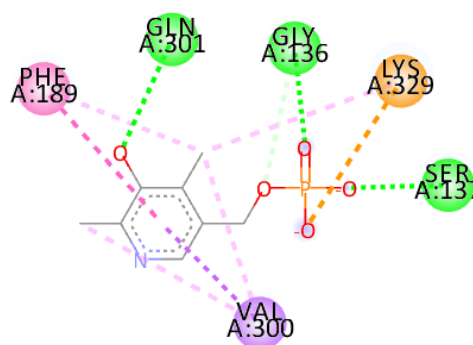


Figure 3. 2. The modeled Protein with PLP.



Interactions

- | | |
|-----------------------------------------------------------------|----------------------------------------------------|
| ■ Attractive Charge | ■ Pi-Pi T-shaped |
| ■ Conventional Hydrogen Bond | ■ Alkyl |
| ■ Carbon Hydrogen Bond | ■ Pi-Alkyl |
| ■ Pi-Sigma | |

Figure 3. 3. PLP interaction residue before Homology Modeling.

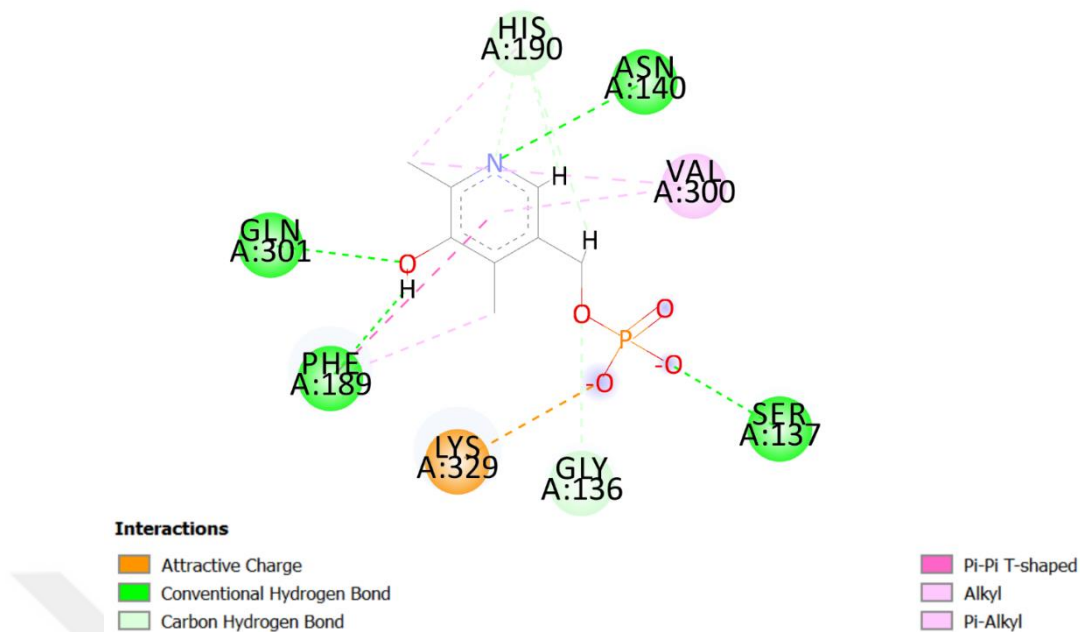


Figure 3. 4. PLP after Homology Modeling.

3.1.1 Align Structures

1OHV and the modeled protein were aligned together to compare the differences between the modeled and the crystal structure loops and α helices and β sheets and plp position after modeling and Root-Mean-Squared Deviation (RMSD) was 0.214 (Figure 3.5). The highlighted with yellow can indicate the 1OHV protein.

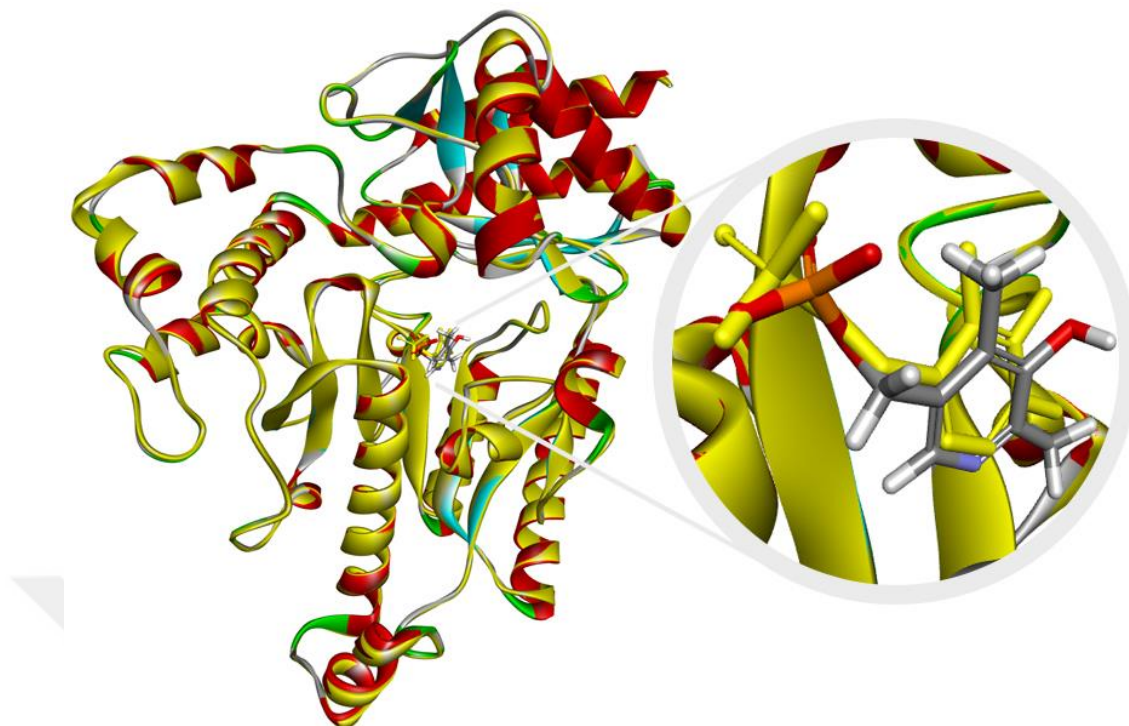


Figure 3. 5. Aligned 1OHV with PLP (yellow highlighted) and modeled protein with PLP.

3.1.2 Ramachandran Plot

Ramachandran plot used to evaluate the energetically acceptable regions of the modeled protein. The regions of alpha-helical and beta-sheet conformations with no steric clashes upon rotation around torsion angles phi and psi, 92.2% of the residues located at the most favored regions and 2.2% of residues located at the allowed regions and 0.8% located at generally allowed regions and 0.2% of residues located at disallowed regions, these results can give us a comprehensive picture of the modeled protein is acceptable (Figure 3.6).

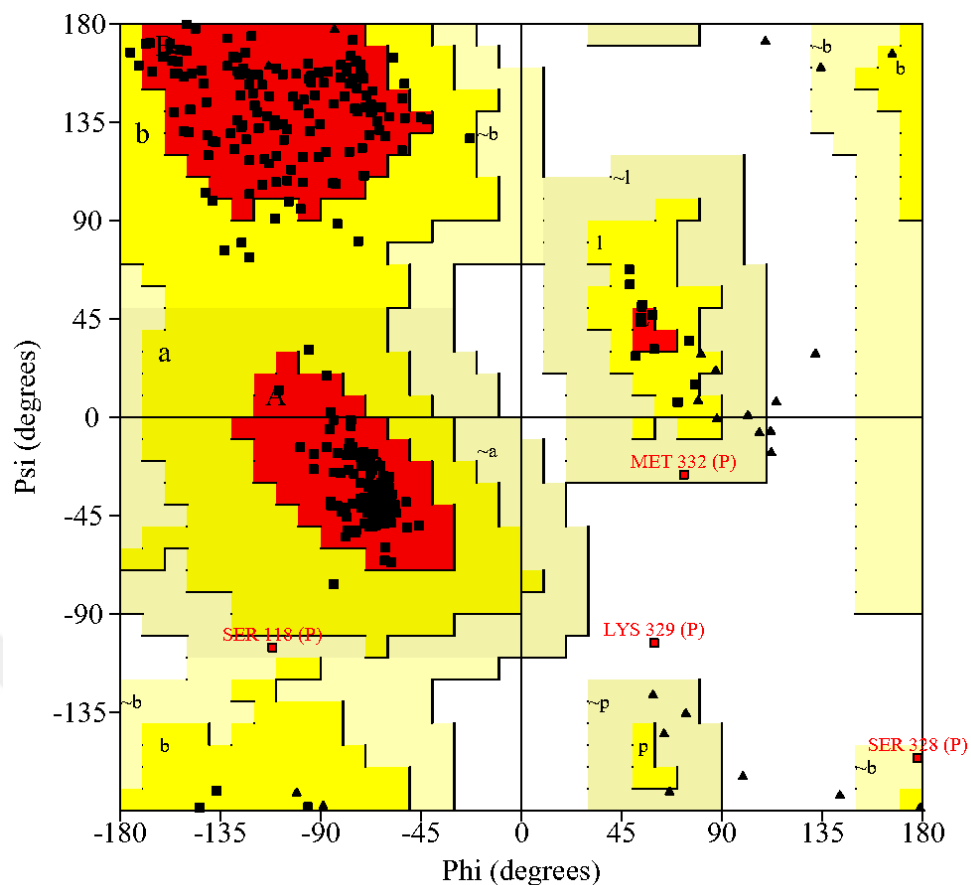


Figure 3. 6. Ramachandran plot showing the energetically allowed regions of the modeled protein.

3.1.3 ProSA-web

The 3D structure was also validated by using ProSA-web to recognize if there are any errors with the GABA-AT 3D structure. We can clearly see the GABA -AT modeled 3D structure located at the accepted X-ray regions (Figure 3.7).

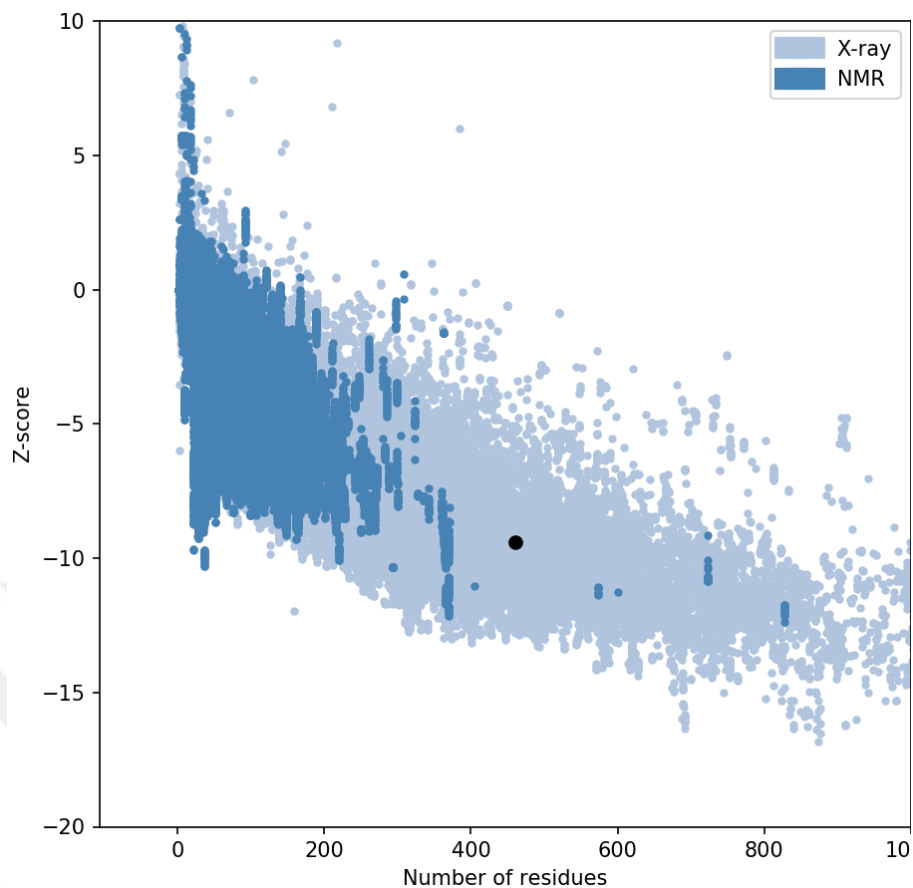


Figure 3. 7. Modeled GABA-AT result from ProSA-web, ● indicates the GABA-AT location between the X-ray regions.

3.1.4 Verify 3D

The modeled GABA-AT with plp was further verified with Verify 3D. verify3D produced averaged data points with 89.59% of the residues have averaged 3D score ≥ 0.2 , assuring a considerable high model quality (Figure 3.8).



Figure 3. 8. Verify 3D shows 89.59% of the residues have averaged 3D score ≥ 0.2 .

3.1.5 MD Simulation

MD simulation carried out to check the stability of the free modeled protein and to analyze the RMSD, Root-Mean-Squared Fluctuations (RMSF) and radius of gyration (Rg). By using CHARMMGUI server. The free modeled protein was prepared for MD simulation and set the minimization for 10000 and equilibrated for 5 nanoseconds and simulated for 50 nanoseconds by using NAMD. The result of the MD simulation shows very high stability and the RMSD has been stabilized approximately between 3 and 3.5 Å (Figure 3.9). The RMSF fluctuated low except the loop's residues (LEU30, MET96, LYS125, PHE161, and MET194) (Figure 3.10A). The Rg through md simulation shows a stable and steady fluctuation between 1.32 and 1.44 Å (Figure 3.10B).

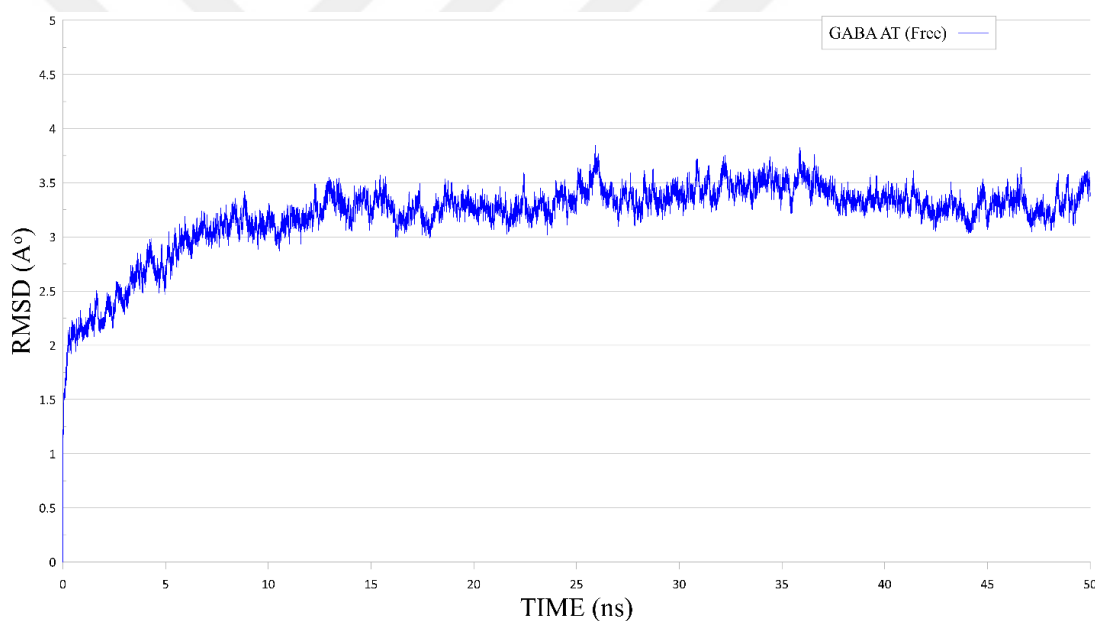


Figure 3. 9. Modeled GABA-AT free RMSD for 50 Nanoseconds.

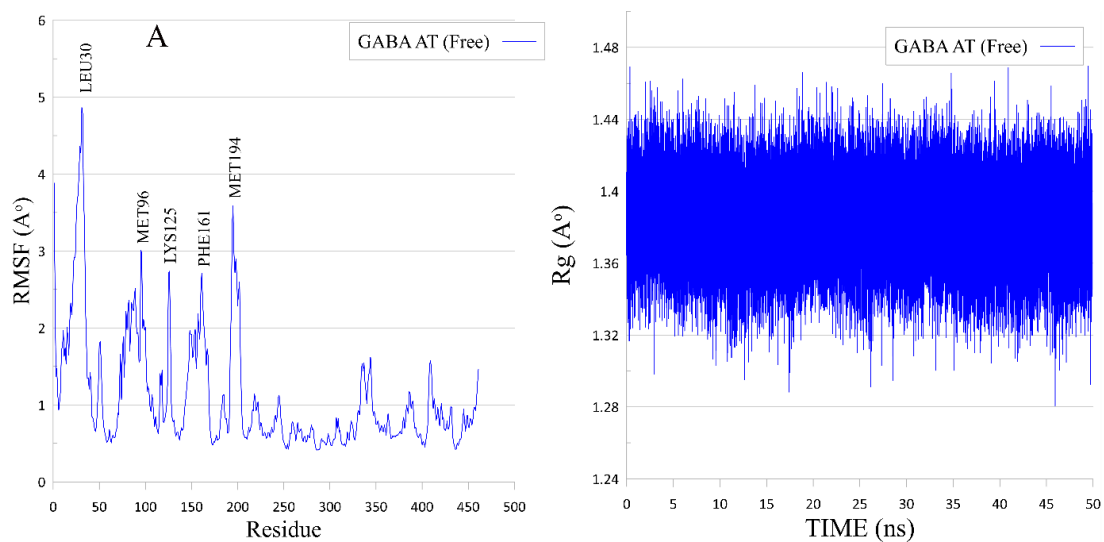


Figure 3. 10 A. Modeled GABA-AT RMSF, **B.** Modeled GABA-AT Rg.

The last frame from MD simulation was taken and analyzed to check the stability of the modeled GABA-AT. The plp during the MD simulation was stabilized and didn't leave the cavity (Figures 3.11, 3.12).

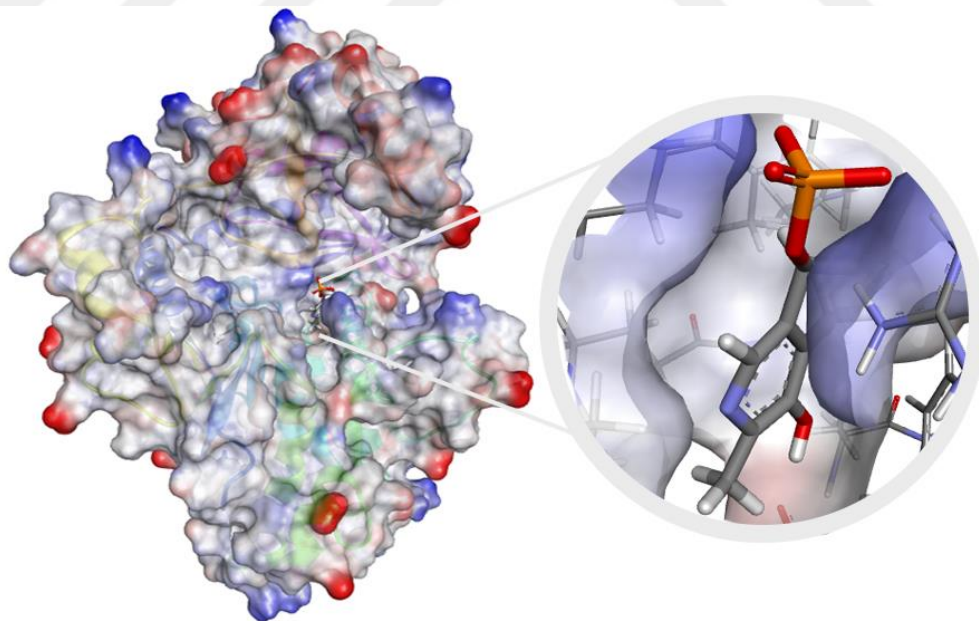


Figure 3. 11. Modeled GABA-AT after MD simulation showing charge surface with PLP interaction.

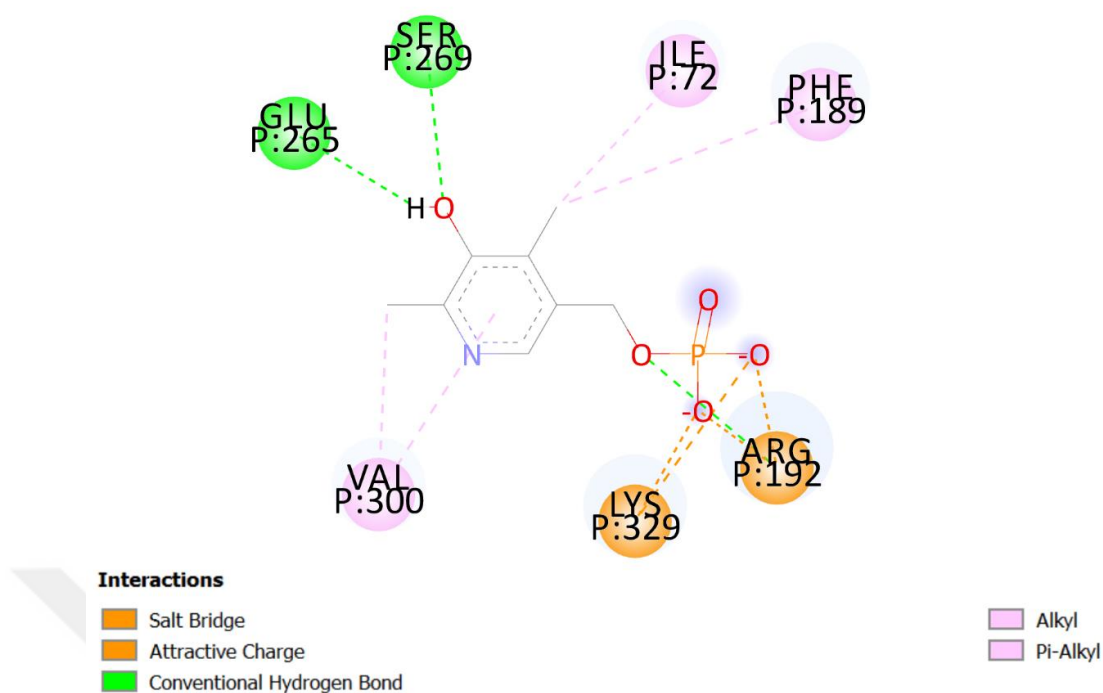


Figure 3. 12. PLP interaction after MD Simulation.

3.1.6 Known Inhibitors

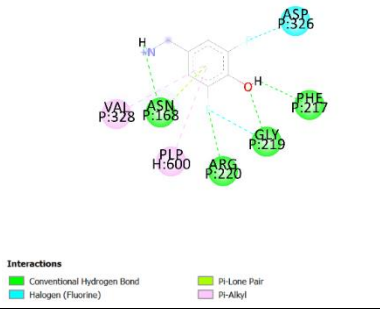
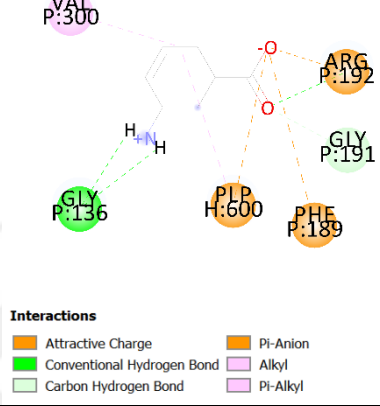
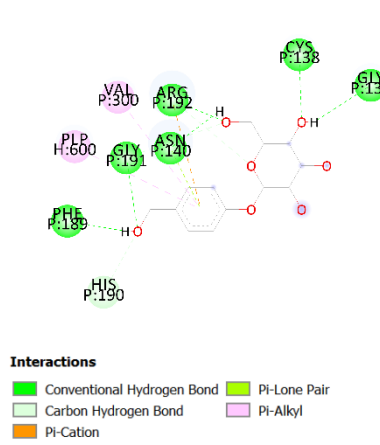
For checking the modeled GABA-AT, we docked known inhibitors to modeled GABA-AT and compared their experimental results with docked results and check the interaction between the active site which retrieved from (Toney, Pascarella, & De Biase, 1995). 8 of known inhibitors have experimented on human and 13 were experimented on the rat. The 21 known inhibitors prepared by using “prepare ligands” plugin tool in biovia DS and docked by using AutoDock with a setting of GA runs set for 20 and the maximum number of evals set for long (25,000,000) and the maximum number of generations set for 27,000 (Tables 3.2, 3.3).

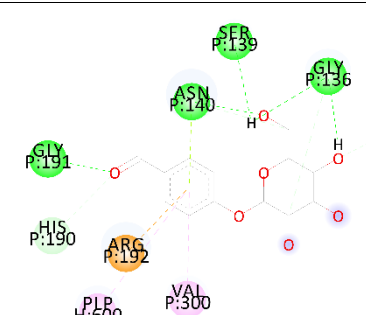
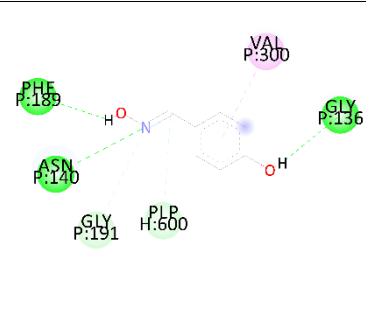
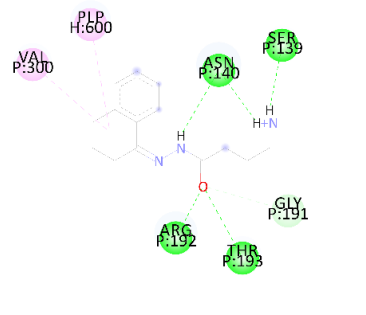
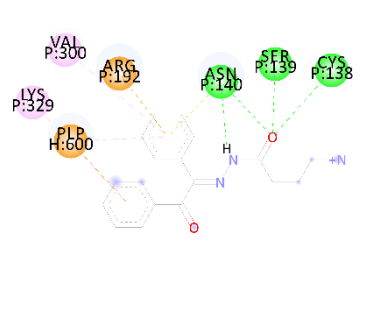
Table 3. 2. Known Inhibitors and the Active site residues interactions.

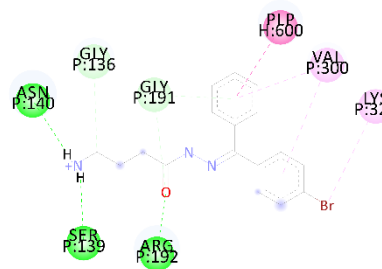
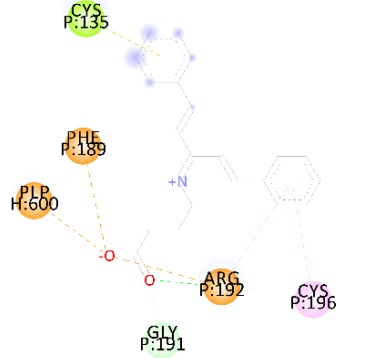
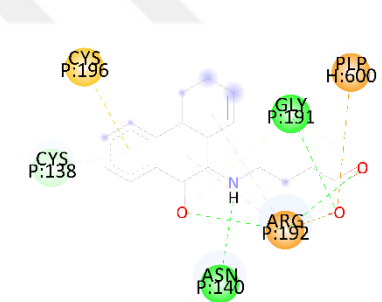
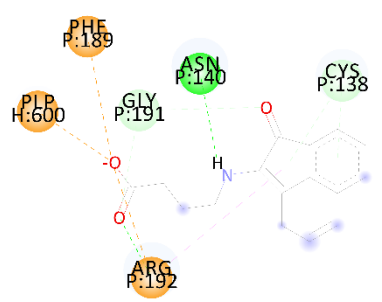
Inhibitor Name	Active Site residues									
	CYS 138	GLY 136	ASN 140	PHE 189	HIS 190	GLY 191	ASP 298	VAL 300	LYS 329	PLP
VIGABATRIN	✓	✓	✓							✓
Aryl aminopyridine derivative of GABA			✓	✓		✓				✓
“208” derivative of difluorophenol		✓	✓	✓		✓		✓		✓
“209” derivative of difluorophenol			✓	✓		✓	✓	✓		✓
Cyclohexene analogue		✓		✓		✓		✓		✓
GASTRODIN	✓	✓	✓	✓	✓	✓		✓		✓
HELICIDE		✓	✓		✓	✓		✓		✓
4-Hydroxybenzaldehyde		✓	✓	✓		✓		✓		✓
Tetrahydronaphthalen-1-one			✓			✓		✓		✓
CHEMBL2283209	✓		✓					✓	✓	✓
CHEMBL2283210		✓	✓			✓		✓	✓	✓
CHEMBL2283211				✓		✓				✓
CHEMBL2283213	✓		✓			✓				✓
CHEMBL2283214	✓		✓	✓		✓				✓
CHEMBL2283217	✓		✓	✓				✓		✓
CHEMBL2283220	✓			✓		✓				✓
CHEMBL2283221	✓	✓						✓		✓
CHEMBL2283223						✓		✓	✓	✓
CHEMBL2283224		✓	✓					✓		✓
CHEMBL2283226	✓		✓	✓		✓		✓		✓
CHEMBL2283227			✓	✓		✓		✓	✓	✓

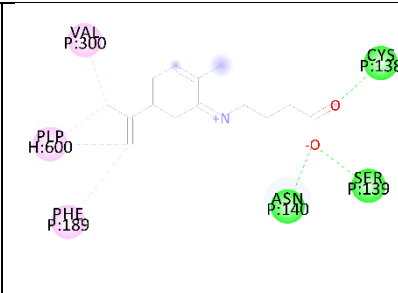
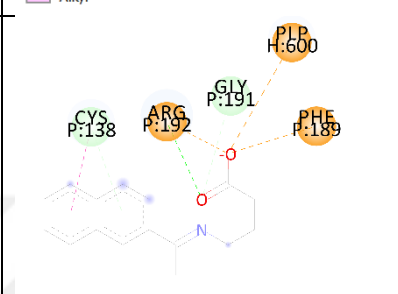
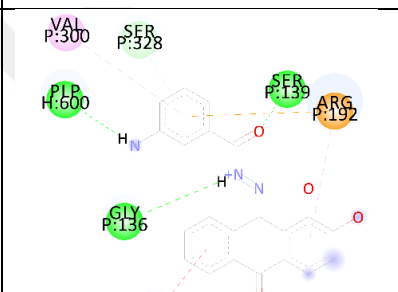
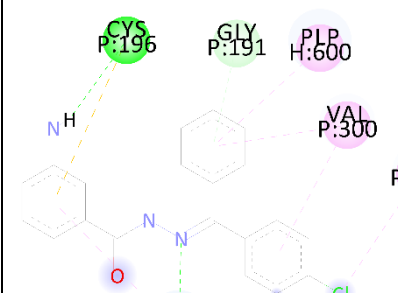
Table 3. 3. Known inhibitors and their experimental Ki and IC50 with docked Ki results with binding affinity and with 2D structures of their interactions.

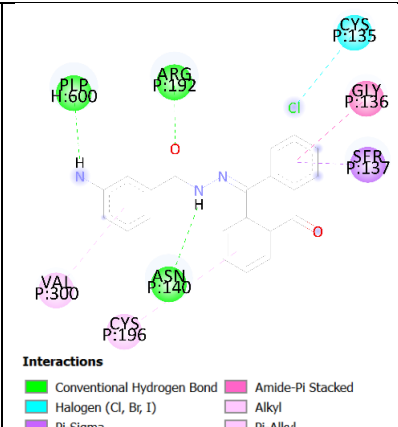
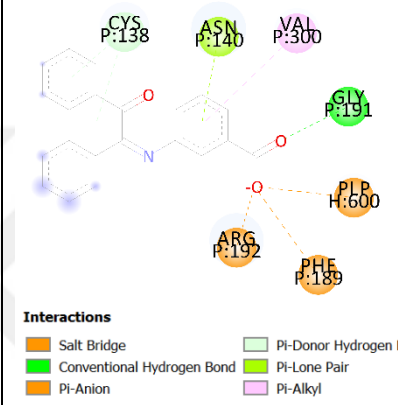
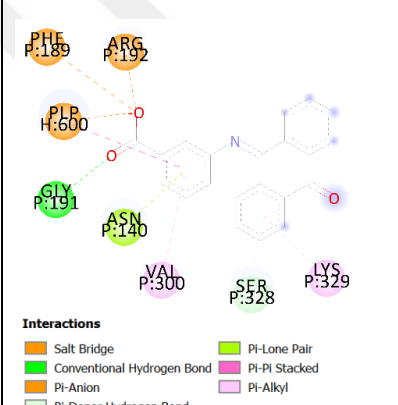
Inhibitor Name	Experimental Ki μM	Docked Ki μM	Binding affinity Kcal/mol	2D Interaction
VIGABATRIN	850	109.66	-5.40	<p>Interactions</p> <ul style="list-style-type: none"> Conventional Hydrogen Bond Carbon Hydrogen Bond Pi-Alkyl
Aryl aminopyridine derivative of GABA	91	27.87	-6.20	<p>Interactions</p> <ul style="list-style-type: none"> Attractive Charge Conventional Hydrogen Bond Carbon Hydrogen Bond Pi-Alkyl Pi-Anion
“208” derivative difluorophenol	6300	1070	-4.05	<p>Interactions</p> <ul style="list-style-type: none"> Conventional Hydrogen Bond Halogen (Fluorine) Pi-Lone Pair Pi-Alkyl

<p>“209” derivative of difluorophenol</p>	<p>11000</p>	<p>1800</p>	<p>-3.75</p>	 <p>Interactions</p> <ul style="list-style-type: none"> Conventional Hydrogen Bond Halogen (Fluorine) Pi-Lone Pair Pi-Alkyl
<p>Cyclohexene analogue</p>	<p>2300</p>	<p>291.69</p>	<p>-4.82</p>	 <p>Interactions</p> <ul style="list-style-type: none"> Attractive Charge Conventional Hydrogen Bond Carbon Hydrogen Bond Pi-Anion Alkyl Pi-Alkyl
<p>Inhibitor Name</p>	<p>Experimental IC₅₀ μM</p>	<p>Docked Ki</p>	<p>Binding affinity Kcal/mol</p>	<p>Interaction</p>
<p>GASTRODIN</p>	<p>1000</p>	<p>2.67</p>	<p>-7.60</p>	 <p>Interactions</p> <ul style="list-style-type: none"> Conventional Hydrogen Bond Carbon Hydrogen Bond Pi-Lone Pair Pi-Alkyl Pi-Cation

HELICIDE	1000	0.718	-8.38	 <p>Interactions</p> <ul style="list-style-type: none"> Conventional Hydrogen Bond Carbon Hydrogen Bond Pi-Cation Pi-Lone Pair Pi-Alkyl
4-hydroxybenzaldehyd	1000	477.71	-4.53	 <p>Interactions</p> <ul style="list-style-type: none"> Conventional Hydrogen Bond Carbon Hydrogen Bond Pi-Alkyl
Tetrahydronaphthalen-1-one	0.28	3.71	-7.40	 <p>Interactions</p> <ul style="list-style-type: none"> Conventional Hydrogen Bond Carbon Hydrogen Bond Alkyl Pi-Alkyl
CHEMBL2283209	0.3	2.73	-7.59	 <p>Interactions</p> <ul style="list-style-type: none"> Conventional Hydrogen Bond Pi-Cation Pi-Anion Pi-Lone Pair Pi-Alkyl

CHEMBL2283210	0.56	0.547	-8.54	 <p>Interactions</p> <ul style="list-style-type: none"> Conventional Hydrogen Bond Carbon Hydrogen Bond Pi-Donor Hydrogen Bond Pi-Pi Stacked Alkyl Pi-Alkyl
CHEMBL2283211	9.95	12.05	-6.71	 <p>Interactions</p> <ul style="list-style-type: none"> Attractive Charge Conventional Hydrogen Bond Carbon Hydrogen Bond Pi-Anion Pi-Lone Pair Pi-Alkyl
CHEMBL2283213	15.53	2.38	-7.67	 <p>Interactions</p> <ul style="list-style-type: none"> Attractive Charge Conventional Hydrogen Bond Carbon Hydrogen Bond Pi-Anion Pi-Donor Hydrogen Bond Pi-Sulfur Alkyl Pi-Alkyl
CHEMBL2283214	16.78	5.43	-7.18	 <p>Interactions</p> <ul style="list-style-type: none"> Attractive Charge Conventional Hydrogen Bond Carbon Hydrogen Bond Pi-Anion Pi-Donor Hydrogen Bond Pi-Alkyl

CHEMBL2283217	23.48	29.94	-6.17	 <p>Interactions</p> <ul style="list-style-type: none"> Conventional Hydrogen Bond Alkyl PI-Alkyl
CHEMBL2283220	44.06	12.85	-6.67	 <p>Interactions</p> <ul style="list-style-type: none"> van der Waals Attractive Charge Conventional Hydrogen Bond Carbon Hydrogen Bond PI-Anion PI-Donor Hydrogen Bond Amide-PI Stacked PI-Alkyl
CHEMBL2283221	0.24	1.40	-7.99	 <p>Interactions</p> <ul style="list-style-type: none"> Conventional Hydrogen Bond PI-Cation PI-Donor Hydrogen Bond Amide-PI Stacked PI-Alkyl
CHEMBL2283223	0.37	1.22	-8.07	 <p>Interactions</p> <ul style="list-style-type: none"> Conventional Hydrogen Bond PI-Donor Hydrogen Bond PI-Sulfur Alkyl PI-Alkyl

CHEMBL2283224	0.46	1.30	-8.03	 <p>Interactions</p> <ul style="list-style-type: none"> Conventional Hydrogen Bond Halogen (Cl, Br, I) Pi-Sigma Amide-Pi Stacked Alkyl Pi-Alkyl
CHEMBL2283226	2.78	3.96	-7.37	 <p>Interactions</p> <ul style="list-style-type: none"> Salt Bridge Conventional Hydrogen Bond Pi-Anion Pi-Donor Hydrogen Bond Pi-Lone Pair Pi-Alkyl
CHEMBL2283227	4.96	16.51	-6.52	 <p>Interactions</p> <ul style="list-style-type: none"> Salt Bridge Conventional Hydrogen Bond Pi-Anion Pi-Donor Hydrogen Bond Pi-Lone Pair Pi-Pi Stacked Pi-Alkyl

3.1.3.1 Vigabatrin MD Simulation

After docking known inhibitors, Vigabatrin was chosen for MD simulation. The estimated free energy of Vigabatrin binding was -5.40 Kcal/mol and the estimated inhibition constant K_i was 109.66 μM and the complex (Vigabatrin and modeled GABA-AT) was prepared for MD simulation by using CHARMM GUI server and set the minimization for 10000 and equilibrated for 5 nanoseconds and simulated for 50

nanoseconds by using NAMD. The result shows the complex was stable and the RMSD has stabled approximately at 2.8 Å (Figure 3.13). RMSF shows the low fluctuation for all protein residues except for LEU30 and MET 194 which they are located at loops region (Figure 3.14A). Rg shows a stable and steady fluctuation between 1.32 and 1.44 Å (Figure 3.14B).

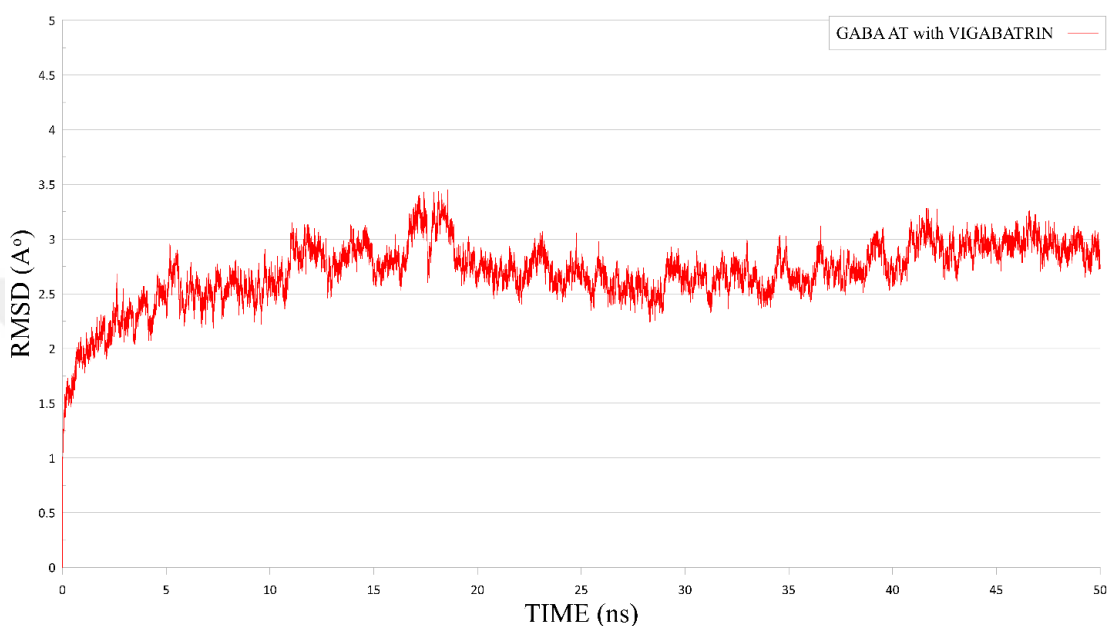


Figure 3. 13. The modeled complex (GABA-AT with Vigabatrin) RMSD.

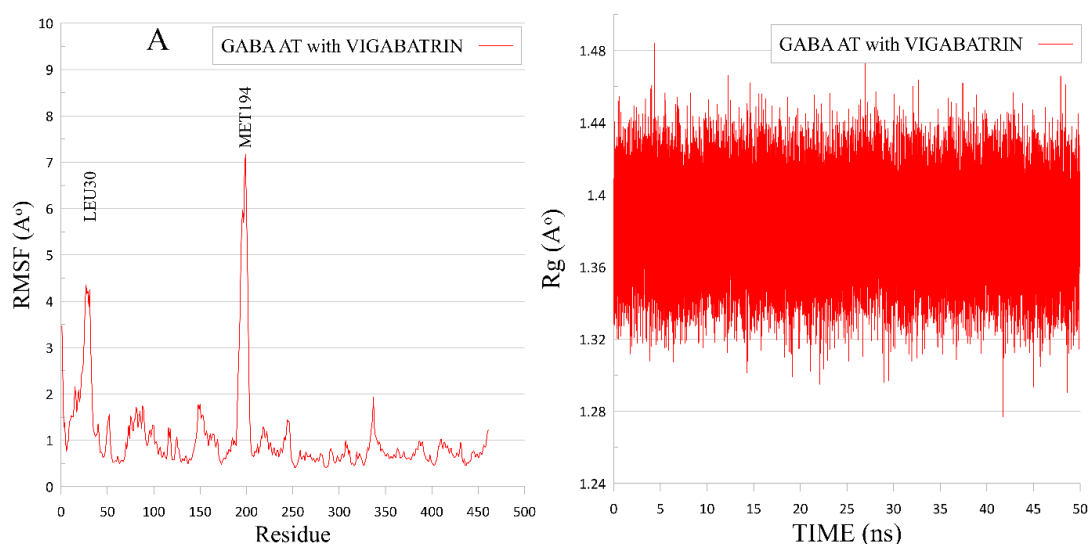


Figure 3. 14 A. GABA-AT with VIGABATRIN RMSF, **B.** GABA-AT with VIGABATRIN Rg.

By analyzing the simulated complex and compare the result with the docked complex before MD simulation, we can see that the Vigabatrin stable and maintain the interaction with the active site and with plp (Figures 3.15, 3.16, 3.17).

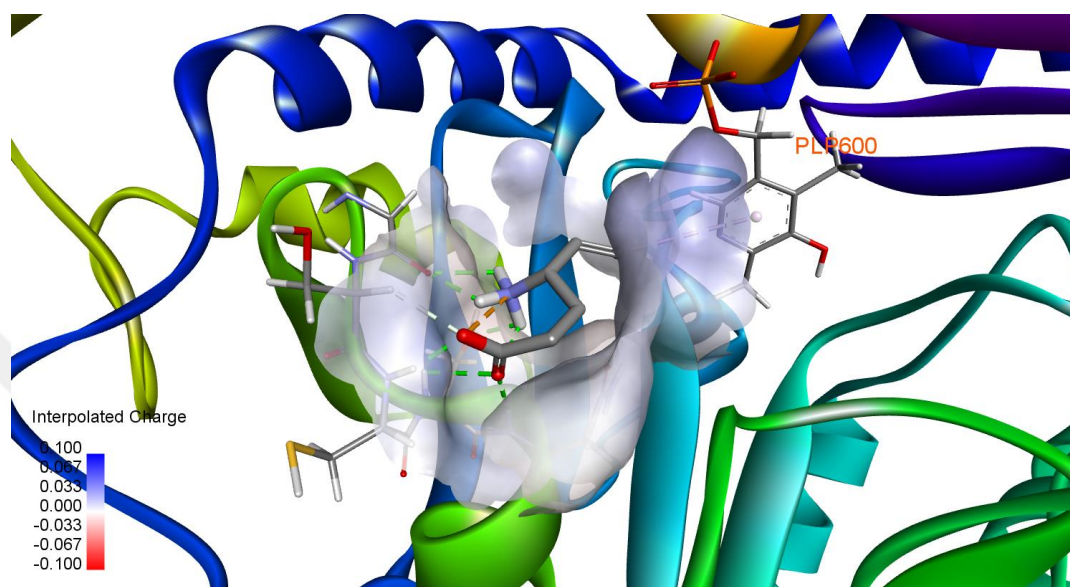


Figure 3. 15. Docked Vigabatrin interaction with the Active Site and PLP.

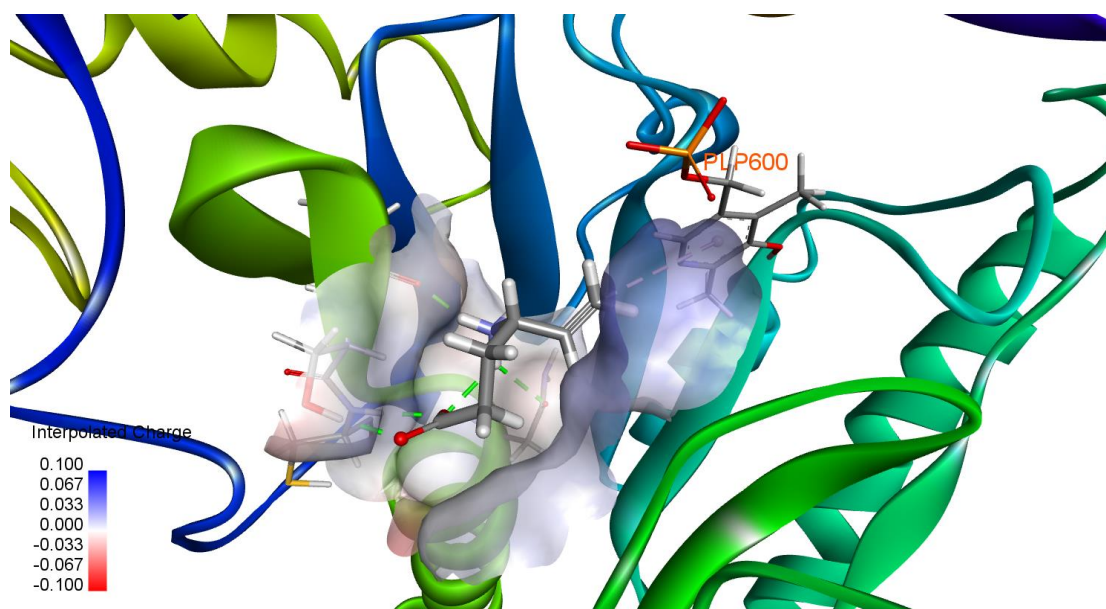


Figure 3. 16. Simulated Vigabatrin interaction with the Active Site and PLP.

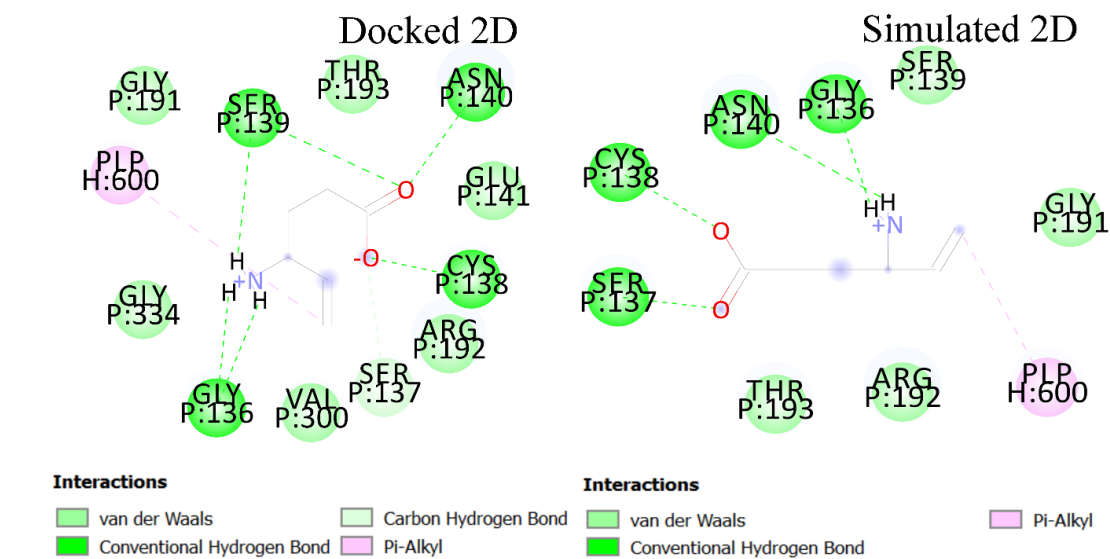


Figure 3. 17. Docked and Simulated Vigabatrin 2D interactions with the Active Site and PLP.

2.5 Virtual screening

3.2.1 Database

A total of 6,872,833 ligands were retrieved from different libraries 5,000,000 of them were from Zinc15 database and 2,372 of them were from Otava database and 1,870,461 of them were from ChEMBL. All ligands are drug-like and their LogP were ranging between -1 and 4.5 and prepared with biovia DS protocols.

2.5.2 ADMET and Lipinski's Rule of Five

All ligands from Zinc, Otava and ChEMBL databases were performed for ADMET via biovia DS "ADMET Descriptors". BBB is divided to five levels of penetration: 0 refers to very high penetration, 1 refers to high penetration, 2 for medium penetration, 3 low penetration and 4 describes no penetration state. Lipinski's rule of five stated that for any small molecule to be considered as a drug-like, the molecule should follow these criteria: molecular mass less than 500 Dalton, no more than 5 hydrogen bond donors, no more than 10 hydrogen bond acceptors, and logP less than 5. All ligands filtered depending on

ADMET and Lipinski's rule of five results. Zinc15 database filtered to 495,539 ligands and Otava database filtered to 2000 ligands and ChEMBL database filtered to 10333 ligands (Figure 3.18).

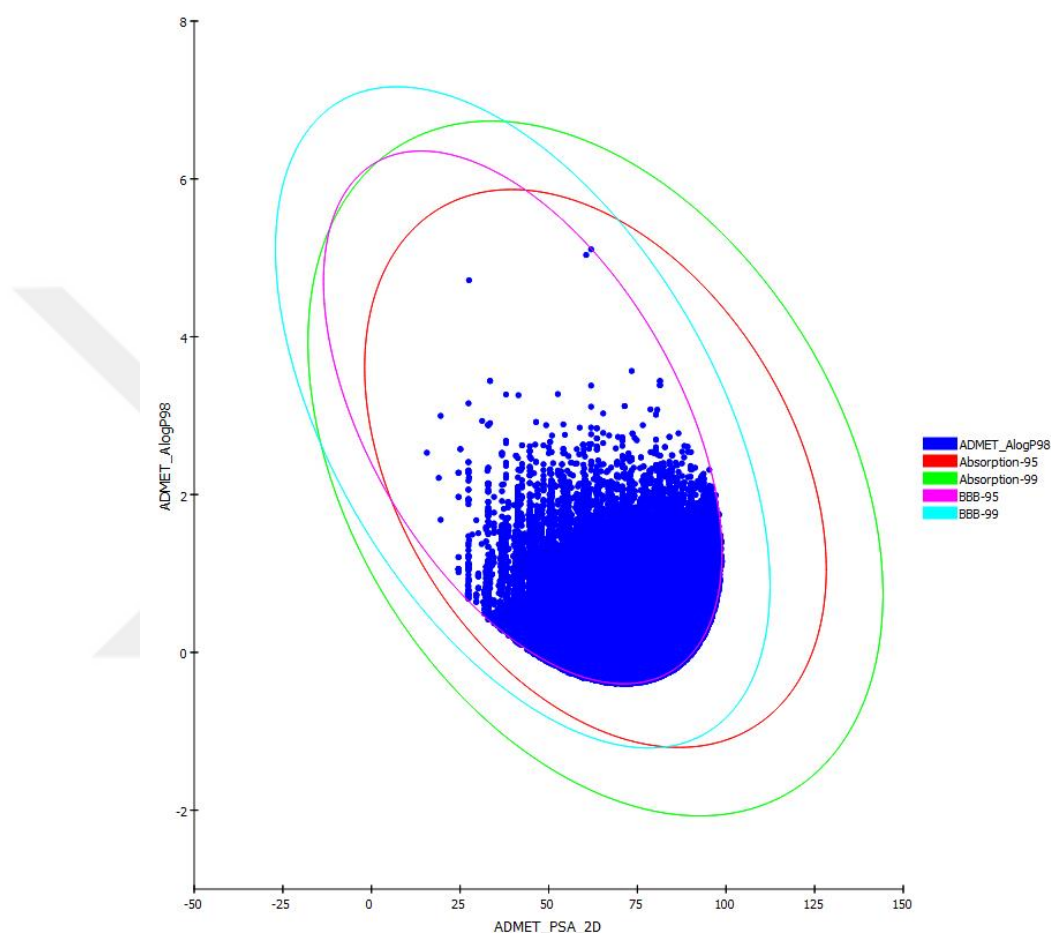


Figure 3. 18. ADMET Descriptors for Zinc, Otava and ChEMBL databases.

3.2.3 Gold

Before using GOLD for virtual screening, we docked known inhibitors against modeled GABA-AT by using GOLD to create a criteria for virtual screening, we docked the 21 known inhibitors with the XYZ coordinate of the active site (-20×8×2) and by using ChemPLP scoring function and 10 GA runs and select all atoms within 10 Å and with default protocols. The results show known inhibitors scores were between 27.39 and

52.73. By taking an average which will be 41.83 we create criteria of 45 score. Any ligand will show less score than 45 scores will be excluded (Table 3.4).

Table 3. 4. Gold CHEMPLP Scoring Function scores for Known Inhibitors.

Known Inhibitor Name	Gold CHEMPLP Score
VIGABATRIN	27.92
Aryl aminopyridine derivative of GABA	41.22
“208” derivative of difluorophenol	30.45
“209” derivative of difluorophenol	32.13
Cyclohexene analogue	27.39
GASTRODIN	41.26
HELICIDE	39.49
4-Hydroxybenzaldehyde	28.23
Tetrahydronaphthalen-1-one	43.65
CHEMBL2283209	52.59
CHEMBL2283210	52.73
CHEMBL2283211	52.34
CHEMBL2283213	45.52
CHEMBL2283214	47.79
CHEMBL2283217	39.96
CHEMBL2283220	42.37
CHEMBL2283221	47.5
CHEMBL2283223	47.46
CHEMBL2283224	47.95
CHEMBL2283226	44.84
CHEMBL2283227	45.84

After docking all databases against our model, 29,840, 803 and 160 from Zinc15, Otava and ChEMBL, respectively passed the criteria of 45 score.

3.2.4 Vina

All passed ligands after gold were picked up and docked by Vina. The highest 90 ligands from Zinc, Otava and ChEMBL were selected based on their binding affinity and interactions with the active site of GABA-AT to continue the study.

3.2.5 AutoDock

All 90 ligands were docked against our model via AutoDock 4.2. The best 2 from zinc database (ZINC000364721779, ZINC000635903250) and the best 1 ligand from Otava database (P6240926) and the best 2 ligands from ChEMBL database (CHEMBL1740350, CHEMBL1235738) were chosen depending on their estimated free energy of binding and their estimated inhibition constant K_i and on the interaction between the ligands with the active site. A total set of 5 ligands among the best 30 ligands from diverse databases were selected for MD simulation (Table 3.5).

Table 3. 5. Best 30 ligand's binding energy and K_i .

Molecule name	Binding energy Kcal/mol	K_i nM
ZINC000364721779	-9.41	127.55
ZINC000635903250	-9.00	250.84
ZINC000361908791	-8.89	304.76
ZINC000348987184	-8.86	319.66
ZINC001337417339	-8.82	344.39
ZINC001109206495	-8.77	374.77
ZINC001100325757	-8.69	423.25
ZINC001100325415	-8.67	444.61
ZINC000653739378	-8.63	470.78
ZINC000845925012	-8.62	476.28
P6240926	-8.67	437.67
P1308591	-8.51	579.05
P0116730119	-8.51	576.43

P1309903	-8.49	601.62
P6666635	-8.37	733.33
P6247875	-8.35	758.11
P7016350065	-8.29	834.25
P6236830	-8.24	904.59
P6667393	-8.21	963.78
P6666710	-8.17	1020
CHEMBL1740350	-7.64	2510
CHEMBL1235738	-7.09	6330
CHEMBL291584	-7.01	7300
CHEMBL3774671	-6.97	7810
CHEMBL49903	-6.93	8380
CHEMBL1201260	-6.87	9220
CHEMBL2007010	-6.87	9250
CHEMBL1199204	-6.7	12170
CHEMBL2206400	-6.68	12680
CHEMBL2333147	-6.33	22730

3.2.6 MD Simulation Analysis

The best results from AutoDock were performed for MD simulation. The complexes ZINC000364721779, ZINC000635903250, P6240926, CHEMBL1235738 and CHEMBL1740350 with modeled GABA-AT were prepared for MD simulation by using CHARMM GUI server and set the minimization for 10000 and equilibrated for 5 nanoseconds and simulated for 50 nanoseconds for each by using NAMD. The MD results show complexes ZINC000364721779, ZINC000635903250, P6240926, CHEMBL1740350 and CHEMBL1235738 with modeled GABA-AT were stable through the 50 nanoseconds of simulation and the RMSD for ZINC000364721779,

ZINC000635903250, P6240926, ChEMBL1740350 and ChEMBL1235738 was stabled approximately at 2.5 Å (Figures 3.19, 3.23, 3.27, 3.31, 3.35). We can clearly see the docked complexes interactions 2D and 3D with active site residues between the modeled GABA-AT and ZINC000364721779, ZINC000635903250, P6240926, ChEMBL1235738 and ChEMBL1740350 before and after MD simulation. We can see the system energy calculated by using PBSA from biovia DS for all systems after MD simulations and the ligand binding energy for all systems after MD simulations (Figures 3.21, 3.22, 3.25, 3.26, 3.29, 3.30, 3.33, 3.34, 3.37, 3.38) and (Tables 3.6, 3.7). Figures 3.39 and 3.40 show the comparison between all system's RMSD, RMSF and Rg. Table 3.8 shows the physiochemical features for the top-ranked ligands. Six systems have been assigned to CaFE tool for calculate the free energy for each ligand and it's active site. Mm for each system was set for 1, pb was set for 2, pb_indi was set for 1.0, pb_exdi was set for 80.0, pb_prbrad was set for 1.4 and pb_scale was set for 2.0. The free energy for the six systems were ranging between (-223 to -255 kcal/mol) which give the explanation of all systems were at the same range of energy which can indicate that our system is energetically stable and all ligands were stabilized at the active site as shown in table 3.9.

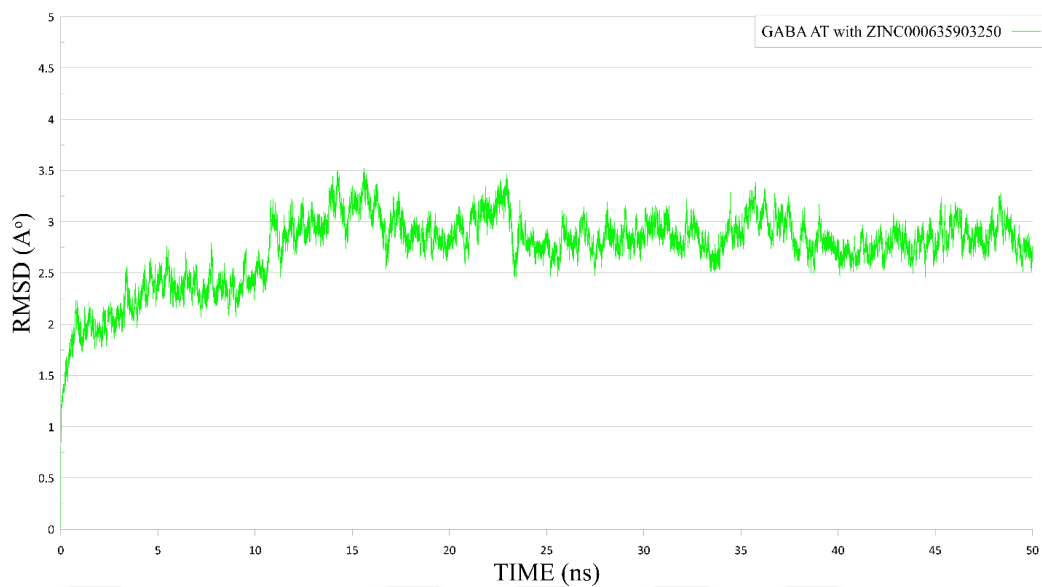


Figure 3. 19. GABA-AT and ZINC000635903250 complex's RMSD.

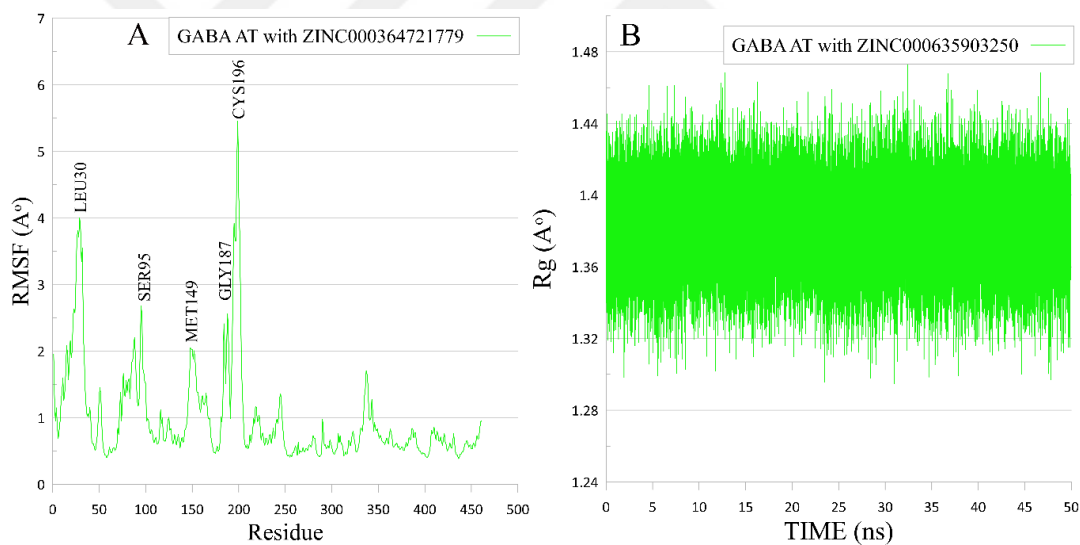


Figure 3. 20 A. GABA-AT and ZINC000635903250 complex's RMSF, **B.** GABA-AT and ZINC000635903250 complex's Rg.

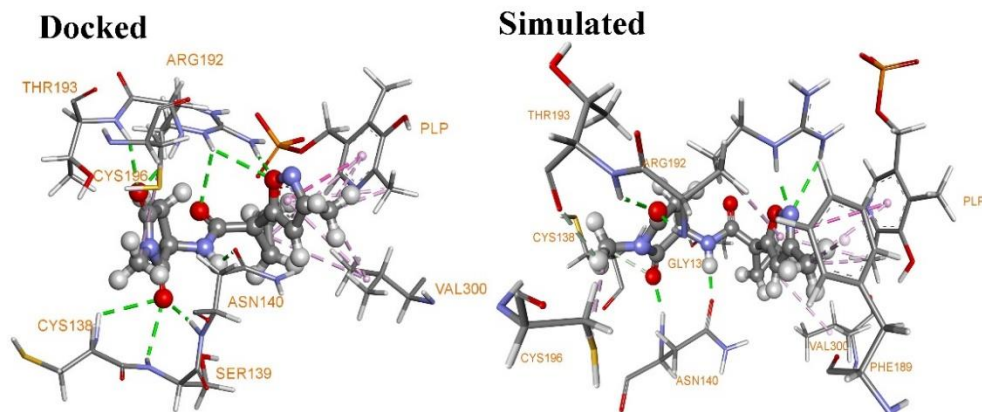


Figure 3. 21. Docked 3D and simulated 3D for ZINC000635903250.

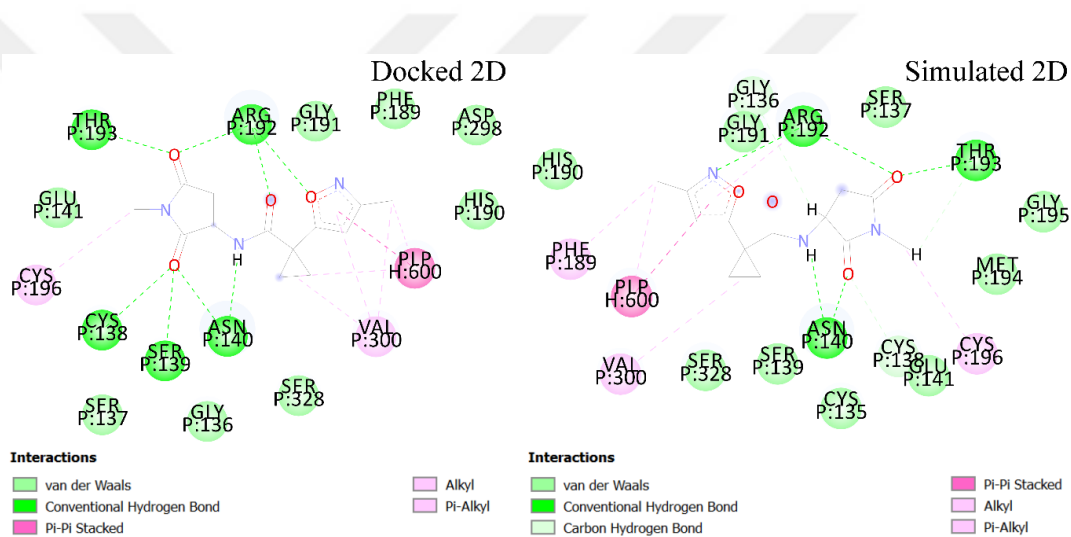


Figure 3. 22. Docked 2D and simulated 2D for ZINC000635903250.

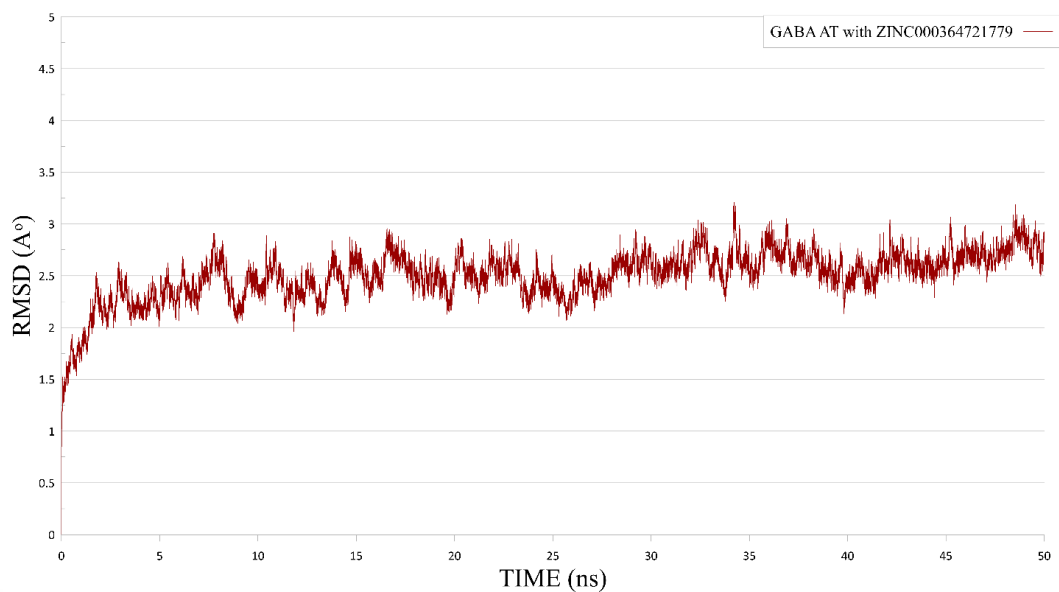


Figure 3. 23. GABA-AT and ZINC000364721779 complex's RMSD.

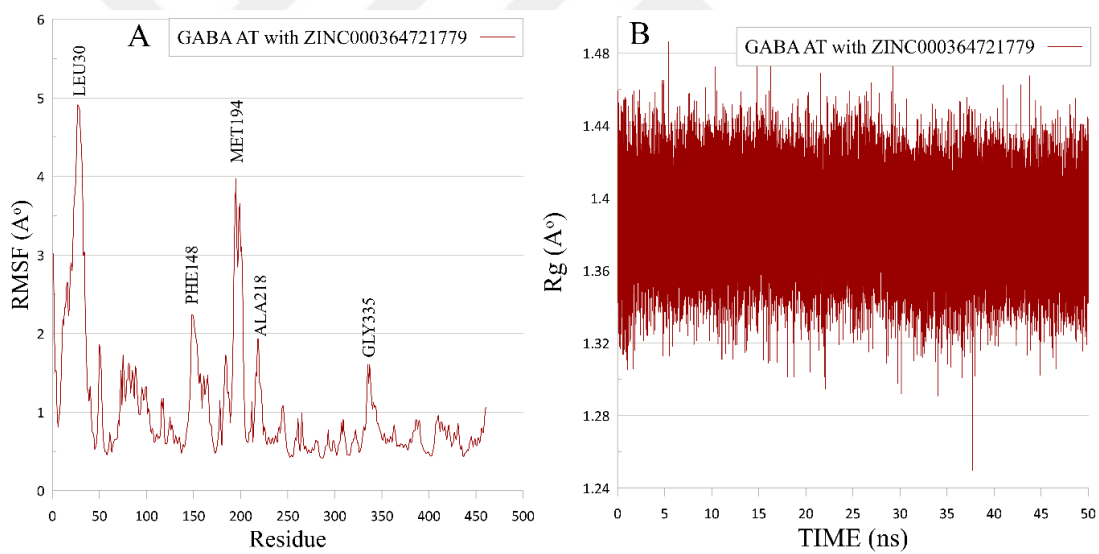


Figure 3. 24 A. GABA-AT and ZINC000364721779 complex's RMSF, **B.** GABA-AT and ZINC000364721779 complex's Rg.

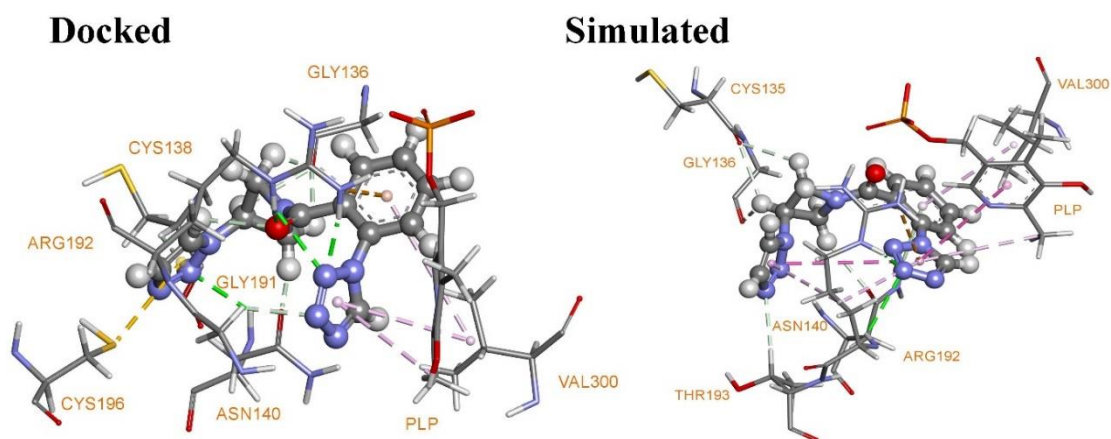


Figure 3. 25. Docked 3D and simulated 3D for ZINC000364721779.

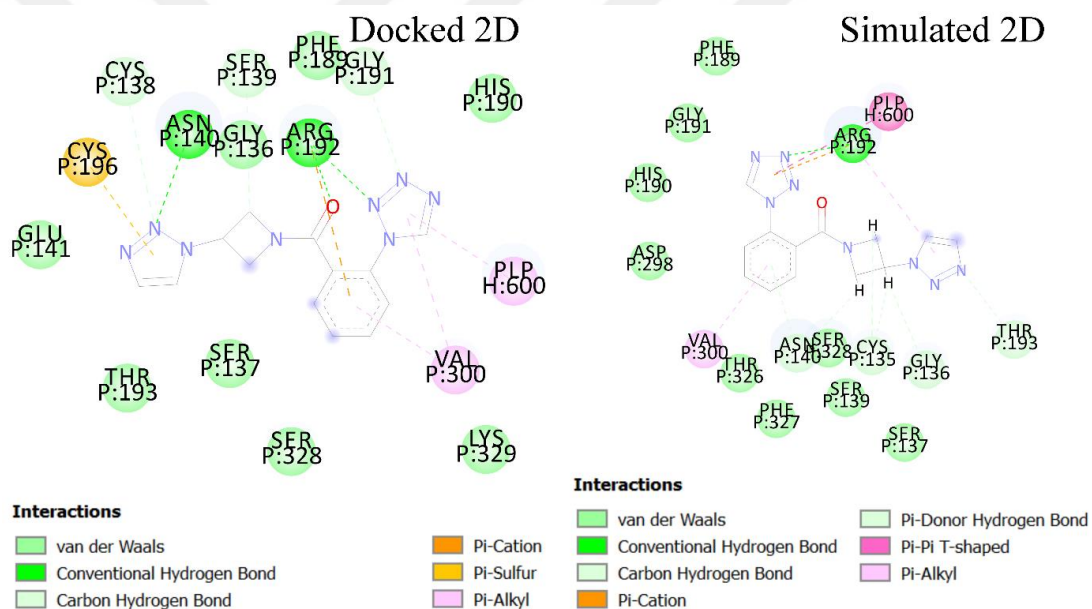


Figure 3. 26. Docked 2D and simulated 2D for ZINC000364721779.

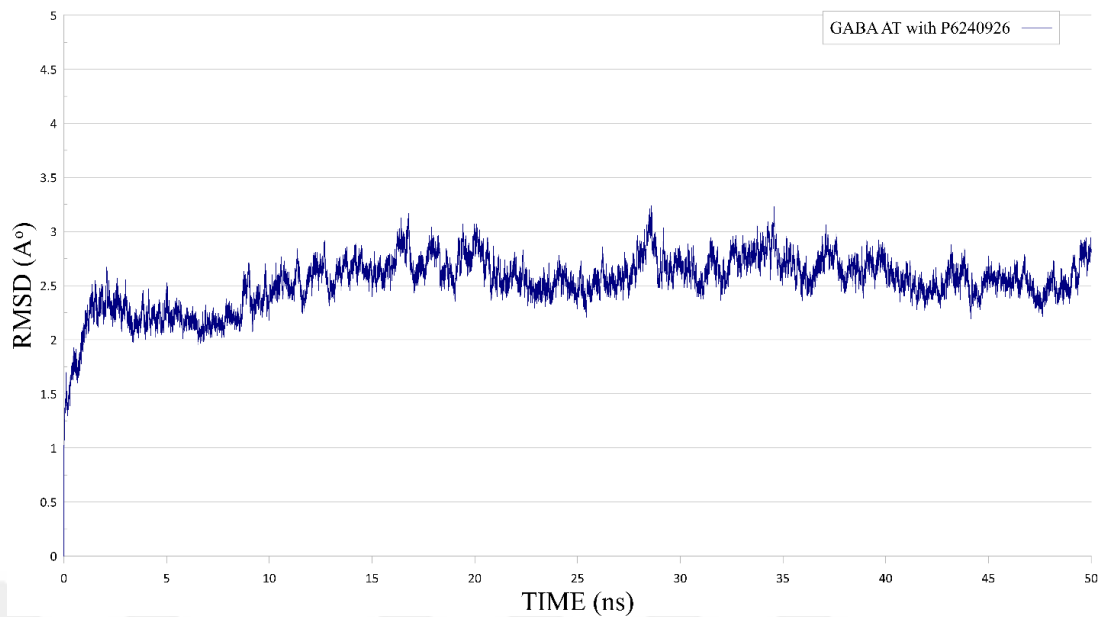


Figure 3. 27. GABA-AT and P6240926 complex's RMSD.

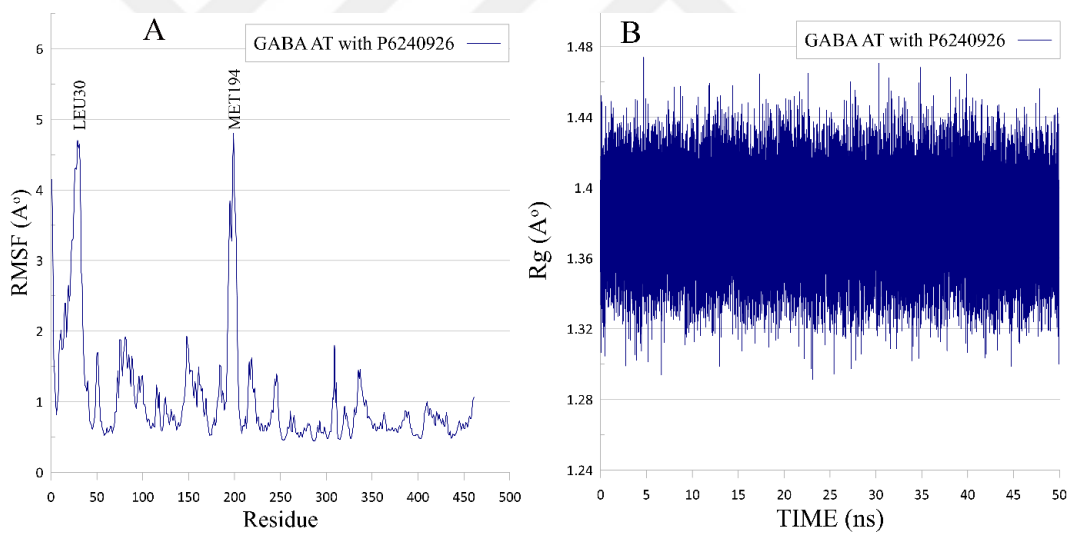


Figure 3. 28 A. GABA-AT and P6240926 RMSF, **B.** GABA-AT and P6240926 Rg.

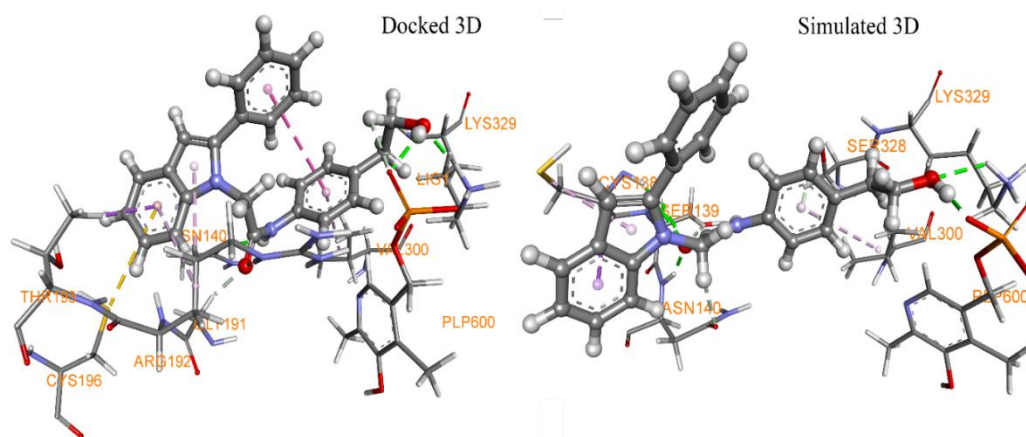


Figure 3. 29. Docked 3D and simulated 3D for P6240926.

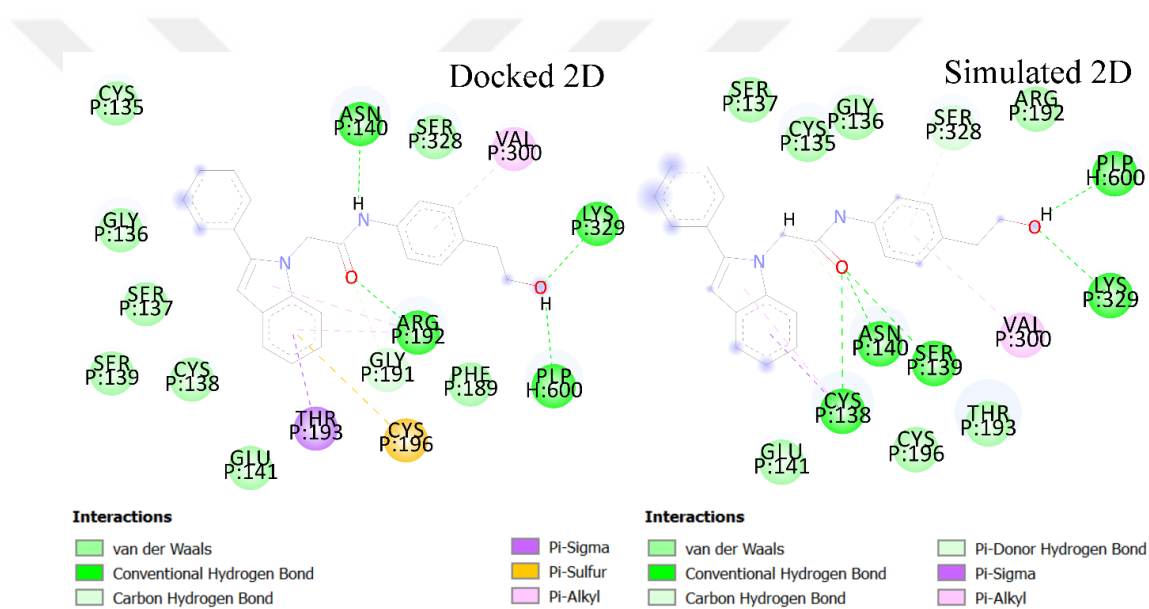


Figure 3. 30. Docked 2D and simulated 2D for P6240926.

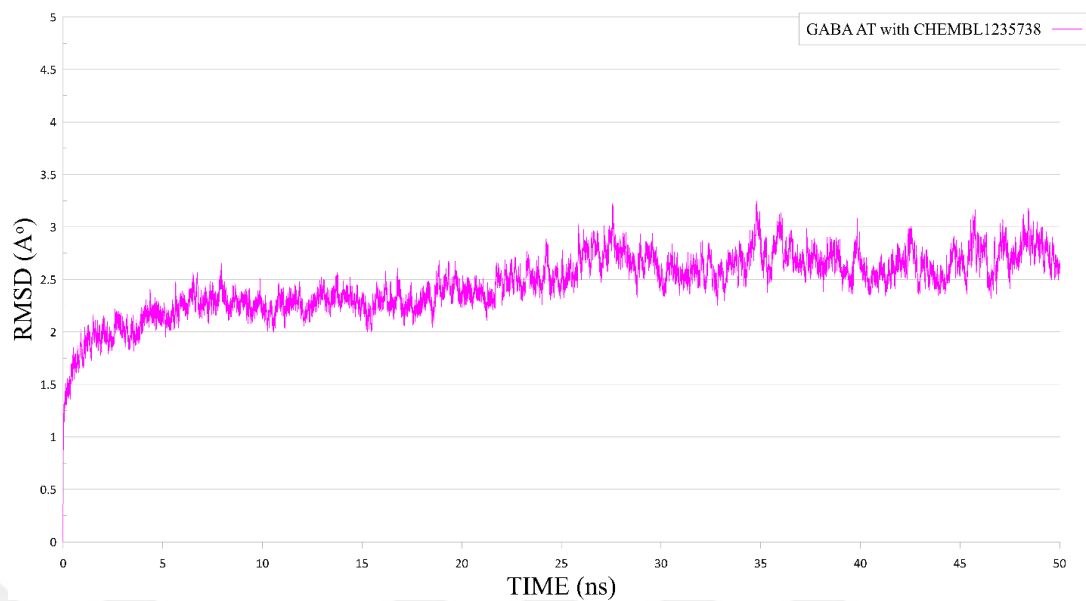


Figure 3. 31. GABA-AT and CHEMBL1235738 complex's RMSD.

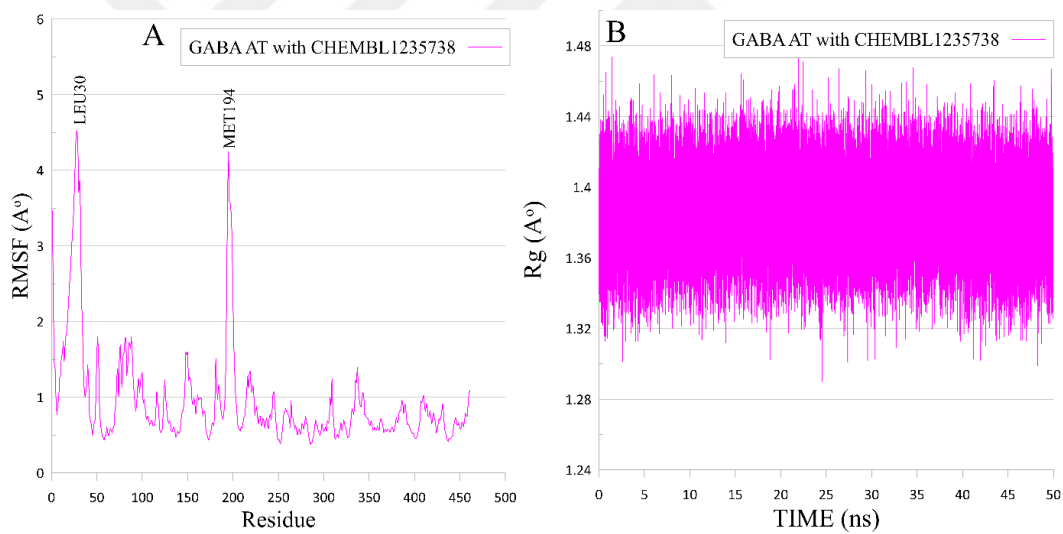


Figure 3. 32 A. GABA-AT and CHEMBL1235738 RMSF, **B.** GABA-AT and CHEMBL1235738 Rg.

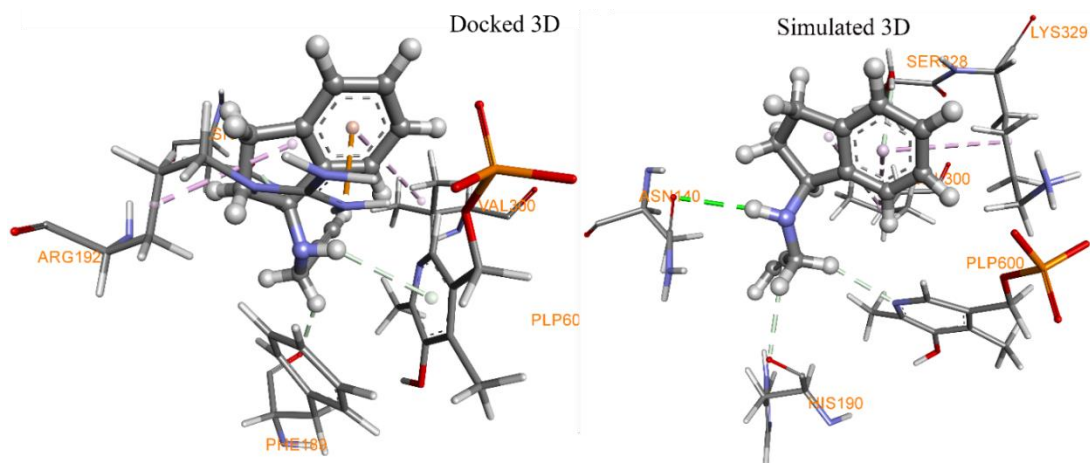


Figure 3.33. Docked 3D and simulated 3D for CHEMBL1235738.

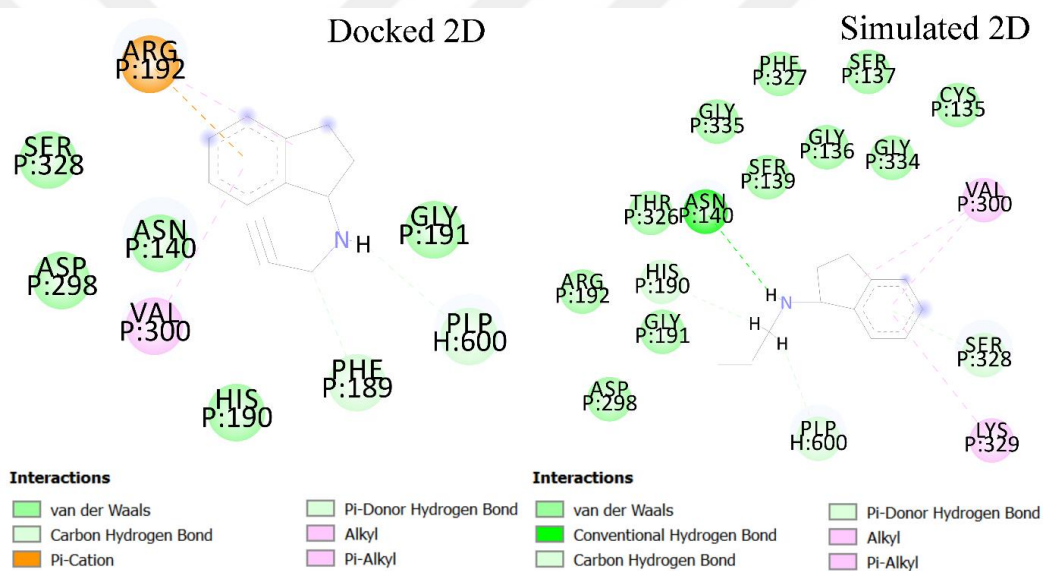


Figure 3.34. Docked 2D and simulated 2D for CHEMBL1235738.

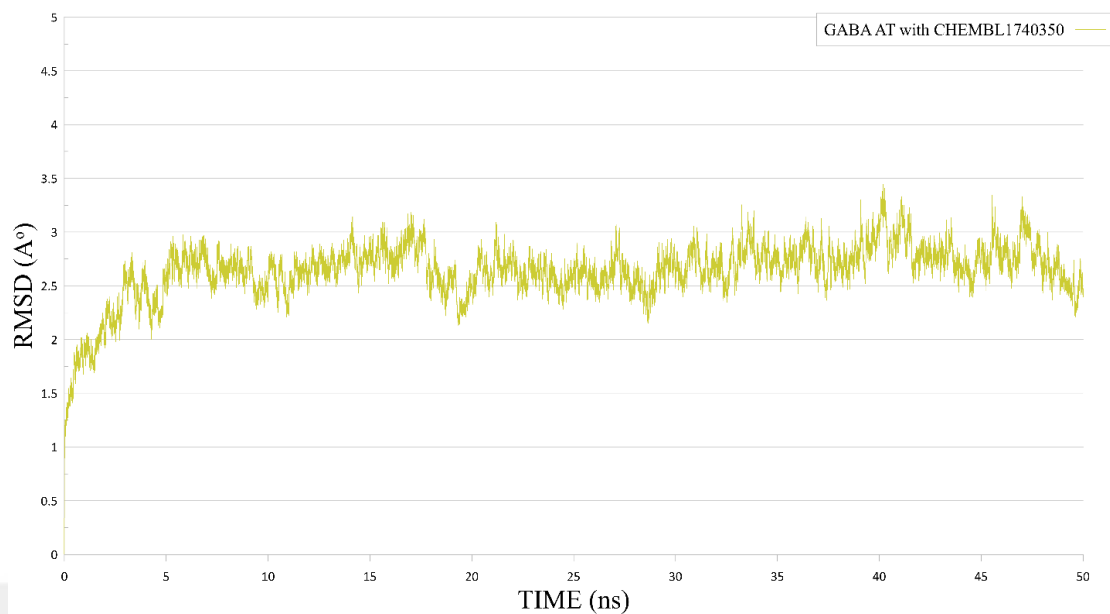


Figure 3. 35. GABA-AT and CHEMBL1740350 complex's RMSD.

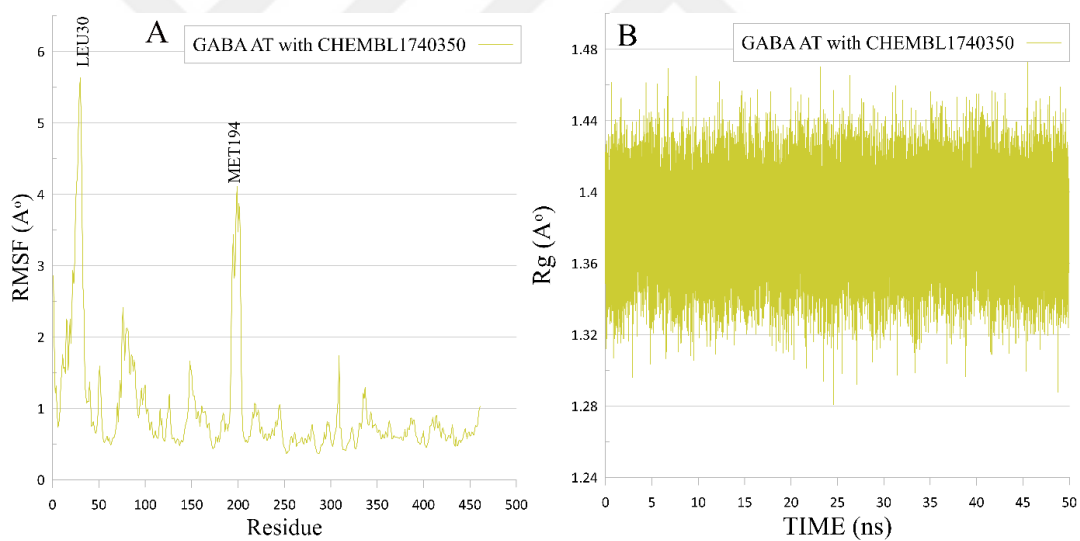


Figure 3. 36 A. GABA-AT and CHEMBL1740350 RMSF, **B.** GABA-AT and CHEMBL1740350 Rg.

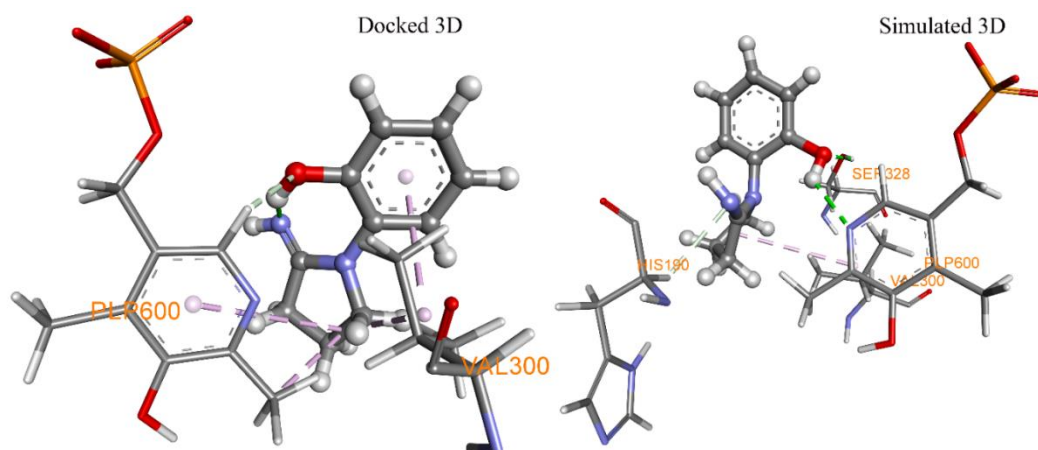


Figure 3.37. Docked 3D and simulated 3D for CHEMBL1740350.

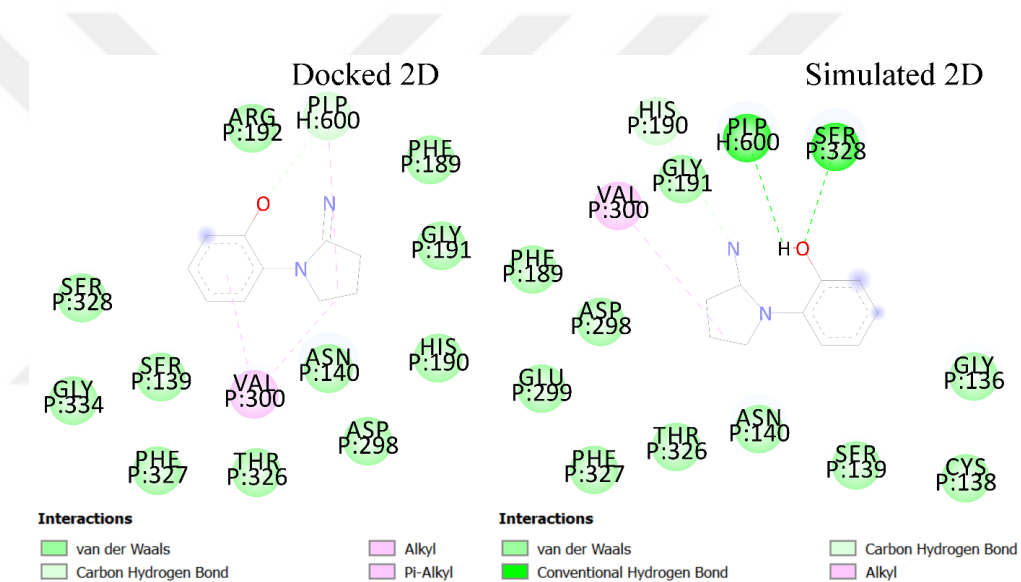


Figure 3.38. Docked 2D and simulated 2D for CHEMBL1740350.

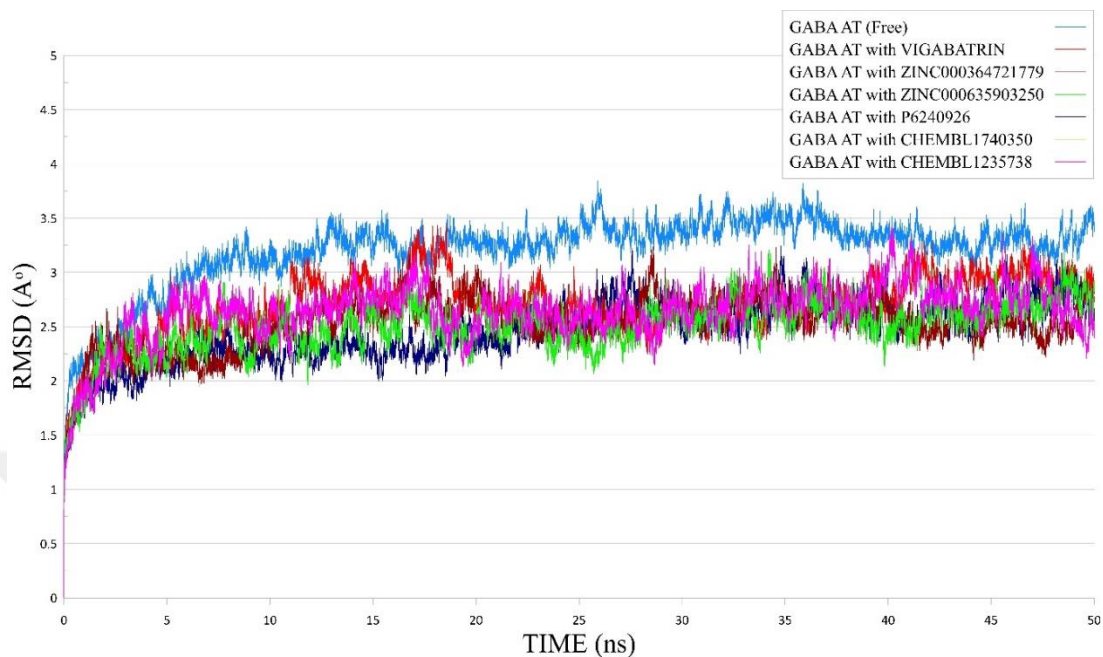


Figure 3.39. Comparison of all systems' RMSD.

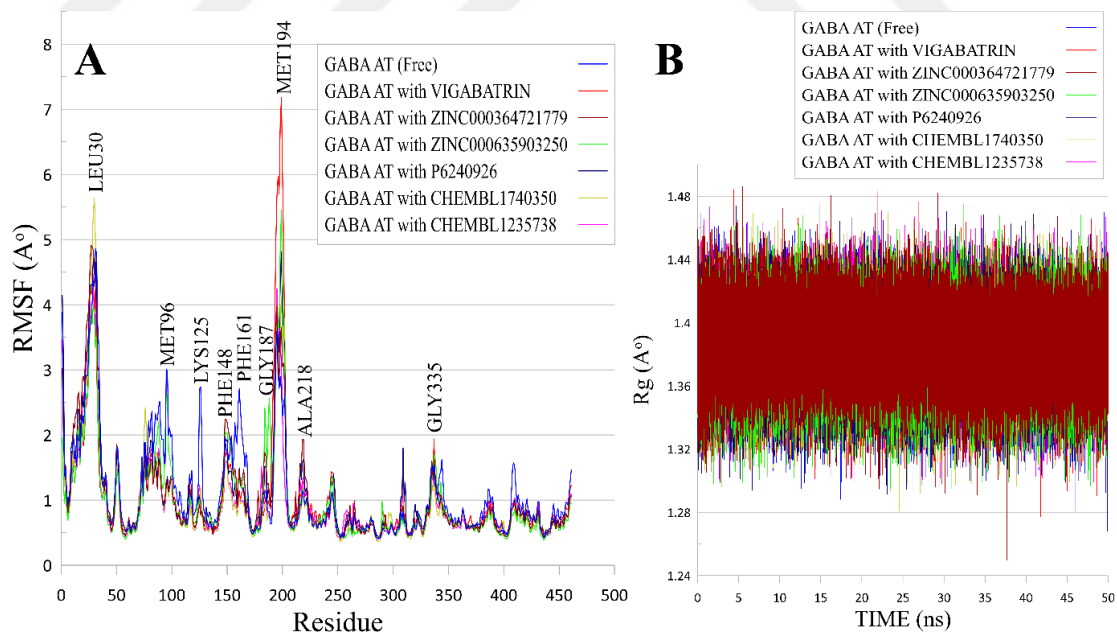


Figure 3.40 A. Comparison of all systems' RMSF **B.** Comparison of all systems' Rg.

Table 3. 6. The best 5-ligand interaction with Active Site before and after MD Simulation.

Ligand Name	CYS 138	GLY 136	ASN 140	PHE 189	HIS 190	GLY 191	ARG 192	VAL 300	LYS 329	PLP
ZINC000635903250 before MD	✓	✓	✓	✓	✓	✓	✓	✓		✓
ZINC000635903250 after MD	✓	✓	✓	✓	✓	✓	✓	✓		✓
ZINC000364721779 before MD	✓	✓	✓	✓	✓	✓	✓	✓	✓	✓
ZINC000364721779 after MD		✓	✓	✓	✓	✓	✓	✓		✓
P6240926 before MD	✓	✓	✓	✓		✓	✓	✓	✓	✓
P6240926 after MD	✓	✓	✓					✓	✓	✓
CHEMBL1235738 before MD			✓	✓	✓	✓	✓	✓		✓
CHEMBL1235738 after MD		✓	✓		✓	✓	✓	✓	✓	✓
CHEMBL1740350 before MD			✓	✓	✓	✓	✓	✓		✓
CHEMBL1740350 after MD	✓	✓	✓	✓	✓	✓		✓		✓

Table 3. 7. System energy for free GABA-AT and VIGABATRIN and the best 5 compounds after MD simulation and Ligand ΔG .

Name	Potential Energy (kcal/mol)	Van der Waals Energy (kcal/mol)	Electrostatic Energy (kcal/mol)	Solvation Energy (kcal/mol)	Free Energy (kcal/mol)	Ligand ΔG (kcal/mol)
FREE	-13064	-3540	-18029	-5896	-18840	N/A
VIGABATRIN	-12833	-3481	-17970	-5908	-18620	-5.77
P6240926	-13171	-3540	-18133	-5681	-18733	-5.42
CHEMBL1235738	-13057	-3514	-18015	-5866	-18802	-6.70
CHEMBL1740350	-12845	-3590	-17707	-6177	-18900	-6.96
ZINC000364721779	-12863	-3585	-17880	-5897	-18642	-6.82
ZINC000635903250	-12829	-3479	-18036	-5826	-18534	-7.48

Table 3. 8. physiochemical features for the top-ranked ligands.

Ligand name	Molecular weight	Hydrogen acceptor	Hydrogen donor	logP	BB level	Aqueous solubility	HIA level
ZINC000364721779	296.287	9	0	-0.191	3	-1.821	0
ZINC000635903250	277.276	7	1	-0.272	3	-2.065	0
P6240926	370.444	4	2	4.492	1	-5.025	0
CHEMBL1740350	176.215	3	2	1.224	3	-1.613	0
CHEMBL1235738	171.238	1	1	3.119	1	-2.141	1

Table 3. 9 MM/PBSA energy calculation for the six systems via CaFE tool.

Complex Name	ΔE Electrostatic	ΔE Van der Waal	ΔE polar	SASA	ΔE binding
VIGABATRIN	-309 +/- 27	-10 +/- 4	-209 +/- 12	-2.9 +/- 0.1	-223 +/- 11
P6240926	-331 +/- 20	-35 +/- 4	-212 +/- 8	-4.3 +/- 0.1	-251 +/- 7.2
CHEMBL1235738	-326 +/- 20	-21 +/- 4	-230 +/- 7	-3.3 +/- 0.1	-255 +/- 6.5
CHEMBL1740350	-275 +/- 19	-23 +/- 4	-222 +/- 8	-3.0 +/- 0.0	-248 +/- 8.2
ZINC000364721779	-337 +/- 25	-37 +/- 4	-193 +/- 8	-4.0 +/- 0.1	-235 +/- 7.6
ZINC000635903250	-195 +/- 24	-30 +/- 4	-207 +/- 6	-3.8 +/- 0.1	-241 +/- 6.8

4. Conclusion

GABA plays a crucial role as a neurotransmitter in the brain and GABA-AT is an enzyme that regulates the level of GABA. That is why GABA-AT is a prominent target for drug design for neurological disorders. *In silico* drug design significantly contributed to the development of GABA-AT inhibitors. Herein, we employed various computational methods to identify novel and highly potent human GABA-AT inhibitors such as homology modeling, structure-based virtual screening and molecular docking, physicochemical properties analysis and molecular dynamic simulation. Our homology modeling was successfully generated and validated. According to our virtual screening studies, ZINC000364721779, ZINC000635903250, P6240926, ChEMBL1740350 and ChEMBL1235738 compounds have shown the highest binding affinities to human GABA-AT. These compounds have obeyed Lipinski's rule of five and have been considered as drug-like candidates based on the ADMET profile. All studied systems remained in the steady state in the MD simulation over time and in energy calculations suggesting high stability of our homology modeled GABA-AT, GABA-AT-ZINC000364721779, GABA-AT-ZINC000635903250, GABA-AT-P6240926, GABA-AT-ChEMBL1740350 and GABA-AT-ChEMBL1235738 complexes. The most promising molecules such as ZINC000364721779, ZINC000635903250, P6240926, ChEMBL1740350 and ChEMBL1235738 might be experimentally tested in future work for further evaluation.

References:

- Agrawal, P. (2013). Structure-Based Drug Design. *Journal of Pharmacovigilance*, 01(04), 1–2. <https://doi.org/10.4172/2329-6887.1000e111>
- Al-Obaidi, A., Elmezayen, A. D., & Yelekçi, K. (2020). Homology modeling of human GABA-AT and devise some novel and potent inhibitors via computer-aided drug design techniques. *Journal of Biomolecular Structure & Dynamics*, 1–11. <https://doi.org/10.1080/07391102.2020.1774417>
- Altschul, S. F., Gish, W., Miller, W., Myers, E. W., & Lipman, D. J. (1990). Basic local alignment search tool. *Journal of Molecular Biology*, 215(3), 403–410. [https://doi.org/10.1016/S0022-2836\(05\)80360-2](https://doi.org/10.1016/S0022-2836(05)80360-2)
- Aqvist, J., Luzhkov, V. B., & Brandsdal, B. O. (2002). Ligand binding affinities from MD simulations. *Accounts of Chemical Research*, 35(6), 358–365. <https://doi.org/10.1021/ar010014p>
- Arodola, O. A., & Soliman, M. E. S. (2017). Quantum mechanics implementation in drug-design workflows: does it really help? *Drug Design, Development and Therapy, Volume 11*, 2551–2564. <https://doi.org/10.2147/DDDT.S126344>
- Bansal, S. K., Sinha, B. N., & Khosa, R. L. (2013). γ -Amino butyric acid analogs as novel potent GABA-AT inhibitors: Molecular docking, synthesis, and biological evaluation. *Medicinal Chemistry Research*, 22(1), 134–146. <https://doi.org/10.1007/s00044-012-0023-0>
- Bateman, A. (2019). UniProt: A worldwide hub of protein knowledge. *Nucleic Acids Research*, 47(D1), D506–D515. <https://doi.org/10.1093/nar/gky1049>
- Bayly, C. I., Merz, K. M., Ferguson, D. M., Cornell, W. D., Fox, T., Caldwell, J. W., ... Spellmeyer, D. C. (1995). A Second Generation Force Field for the Simulation of Proteins, Nucleic Acids, and Organic Molecules. *Journal of the American Chemical Society*, 117(19), 5179–5197. <https://doi.org/10.1021/ja00124a002>
- Berman, H. M., Westbrook, J., Feng, Z., Gilliland, G., Bhat, T. N., Weissig, H., ... Bourne, P. E. (2000). The Protein Data Bank. *Nucleic Acids Research*, 28(1), 235–242. <https://doi.org/10.1093/nar/28.1.235>
- Biasini, M., Bienert, S., Waterhouse, A., Arnold, K., Studer, G., Schmidt, T., ... Schwede, T. (2014). SWISS-MODEL: Modelling protein tertiary and quaternary structure using evolutionary information. *Nucleic Acids Research*, 42(W1), W252–W258. <https://doi.org/10.1093/nar/gku340>
- BIOVIA, D. S. (2017). BIOVIA Discovery Studio 2017 R2: A comprehensive

predictive science application for the Life Sciences. *San Diego, CA, USA*. San Diego, CA, USA.

- Boonstra, E., de Kleijn, R., Colzato, L. S., Alkemade, A., Forstmann, B. U., & Nieuwenhuis, S. (2015). Neurotransmitters as food supplements: The effects of GABA on brain and behavior. *Frontiers in Psychology*, *6*(OCT), 6–11. <https://doi.org/10.3389/fpsyg.2015.01520>
- Bowery, N. G., Bettler, B., Froestl, W., Gallagher, J. P., Marshall, F., Raiteri, M., ... Enna, S. J. (2002). International Union of Pharmacology. XXXIII. Mammalian γ -aminobutyric acid receptors: Structure and function. *Pharmacological Reviews*, *54*(2), 247–264. <https://doi.org/10.1124/pr.54.2.247>
- Bowie, J. U., Lüthy, R., & Eisenberg, D. (1991). A method to identify protein sequences that fold into a known three-dimensional structure. *Science*, *253*(5016), 164–170. <https://doi.org/10.1126/science.1853201>
- Browne, T. R. (1998). Pharmacokinetics of antiepileptic drugs. *Neurology*, *51*(Issue 5, Supplement 4), S2–S7. https://doi.org/10.1212/WNL.51.5_Suppl_4.S2
- Cellini, B., Montioli, R., Oppici, E., & Voltattorni, C. B. (2012). Biochemical and computational approaches to improve the clinical treatment of dopa decarboxylase-related diseases: an overview. *The Open Biochemistry Journal*, *6*(1), 131–138. <https://doi.org/10.2174/1874091X01206010131>
- Centeno, N. B., Planas-Iglesias, J., & Oliva, B. (2005). Comparative modelling of protein structure and its impact on microbial cell factories. *Microbial Cell Factories*, *4*, 1–11. <https://doi.org/10.1186/1475-2859-4-20>
- Cheng, A., & Merz, K. M. (2003). Prediction of aqueous solubility of a diverse set of compounds using quantitative structure-property relationships. *Journal of Medicinal Chemistry*, *46*(17), 3572–3580. <https://doi.org/10.1021/jm020266b>
- Choi, S., & Silverman, R. B. (2002a). Inactivation and inhibition of γ -aminobutyric acid aminotransferase by conformationally restricted vigabatrin analogues. *Journal of Medicinal Chemistry*, *45*(20), 4531–4539. <https://doi.org/10.1021/jm020134i>
- Choi, S., & Silverman, R. B. (2002b). Inactivation and inhibition of γ -aminobutyric acid aminotransferase by conformationally restricted vigabatrin analogues. *Journal of Medicinal Chemistry*, *45*(20), 4531–4539. <https://doi.org/10.1021/jm020134i>
- Chothia, C., & Lesk, A. M. (1986). The relation between the divergence of sequence and structure in proteins. *The EMBO Journal*, *5*(4), 823–826. <https://doi.org/10.1002/j.1460-2075.1986.tb04288.x>
- Christensen, D. L., Braun, K. V. N., Baio, J., Bilder, D., Charles, J., Constantino, J. N., ... Yeargin-Allsopp, M. (2018). Prevalence and Characteristics of Autism Spectrum Disorder Among Children Aged 8 Years - Autism and Developmental Disabilities Monitoring Network, 11 Sites, United States, 2012. *Morbidity and Mortality Weekly Report. Surveillance Summaries (Washington, D.C. : 2002)*, *65*(13), 1–23. <https://doi.org/10.15585/mmwr.ss6513a1>
- Clayton, L. M., Stern, W. M., Newman, W. D., Sander, J. W., Acheson, J., & Sisodiya,

- S. M. (2013). Evolution of visual field loss over ten years in individuals taking vigabatrin. *Epilepsy Research*, 105(3), 262–271. <https://doi.org/10.1016/j.eplepsyres.2013.02.014>
- Clift, M. D., & Silverman, R. B. (2008). Synthesis and evaluation of novel aromatic substrates and competitive inhibitors of GABA aminotransferase. *Bioorganic and Medicinal Chemistry Letters*, 18(10), 3122–3125. <https://doi.org/10.1016/j.bmcl.2007.10.060>
- Coupez, B., & Lewis, R. A. (2006). Docking and scoring--theoretically easy, practically impossible? *Current Medicinal Chemistry*, 13(25), 2995–3003. <https://doi.org/10.2174/092986706778521797>
- Dalal, S., Balasubramanian, S., & Regan, L. (1997). Transmuting α helices and β sheets. *Folding and Design*, 2(5), R71–R79. [https://doi.org/10.1016/S1359-0278\(97\)00036-9](https://doi.org/10.1016/S1359-0278(97)00036-9)
- Dar, A. M., & Mir, S. (2017). Molecular Docking: Approaches, Types, Applications and Basic Challenges. *Journal of Analytical & Bioanalytical Techniques*, 08(02), 8–10. <https://doi.org/10.4172/2155-9872.1000356>
- de Boer, A. G., van der Sandt, I. C. J., & Gaillard, P. J. (2003). The role of drug transporters at the blood-brain barrier. *Annual Review of Pharmacology and Toxicology*, 43(1), 629–656. <https://doi.org/10.1146/annurev.pharmtox.43.100901.140204>
- de Lau, L. M., & Breteler, M. M. (2006). Epidemiology of Parkinson's disease. *Lancet Neurology*, 5(6), 525–535. [https://doi.org/10.1016/S1474-4422\(06\)70471-9](https://doi.org/10.1016/S1474-4422(06)70471-9)
- Egan, W. J., & Lauri, G. (2002). Prediction of intestinal permeability. *Advanced Drug Delivery Reviews*, 54(3), 273–289. [https://doi.org/10.1016/s0169-409x\(02\)00004-2](https://doi.org/10.1016/s0169-409x(02)00004-2)
- Elmezayen, A. D., Al-Obaidi, A., Şahin, A. T., & Yelekçi, K. (2020). Drug repurposing for coronavirus (COVID-19): in silico screening of known drugs against coronavirus 3CL hydrolase and protease enzymes. *Journal of Biomolecular Structure and Dynamics*, 0(0), 1–12. <https://doi.org/10.1080/07391102.2020.1758791>
- Gaulton, A., Bellis, L. J., Bento, A. P., Chambers, J., Davies, M., Hersey, A., ... Overington, J. P. (2012). ChEMBL: a large-scale bioactivity database for drug discovery. *Nucleic Acids Research*, 40(Database issue), D1100-7. <https://doi.org/10.1093/nar/gkr777>
- Graff, C. L., & Pollack, G. M. (2004). Drug transport at the blood-brain barrier and the choroid plexus. *Current Drug Metabolism*, 5(1), 95–108. <https://doi.org/10.2174/1389200043489126>
- Gram, L., Larsson, O. M., Johnsen, A., & Schousboe, A. (1989). Experimental studies of the influence of vigabatrin on the GABA system. *British Journal of Clinical Pharmacology*, 27 Suppl 1(1 S), 13S-17S. <https://doi.org/10.1111/j.1365-2125.1989.tb03455.x>
- Guedes, I. A., de Magalhães, C. S., & Dardenne, L. E. (2014). Receptor-ligand

- molecular docking. *Biophysical Reviews*, 6(1), 75–87.
<https://doi.org/10.1007/s12551-013-0130-2>
- Gulerez, I. E., & Gehring, K. (2014). X-ray crystallography and NMR as tools for the study of protein tyrosine phosphatases. *Methods (San Diego, Calif.)*, 65(2), 175–183. <https://doi.org/10.1016/j.ymeth.2013.07.032>
- Han, Y., Zhang, J., Hu, C. Q., Zhang, X., Ma, B., & Zhang, P. (2019). In silico ADME and Toxicity Prediction of Ceftazidime and Its Impurities. *Frontiers in Pharmacology*, 10(APR), 434. <https://doi.org/10.3389/fphar.2019.00434>
- Hawker, D. D., & Silverman, R. B. (2012). Synthesis and evaluation of novel heteroaromatic substrates of GABA aminotransferase. *Bioorganic & Medicinal Chemistry*, 20(19), 5763–5773. <https://doi.org/10.1016/j.bmc.2012.08.009>
- Jeremiah, S., & Povey, S. (1981). The biochemical genetics of human gamma-aminobutyric acid transaminase. *Annals of Human Genetics*, 45(3), 231–236. <https://doi.org/10.1111/j.1469-1809.1981.tb00334.x>
- Jhoti, H., Rees, S., & Solari, R. (2013). High-throughput screening and structure-based approaches to hit discovery: is there a clear winner? *Expert Opinion on Drug Discovery*, 8(12), 1449–1453. <https://doi.org/10.1517/17460441.2013.857654>
- Jiménez, J., Škalič, M., Martínez-Rosell, G., & De Fabritiis, G. (2018). K DEEP : Protein–Ligand Absolute Binding Affinity Prediction via 3D-Convolutional Neural Networks. *Journal of Chemical Information and Modeling*, 58(2), 287–296. <https://doi.org/10.1021/acs.jcim.7b00650>
- Jo, S., Kim, T., Iyer, V. G., & Im, W. (2008). CHARMM-GUI: a web-based graphical user interface for CHARMM. *Journal of Computational Chemistry*, 29(11), 1859–1865. <https://doi.org/10.1002/jcc.20945>
- John, R. A. (1995). Pyridoxal phosphate-dependent enzymes. *Biochimica et Biophysica Acta*, 1248(2), 81–96. [https://doi.org/10.1016/0167-4838\(95\)00025-p](https://doi.org/10.1016/0167-4838(95)00025-p)
- Jones, G., Willett, P., Glen, R. C., Leach, A. R., & Taylor, R. (1997). Development and validation of a genetic algorithm for flexible docking. *Journal of Molecular Biology*, 267(3), 727–748. <https://doi.org/10.1006/jmbi.1996.0897>
- Joó, F. (1993). The blood-brain barrier in vitro: the second decade. *Neurochemistry International*, 23(6), 499–521. [https://doi.org/10.1016/0197-0186\(93\)90098-p](https://doi.org/10.1016/0197-0186(93)90098-p)
- Jorgensen, W. L. (2004). The many roles of computation in drug discovery. *Science (New York, N.Y.)*, 303(5665), 1813–1818. <https://doi.org/10.1126/science.1096361>
- Jorgensen, W. L., & Tirado-Rives, J. (1988). The OPLS [optimized potentials for liquid simulations] potential functions for proteins, energy minimizations for crystals of cyclic peptides and crambin. *Journal of the American Chemical Society*, 110(6), 1657–1666. <https://doi.org/10.1021/ja00214a001>
- Kaila, K., Ruusuvuori, E., Seja, P., Voipio, J., & Puskarjov, M. (2014). GABA actions and ionic plasticity in epilepsy. *Current Opinion in Neurobiology*, 26(Figure 1), 34–41. <https://doi.org/10.1016/j.conb.2013.11.004>

- Kim, Y. S., & Yoon, B.-E. (2017). Altered GABAergic Signaling in Brain Disease at Various Stages of Life. *Experimental Neurobiology*, *26*(3), 122–131. <https://doi.org/10.5607/en.2017.26.3.122>
- Kool, E. T. (2002). Active site tightness and substrate fit in DNA replication. *Annual Review of Biochemistry*, *71*(1), 191–219. <https://doi.org/10.1146/annurev.biochem.71.110601.135453>
- Krnjevic, K. (1974). Chemical nature of synaptic transmission in vertebrates. *Physiological Reviews*, *54*(2), 418–540. <https://doi.org/10.1152/physrev.1974.54.2.418>
- Kuntz, I. D., Blaney, J. M., Oatley, S. J., Langridge, R., & Ferrin, T. E. (1982). A geometric approach to macromolecule-ligand interactions. *Journal of Molecular Biology*, *161*(2), 269–288. [https://doi.org/10.1016/0022-2836\(82\)90153-X](https://doi.org/10.1016/0022-2836(82)90153-X)
- Laskowski, R. A., MacArthur, M. W., Moss, D. S., & Thornton, J. M. (1993). PROCHECK: a program to check the stereochemical quality of protein structures. *Journal of Applied Crystallography*, *26*(2), 283–291. <https://doi.org/10.1107/S0021889892009944>
- Lindberger, M., Luhr, O., Johannessen, S. I., Larsson, S., & Tomson, T. (2003). Serum concentrations and effects of gabapentin and vigabatrin: observations from a dose titration study. *Therapeutic Drug Monitoring*, *25*(4), 457–462. <https://doi.org/10.1097/00007691-200308000-00007>
- Lipinski, C. A., Lombardo, F., Dominy, B. W., & Feeney, P. J. (1997). Experimental and computational approaches to estimate solubility and permeability in drug discovery and development settings. *Advanced Drug Delivery Reviews*, *23*(1–3), 3–25. [https://doi.org/10.1016/S0169-409X\(96\)00423-1](https://doi.org/10.1016/S0169-409X(96)00423-1)
- Liu, H., & Hou, T. (2016). CaFE: a tool for binding affinity prediction using end-point free energy methods. *Bioinformatics*, *32*(14), 2216–2218. <https://doi.org/10.1093/bioinformatics/btw215>
- Luchetti, S., Huitinga, I., & Swaab, D. F. (2011). Neurosteroid and GABA-A receptor alterations in Alzheimer's disease, Parkinson's disease and multiple sclerosis. *Neuroscience*, *191*, 6–21. <https://doi.org/10.1016/j.neuroscience.2011.04.010>
- MacKerell, A. D., Bashford, D., Bellott, M., Dunbrack, R. L., Evanseck, J. D., Field, M. J., ... Karplus, M. (1998). All-atom empirical potential for molecular modeling and dynamics studies of proteins. *The Journal of Physical Chemistry. B*, *102*(18), 3586–3616. <https://doi.org/10.1021/jp973084f>
- Madsen, K. K., Larsson, O. M., & Schousboe, A. (2008). Regulation of excitation by GABA neurotransmission: focus on metabolism and transport. *Results and Problems in Cell Differentiation*, *44*(June), 201–221. https://doi.org/10.1007/400_2007_036
- Maragakis, P., Lindorff-Larsen, K., Eastwood, M. P., Dror, R. O., Klepeis, J. L., Arkin, I. T., ... Shaw, D. E. (2008). Microsecond molecular dynamics simulation shows effect of slow loop dynamics on backbone amide order parameters of proteins. *Journal of Physical Chemistry B*, *112*(19), 6155–6158.

<https://doi.org/10.1021/jp077018h>

- Martí-Renom, M. A., Stuart, A. C., Fiser, A., Sánchez, R., Melo, F., & Sali, A. (2000). Comparative protein structure modeling of genes and genomes. *Annual Review of Biophysics and Biomolecular Structure*, 29(1), 291–325.
<https://doi.org/10.1146/annurev.biophys.29.1.291>
- Masten, A. S., Faden, V. B., Zucker, R. A., & Spear, L. P. (2009). A developmental perspective on underage alcohol use. *Alcohol Research & Health : The Journal of the National Institute on Alcohol Abuse and Alcoholism*, 32(1), 3–15.
https://doi.org/10.1007/978-3-319-45641-6_11
- McConkey, B. J., Sobolev, V., & Edelman, M. (2002). The performance of current methods in ligand-protein docking. *Current Science*, 83(7), 845–856.
- Meanwell, N. A. (2011). Synopsis of some recent tactical application of bioisosteres in drug design. *Journal of Medicinal Chemistry*, 54(8), 2529–2591.
<https://doi.org/10.1021/jm1013693>
- Meng, X.-Y., Zhang, H.-X., Mezei, M., & Cui, M. (2011). Molecular docking: a powerful approach for structure-based drug discovery. *Current Computer-Aided Drug Design*, 7(2), 146–157. <https://doi.org/10.2174/157340911795677602>
- Moitessier, N., Englebienne, P., Lee, D., Lawandi, J., & Corbeil, C. R. (2008). Towards the development of universal, fast and highly accurate docking/scoring methods: a long way to go. *British Journal of Pharmacology*, 153 Suppl(SUPPL. 1), S7-26.
<https://doi.org/10.1038/sj.bjp.0707515>
- Morris, G. M., Huey, R., Lindstrom, W., Sanner, M. F., Belew, R. K., Goodsell, D. S., & Olson, A. J. (2009). AutoDock4 and AutoDockTools4: Automated docking with selective receptor flexibility. *Journal of Computational Chemistry*, 30(16), 2785–2791. <https://doi.org/10.1002/jcc.21256>
- Oostenbrink, C., Villa, A., Mark, A. E., & van Gunsteren, W. F. (2004). A biomolecular force field based on the free enthalpy of hydration and solvation: the GROMOS force-field parameter sets 53A5 and 53A6. *Journal of Computational Chemistry*, 25(13), 1656–1676. <https://doi.org/10.1002/jcc.20090>
- Pan, Y., Qiu, J., & Silverman, R. B. (2003). Design, synthesis, and biological activity of a difluoro-substituted, conformationally rigid vigabatrin analogue as a potent gamma-aminobutyric acid aminotransferase inhibitor. *Journal of Medicinal Chemistry*, 46(25), 5292–5293. <https://doi.org/10.1021/jm034162s>
- Park, J., Teichmann, S. A., Hubbard, T., & Chothia, C. (1997). Intermediate sequences increase the detection of homology between sequences. *Journal of Molecular Biology*, 273(1), 349–354. <https://doi.org/10.1006/jmbi.1997.1288>
- Pearl, P. L. (2018). Epilepsy Syndromes in Childhood. *Continuum (Minneapolis, Minn.)*, 24(1, Child Neurology), 186–209.
<https://doi.org/10.1212/CON.0000000000000568>
- Percudani, R., & Peracchi, A. (2003). A genomic overview of pyridoxal-phosphate-dependent enzymes. *EMBO Reports*, 4(9), 850–854.

<https://doi.org/10.1038/sj.embor.embor914>

- Pevsner, J. (2009). Bioinformatics and Functional Genomics: Second Edition. In *Bioinformatics and Functional Genomics: Second Edition*.
<https://doi.org/10.1002/9780470451496>
- Phillips, J. C., Braun, R., Wang, W., Gumbart, J., Tajkhorshid, E., Villa, E., ... Schulten, K. (2005). Scalable molecular dynamics with NAMD. *Journal of Computational Chemistry*, 26(16), 1781–1802. <https://doi.org/10.1002/jcc.20289>
- Ringe, D., & Petsko, G. A. (2008). Biochemistry. How enzymes work. *Science (New York, N.Y.)*, 320(5882), 1428–1429. <https://doi.org/10.1126/science.1159747>
- Rokita, S. (2000). The Organic Chemistry of Enzyme-Catalyzed Reactions By Richard B. Silverman (Northwestern University). Academic Press: San Diego. 2000. xviii + 718 pp. \$89.95. ISBN 0-12-643745-9. *Journal of the American Chemical Society*, 122(33), 8103–8104. <https://doi.org/10.1021/ja004710g>
- Seeliger, D., & De Groot, B. L. (2010). Ligand docking and binding site analysis with PyMOL and Autodock/Vina. *Journal of Computer-Aided Molecular Design*, 24(5), 417–422. <https://doi.org/10.1007/s10822-010-9352-6>
- Seyfried, T. N., & Yu, R. K. (1980). Heterosis for brain myelin content in mice. *Biochemical Genetics*, 18(11–12), 1229–1238.
<https://doi.org/10.1007/BF00484350>
- Shoichet, B. K., McGovern, S. L., Wei, B., & Irwin, J. J. (2002). Lead discovery using molecular docking. *Current Opinion in Chemical Biology*, 6(4), 439–446.
[https://doi.org/10.1016/S1367-5931\(02\)00339-3](https://doi.org/10.1016/S1367-5931(02)00339-3)
- Silverman, R. B. (2018). Design and Mechanism of GABA Aminotransferase Inactivators. Treatments for Epilepsies and Addictions. *Chemical Reviews*, 118(7), 4037–4070. <https://doi.org/10.1021/acs.chemrev.8b00009>
- Silverman, R. B., & Holladay, M. W. (2015). The Organic Chemistry of Drug Design and Drug Action: Third Edition. In *The Organic Chemistry of Drug Design and Drug Action: Third Edition*. <https://doi.org/10.1016/C2009-0-64537-2>
- Solomon, N., & McHale, K. (2012). An overview of epilepsy in children and young people. *Nursing Children and Young People*, 24(6), 28–35; quiz 36.
<https://doi.org/10.7748/ncyp2012.07.24.6.28.c9190>
- Sterling, T., & Irwin, J. J. (2015). ZINC 15--Ligand Discovery for Everyone. *Journal of Chemical Information and Modeling*, 55(11), 2324–2337.
<https://doi.org/10.1021/acs.jcim.5b00559>
- Storici, P., De Biase, D., Bossa, F., Bruno, S., Mozzarelli, A., Peneff, C., ... Schirmer, T. (2004). Structures of gamma-aminobutyric acid (GABA) aminotransferase, a pyridoxal 5'-phosphate, and [2Fe-2S] cluster-containing enzyme, complexed with gamma-ethynyl-GABA and with the antiepilepsy drug vigabatrin. *The Journal of Biological Chemistry*, 279(1), 363–373. <https://doi.org/10.1074/jbc.M305884200>
- Surabhi, S., & Singh, B. (2018). COMPUTER AIDED DRUG DESIGN: AN OVERVIEW. *Journal of Drug Delivery and Therapeutics*, 8(5), 504–509.

<https://doi.org/10.22270/jddt.v8i5.1894>

- Tao, Y.-H., Yuan, Z., Tang, X.-Q., Xu, H.-B., & Yang, X.-L. (2006). Inhibition of GABA shunt enzymes' activity by 4-hydroxybenzaldehyde derivatives. *Bioorganic & Medicinal Chemistry Letters*, *16*(3), 592–595. <https://doi.org/10.1016/j.bmcl.2005.10.040>
- Toney, M. D., Pascarella, S., & De Biase, D. (1995). Active site model for γ -aminobutyrate aminotransferase explains substrate specificity and inhibitor reactivities. *Protein Science*, *4*(11), 2366–2374. <https://doi.org/10.1002/pro.5560041115>
- Trott, O., & Olson, A. J. (2010). AutoDock Vina: improving the speed and accuracy of docking with a new scoring function, efficient optimization, and multithreading. *Journal of Computational Chemistry*, *31*(2), 455–461. <https://doi.org/10.1002/jcc.21334>
- Tulloch, J. K., Carr, R. R., & Ensom, M. H. H. (2012). A systematic review of the pharmacokinetics of antiepileptic drugs in neonates with refractory seizures. *The Journal of Pediatric Pharmacology and Therapeutics : JPPT : The Official Journal of PPAG*, *17*(1), 31–44. <https://doi.org/10.5863/1551-6776-17.1.31>
- Tunncliffe, G. (1989). Inhibitors of brain GABA aminotransferase. *Comparative Biochemistry and Physiology. A, Comparative Physiology*, *93*(1), 247–254. [https://doi.org/10.1016/0300-9629\(89\)90213-2](https://doi.org/10.1016/0300-9629(89)90213-2)
- Visser, S. N., Danielson, M. L., Bitsko, R. H., Perou, R., & Blumberg, S. J. (2013). Convergent Validity of Parent-Reported Attention-Deficit/Hyperactivity Disorder Diagnosis. *JAMA Pediatrics*, *167*(7), 674. <https://doi.org/10.1001/jamapediatrics.2013.2364>
- Wang, X., Song, K., Li, L., & Chen, L. (2018). Structure-Based Drug Design Strategies and Challenges. *Current Topics in Medicinal Chemistry*, *18*(12), 998–1006. <https://doi.org/10.2174/1568026618666180813152921>
- Webb, B., & Sali, A. (2016). Comparative Protein Structure Modeling Using MODELLER. *Current Protocols in Bioinformatics*, *54*(June), 5.6.1-5.6.37. <https://doi.org/10.1002/cpbi.3>
- Wermuth, C. G., Bourguignon, J. J., Schlewer, G., Gies, J. P., Schoenfelder, A., Melikian, A., ... Heaulme, M. (1987). Synthesis and structure-activity relationships of a series of aminopyridazine derivatives of gamma-aminobutyric acid acting as selective GABA-A antagonists. *Journal of Medicinal Chemistry*, *30*(2), 239–249. <https://doi.org/10.1021/jm00385a003>
- Wiederstein, M., & Sippl, M. J. (2007). ProSA-web: interactive web service for the recognition of errors in three-dimensional structures of proteins. *Nucleic Acids Research*, *35*(Web Server issue), W407-10. <https://doi.org/10.1093/nar/gkm290>
- Wiley, A. J. (2001). Enzymes. A Practical Introduction to Structure, Mechanism, and Data Analysis, Second ed. Robert A. Copeland. In *Analytical Biochemistry* (Vol. 291). <https://doi.org/10.1006/abio.2001.5023>

Yizhar, O., Fenno, L. E., Prigge, M., Schneider, F., Davidson, T. J., O'Shea, D. J., ... Deisseroth, K. (2011). Neocortical excitation/inhibition balance in information processing and social dysfunction. *Nature*, 477(7363), 171–178. <https://doi.org/10.1038/nature10360>

Zwanzger, P., Baghai, T. C., Schuele, C., Ströhle, A., Padberg, F., Kathmann, N., ... Rupprecht, R. (2001). Vigabatrin decreases cholecystokinin-tetrapeptide (CCK-4) induced panic in healthy volunteers. *Neuropsychopharmacology : Official Publication of the American College of Neuropsychopharmacology*, 25(5), 699–703. [https://doi.org/10.1016/S0893-133X\(01\)00266-4](https://doi.org/10.1016/S0893-133X(01)00266-4)

